Development of a drug discovery protocol through the expression of key mycothiol biosynthetic enzymes from *Mycobacterium tuberculosis*

by

Dirk Antonie Lamprecht

Thesis

presented in partial fulfillment of the

requirements for the degree

Magister Scientiae

in

Chemistry

in the

Faculty of Science

University of Stellenbosch

Supervisor: Dr. M. A. Jardine

Co-supervisor: Dr. E. Strauss

April 2008

Declaration:

I, the undersigned, hereby declare that the work contained in this thesis is my own original work and that I have not previously in its entirety or in part submitted it at any university for a degree.

Signture .....

Date.....

Conference poster presentations

Quantification of Disaccharide Intermediates of the Mycothiol Biosynthetic Pathway using LC-MS/MS.

TUBERCULOSIS DRUG DEVELOPMENT – Gordon Conference
August 26-31, 2007
Magdalen College
Oxford, United Kingdom

SASM - Biotech SA - SASBMB
January 21 – 25, 2008
Grahamstown, South Africa

Manuscripts in preparation

1. Quantification of Disaccharide Intermediates of the Mycothiol Biosynthetic Pathway using LC-MS/MS.
2. The Synthesis and Evaluation of Thioglycoside Substrate Analogs of the Mycothiol Biosynthesis Pathway.
3. Purification and Characterization of *Mycobacterium Tuberculosis* mycothiol disulfide reductase, Mtr.

Summary:

This work focuses on mycothiol (MSH), the low molecular weight thiol of *M. tuberculosis*, the causative agent of pulmonary TB. It has been proven through numerous studies that the enzymes involved in the biosynthesis and related reactions of MSH are good drug targets for the design of new antibiotics against *M. tuberculosis*. Unfortunately, current screening methods are insufficient and do not allow for the high thought-put screening of potential inhibitors against these enzymes. In this work we laid the foundation for an improved method to expedite antitubercular drug discovery.

During this study mycothiol disulfide reductase (Mtr) and the mycothiol biosynthetic enzyme MshB were recombinantly expressed and purified from *E. coli*. The Mtr enzyme was shown to be active in the presence of des-*myo*-inositol mycothiol disulfide (DI-MSSM), a substrate analogue of Mtr. Taken together, these results should greatly facilitate the solution of the first crystal structure of this essential *M. tuberculosis* enzyme. Such a structure would be an essential requirement of structure-based drug development efforts directed at Mtr. Furthermore, we have developed a new ESI/MS(TOF)-HPLC method for the quantitation of MSH and its pathway intermediates. This new analytical method was employed to detect and quantitate three different pathway analytes from a single injection of *M. smegmatis* cell lysate. It was also used to determine the fluctuating MSH:MSSM levels in *M. smegmatis* cells growing under oxidative stress conditions. MshB enzyme reactions were also analyzed using this method.

A series of substrate analogues were also designed and tested against both the expressed enzymes. The first of these, DI-MSSM, was used to test the activity of Mtr. Furthermore, two sets of substrate analogues of MshB – one of thioglycoside-disaccharides and another containing a variety of fluorophores – were designed and synthesized with the goal of using these analogues as scaffolds for the development of new inhibitor libraries. Among these analogues, one of the fluorogenic substrates showed better activity with MshB than its natural substrate. This molecule was also shown to undergo an intramolecular rearrangement, after reacting with MshB. This would be the first time this type of rearrangement is shown to be enzyme mediated. With further development this molecule could be used in a photometric-based assay of MshB.

Summary:

This work focuses on mycothiol (MSH), the low molecular weight thiol of *M. tuberculosis*, the causative agent of pulmonary TB. It has been proven through numerous studies that the enzymes involved in the biosynthesis and related reactions of MSH are good drug targets for the design of new antibiotics against *M. tuberculosis*. Unfortunately, current screening methods are insufficient and do not allow for the high thought-put screening of potential inhibitors against these enzymes. In this work we laid the foundation for an improved method to expedite antitubercular drug discovery.

During this study mycothiol disulfide reductase (Mtr) and the mycothiol biosynthetic enzyme MshB were recombinantly expressed and purified from *E. coli*. The Mtr enzyme was shown to be active in the presence of des-*myo*-inositol mycothiol disulfide (DI-MSSM), a substrate analogue of Mtr. Taken together, these results should greatly facilitate the solution of the first crystal structure of this essential *M. tuberculosis* enzyme. Such a structure would be an essential requirement of structure-based drug development efforts directed at Mtr. Furthermore, we have developed a new ESI/MS(TOF)-HPLC method for the quantitation of MSH and its pathway intermediates. This new analytical method was employed to detect and quantitate three different pathway analytes from a single injection of *M. smegmatis* cell lysate. It was also used to determine the fluctuating MSH:MSSM levels in *M. smegmatis* cells growing under oxidative stress conditions. MshB enzyme reactions were also analyzed using this method.

A series of substrate analogues were also designed and tested against both the expressed enzymes. The first of these, DI-MSSM, was used to test the activity of Mtr. Furthermore, two sets of substrate analogues of MshB – one of thioglycoside-disaccharides and another containing a variety of fluorophores – were designed and synthesized with the goal of using these analogues as scaffolds for the development of new inhibitor libraries. Among these analogues, one of the fluorogenic substrates showed better activity with MshB than its natural substrate. This molecule was also shown to undergo an intramolecular rearrangement, after reacting with MshB. This would be the first time this type of rearrangement is shown to be enzyme mediated. With further development this molecule could be used in a photometric-based assay of MshB.

Opsomming:

Die werkstuk fokus op mikotiol (MSH), wat 'n lae molekulêre gewig tiol van *M. tuberculosis* is. Verskeie studies het alreeds bewys dat die ensieme wat betrokke is by die biosintese en sellulêre funksies van MSH, goeie teikens is vir die ontwikkeling van nuwe *M. tuberculosis* antibiotikums. Huidige metodes vir die evalueering van inhibeerders teen hierdie ensieme is onvoldoende en laat nie die toets van groot hoeveelhede inhibeerders gelyktydig toe nie. In hierdie betrokke werkstuk word die grondslag gelê vir die onwikkeling van 'n verbeterde metode vir die ontdekking van antituberkurale middels.

Gedurende die studie is mikotiol disulfied reduktase (Mtr) en die mikotiol biosintetiese ensiem, MshB, in *E. coli* uitgedruk en gesuiwer. Dit is die eerste suksesvolle uitdrukking van Mtr in *E. coli* en maak dit moontlik om die eerste kristalstruktuur van hierdie essensiële *M. tuberculosis* ensiem op te los. Die Mtr kristalstruktuur sal 'n belangrike hulpmiddel wees vir struktuurgebaseerde ontwikkeling van middele teen Mtr.

Verder, is daar ook 'n nuwe ESI/MS(TOF)-HPLC metode ontwikkel vir die kwantifisering van MSH en sy tussengangers in die biosintese pad. Die nuwe analitiese metode is gebruik om drie verskillende tussengangers op te spoor en te kwantifiseer. Al drie tussengangers is in 'n enkele inspuiting van *M. smegmatis* sel vervloeiing opgespoor. Die metode is ook gebruik om die verandering in MSH:MSSM verhoudings te ondersoek in *M. smegmatis* selle wat onder oksidatiewe toestande opgegroei is. Ensiemreaksies met MshB is ook geanaliseer met die metode.

'n Reeks substraatanaloë is ook ontwikkel en getoets teen Mtr en MshB. Des-*myo*-inositol mikotiol disulfied (DI-MSSM) is gebruik om die aktiwiteit van Mtr te toets. Verder is twee groepe substraatanaloë teen MshB ontwikkel, tioglikosidiese-disakkariede en fluoroserende substrate, met die doel om as raamwerk te dien vir die ontwikkeling van inhibeerders teen MshB. Daar is gevind dat een van die fluoroserende substrate beter aktiwiteit toon met MshB as die natuurlike substraat. Dit is ook gewys dat die molekule intramolekulêre herrangskiking ondergaan na die inwerking van MshB. Hierdie ondekking dien eerste bewys dat die tipe intramolekulêre herrangskiking deur 'n ensiem gemedieer kan word. Met verdere onwikkeling kan hierdie molekule gebruik word in die fotometriese analiese van MshB ensiemreaksies.

"The joy of discovery is certainly the liveliest that the mind of man can feel"
Claude Bernard (1813 – 1876)

Acknowledgments

Drs. Anwar Jardine and Erick Strauss, for their guidance and assistance throughout this past two years. Anwar for always seeing the positive prospects in a negative result and the ideas which kept me motivated. Erick for his more objective view of things, helping me to be focused on the task at hand. Thank you for being the best supervisor pair a new, insecure researcher could ask for and helping me make this study a success.

My parents, thank you for teaching me the virtue of hard work and persistence, your love and constant support.

Sindi, the person closest to me, thank you for your love, support and objective opinions. It really made the difficult times more bearable. Thanks for also being a true friend and all your understanding.

My fellow students: Jandrè, Marianne, Renier and Ilse. Most of all, thank you for your friendship and camaraderie. It meant a lot. Also thanks for your help and support, even with the simplest tasks.

Leisl Brand, thanks for all your help, especially with the cloning and expression.

My friends and siblings, thank you for your friendship and having an interest in what I do.

I would also like to thank all University of Stellenbosch support staff for their assistance.

To my heavenly Father, for granting me the abilities to do want I love and for keeping my safe all these years.

Table of content

Cloning, expression and purification of *M. tuberculosis* mycothiol related enzymes

Alternate substrates of MshB and Mtr

Abbreviations

Ac_2O	acetic anhydride
AI	auto induction
αGlcN-DNP	2,4-Dinitrophenyl 2-deoxy-1-thio-α-D-glucopyranose
αGlcNAc-DNP	2,4-Dinitrophenyl2-Acetamido-2-deoxy-1-thio-α-D-glucopyranose
αGlcN-Ins	1-D-myo-inosityl-2-deoxy-α-D-glycopyranoside
αGlcNAc-Ins	1-D-myo-inosityl-2-acetamido-2-deoxy-α-D-glycopyranoside
AMP	adenine monophosphate
ATP	adenine triphosphate
Asp	aspartic acid
BF_3OEt_2	boron trifluoride etherate-complex
BSA	Bovine serum albumin
CoA	coenzyme A
Cys	cysteine
DCM	dichloromethane
ddH_2O	distilled, deionised water
DI-MSSM	des-*myo*-inositol mycothiol disulfide reductase
DiPEA	diisopopyl ethylamine
DMF	N,N-Dimethyl formamide
DNA	deoxyribonucleic acid
DNTB	Ellman's Reagent
EDTA	ethylenediaminetetraacetic acid
E. coli	*Escherichia coli*
EDC	1-Ethyl-3-(3-dimethylaminopropyl)-carbodiimide
ESI-MS	electron spray ionization mass spectroscopy
Et_2O	diethyl ether

EtOH	ethanol
FAD	flavin adenine dinucleotide
FRET	fluorescence resonance energy transfer
Glu	glutamic acid
Gly	glycine
Glygly	glycylglycine
His	histidine
His-tag	6xHistidine tag
HIV	Human immunodeficiency virus
HOBt	N-Hydroxybenzotriazole
HPLC	High pressure liquid chromatography
IPTG	isopropyl-β-D-thiogalactoside
IMAC	Immobilized metal affinity chromatography
Ins	*myo*-inositol
KDa	kilo Dalton
K_m	Michaelis constant
LB	Luria bertani
LCMS	liquid chromatography mass spectroscopy
mBBr	monobromobimane
MBP	maltose binding protein
Mca	mycothiol-S-conjugate amidase
MDR-TB	multi drug-resistant *M. tuberculosis*
MeCN	acetonitrile
MeOH	methanol
M. tuberculosis	*Mycobacterium tuberculosis*
MSH	mycothiol
M. smegmatis	*Mycobacterium smegmatis*

MSSM	mycothiol disulfide
MSSMR	mycothiol disulfide reductase
Mtr	myochiol disulfide reductase
NADPH	nicotinamide adenine dinucleotide phosphate
NMR	nuclear magnetic resonance spectroscopy
OD_{600}	optical density at 600nm
OAc	acetate
PPi	pyrophosphate
RNA	ribonucleic acid
tRNA	transfer ribonucleic acid
Py	pyridine
PCR	polymerase chain reaction
QTOF	quadrupole, time-of-flight tandem mass spectrometer
S. enterica	*Salmonella enterica*
SDS-PAGE	sodium dodecyl sulfate-polyacrylamide gel electrophoresis
TB	pulmonary tuberculosis
TEA	triethylamine
TFA	trifluoroacetic acid
TLC	thin layer chromatography
Tris	2-Amino-2-(hydroxymethyl)-1,3-propanediol
V_{max}	maximum velocity
WHO	World Health Organisation
XDR-TB	Extensively Drug-Resistant *M. tuberculosis*

Chapter 1

Introduction

1.1 Introduction

Mycobacterium tuberculosis is the causative agent of pulmonary tuberculosis (TB) (*1*) and one third of people worldwide are infected with the dormant form of this bacterium. It is only when the bacteria become active – mainly because of a reduction in an individual's immunity – that so-called full-blown TB is developed (*2*). According to the World Health Organization (WHO) an estimated 8.8 million new TB cases were reported in 2005 worldwide. During this period a total of 1.6 million people died, of which 195 000 patients were also infected with HIV (*3*). TB is usually treatable with a course of the first-line anti-TB drugs: pyrazinamide, isoniazid, ethambutol and rifampicin. The course of these drugs is taken for two months, followed by a four-month long course of isoniazid and rifampicin. If misapplied, this drug regime could result in the development of multidrug-resistant *M. tuberculosis* (MDR-TB) strains, which are defined as strains that have become resistant to at least isoniazid and rifampicin (*4*). Almost 4% of new TB cases reported in developing countries are caused by the MDR-TB strain (*2*).

Extremely drug-resistant *M. tuberculosis* (XDR-TB) strains can develop with the continued misuse of second-line anti-TB drugs (Amikacin, Kanamycin and Capreomycin), which are prescribed for MDR-TB patients. A XDR-TB strain is defined as a strain of *M. tuberculosis* that is resistant to at least isoniazid and rifampicin, fluoroquinolones and any one of the second-line anti-TB drugs. Thus making the treatment options for XDR-TB patients dangerously limited (*2, 5*). The continued research and development of new drugs against *M. tuberculosis* is therefore vital in the global fight against TB.

1.2 Mycothiol: structure and function

1-D-*myo*-inositol-2-(*N*-acetyl-L-cysteinyl)-amido-2-deoxy-α-D-glucopyranoside or Mycothiol (MSH), is the major low molecular weight thiol present in wide range of actinomycetes (*6*). MSH plays an important role in protecting the mycobacterial cell similar to the role fulfilled by glutathione in eukaryotic cells,. Some of the main MSH functions are: detoxification of cell from alkylating agents, protection of the bacterial cell against oxidative stress and cell detoxification from formaldehyde (*7-10*). In the formaldehyde detoxification MSH acts as co-factor for the formaldehyde dehydrogenase enzyme in *Amycolatopsis methanolica*. Also, it was recently discovered that MSH serve as a reservoir of biosynthetic precursors and energy-producing metabolites (*11*).

The very unique structure of MSH is shown in Figure 1.1. It consists of two sugar moieties, *N*-glucosamine (red) and inositol (black), bound together by an α(1→1) glycosidic bond. Two amide bonds also form part of the structure, one connecting the cysteine (blue) to the *N*-glucosamine and another connecting the acetyl group (green) to the cysteine. The first chemo-enzymatic synthesis of MSH was attempted by Bornemann *et al.*, in 1997 (*12*).

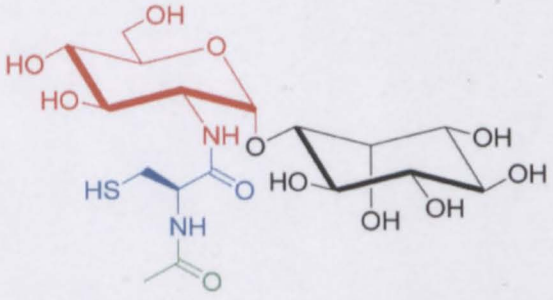

Figure 1.1: Structure of mycothiol

Because of the unique structure of MSH, the enzymes involved in its biosynthesis and metabolism are all potential targets for new drugs against *M. tuberculosis* and other actinomycetes.

1.2.1 Detoxification of alkylating agents and antibiotics

The key enzyme involved in the MSH-dependent detoxification of alkylating agents and antibiotics in *M. tuberculosis* is mycothiol S-conjugate amidase or Mca (*Rv1082* gene product). The enzyme was first discovered in *M. smegmatis*, in a study in which monobromobimane (mBBr) was added to *M. smegmatis* cultures in attempts to alkylate the free thiol of MSH (*7*). It was discovered that derivatised MSH molecules (MSmB) were not exported from the cell. Instead the cysteinyl-glucosamine amide bond of the MSmB molecule was hydrolyzed to produce αGlcN-Ins and a bimane derivatised *N*-acetylcysteine, AcCysmB (a mercapturic acid). The mercapturic acid is transported from the cell either through passive diffusion or a specific export system. The general scheme for this detoxification mechanism is depicted in Figure 1.2. The αGlcN-Ins moiety is retained in the cell and used in the biosynthesis of MSH (*13*).

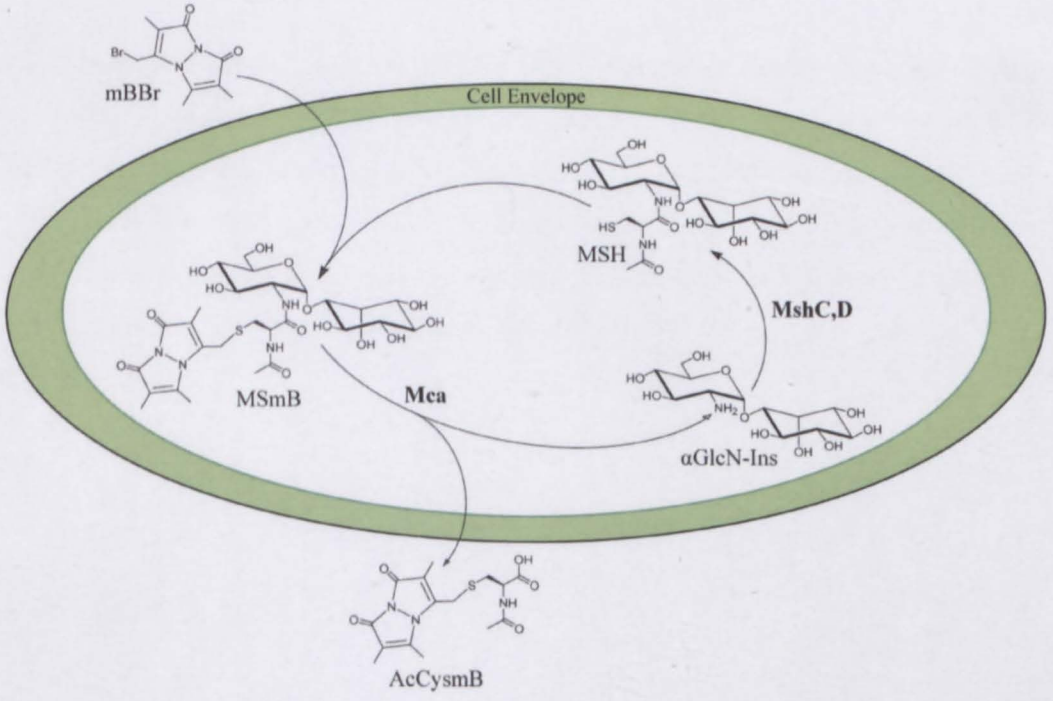

Figure 1.2: The cellular detoxification mechanism of Mca.

Mca has a very high specificity for the mycothiol moiety and the enzyme's activity dropped considerably when either the acetyl or inositol moieties are removed from the MSmB molecule (*7*). Also the amidase activity was observed with a wide range of groups conjugated to the MSH thiol, including an acetophenone moiety which is

structurally similar to isoniazid. The MSH *S*-conjugate of rifamycin S was also shown to be a substrate for Mca (*13*). It is this feature of Mca that is being exploited in the development of inhibitors against this enzyme (*14, 15*). It was also shown by Rawat *et al.* that *M. smegmatis* mutants deficient of Mca is susceptible for antituberculous antibiotics like streptomycin (*16*).

1.2.2 Antioxidant activity

Just like glutathione mycothiol also acts as an antioxidant by reacting with exogenous or endogenous reactive intermediates and thereby maintaining an intracellular redox homeostasis (*17*). During this reaction two equivalents MSH are oxidized to a molecule mycothiol disulfide (MSSM). The reverse reaction, catalyzed by mycothiol disulfide reductase or Mtr, reduces the disulfide and returns the original thiol, thereby maintaining a constant MSH:MSSM ratio (*8*).

Mtr is encoded for by the gene *Rv2855* (*mtr*). Similar to functionally homologous enzymes like glutathione and trypanothione reductase it also depends on bound FAD and NADPH for the reduction of the disulfide bond of MSSM to produce two MSH equivalents (*18*). The catalytically important redox-active disulfide and a histidine-glutamate ion pair is also conserved in these three enzymes. In Mtr these catalytically active residues have been identified as the His444-Glu449 ion pair and Cys39 and Cys44 (*19*).

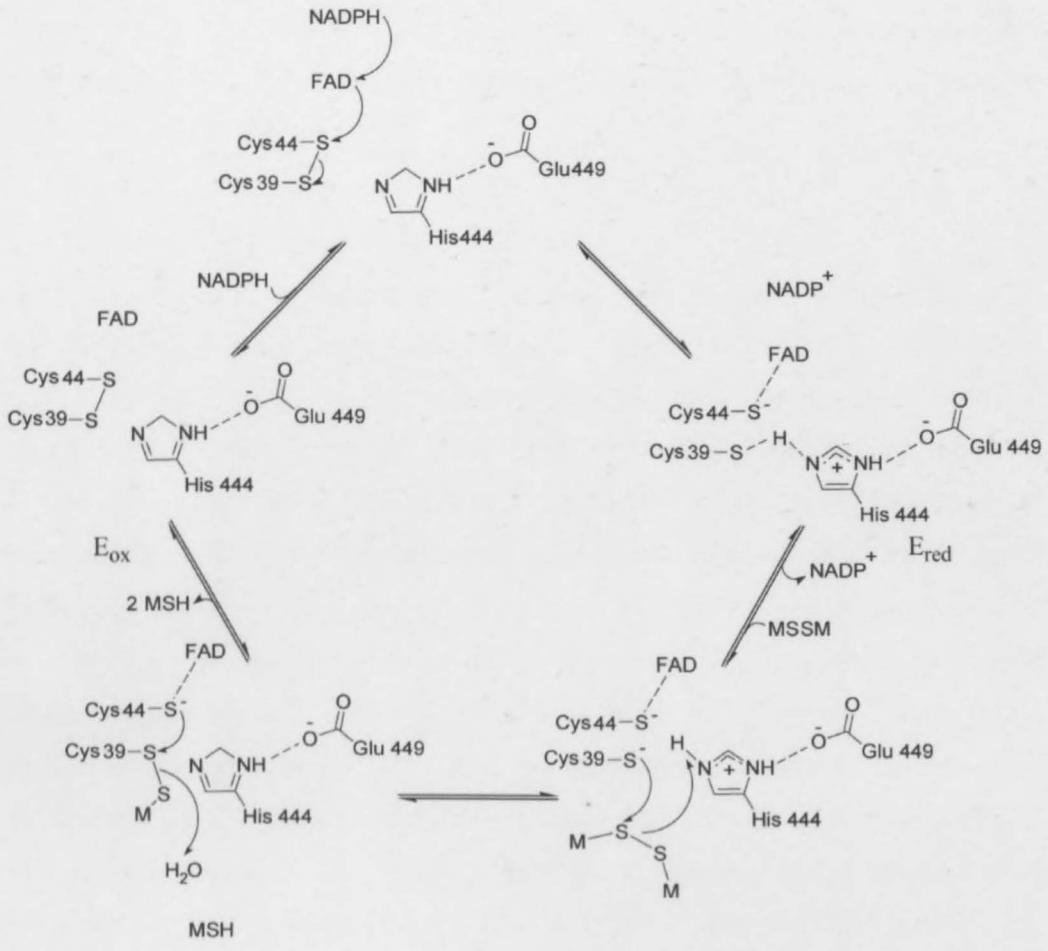

Scheme 1.1: Mtr reaction mechanism as proposed by Patel and Blanchard, 2001 (*19*).

The catalytic mechanism of MSH:MSSM redox shuttling was proposed by Patel and Blanchard (Scheme 1.1) (*19*). Because the Mtr crystal structure coordinates have not yet been determined, the authors relied on pH dependent kinetic studies, the primary sequence and the functional homology between flavoprotein disulfide reductases to deduce the proposed mechanism. They proposed that after the binding of NADPH and subsequent hydride transfer to the bound FAD, electron transfer to the active site follows. The two electron reduced enzyme is stabilized by the protonated His444, which shares a proton with Cys39. After the binding of MSSM, the Cys39 thiolate reacts with the MSSM disulfide. A substrate-enzyme mixed disulfide is formed with the release of the first MSH product. In the final step, an enzymic disulfide is formed with the release of the second MSH product. The authors proposed this mechanism after numerous pH dependent kinetic studies.

The essentiality of Mtr was shown through the application of antisense *mtr* oligonucleotides, which resulted in a 66% reduction of growth in *M. tuberculosis* over a seven day period (*20*).

1.2.3 Storage of cysteine and αGlcN-Ins

Bzymek *et al.* demonstrated during a study with MSH deficient *M. smegmatis* cells, that MSH also serves as a stockpile of available cysteine and αGlcN-Ins. Cells most likely make use of this reserve in times of stress (*11*). The key enzyme in the catabolism of MSH is Mca which cleaves the MSH molecule to produce GlcN-Ins and AcCys. The specific steps of the αGlcN-Ins catabolism have not yet been determined, but the authors postulate that αGlcN is converted to pyruvate via the glycolytic pathway. It was also shown that *myo*-inositol can serve as the only carbon source for *M. smegmatis*, proving that this moiety is also catabolized to produce energy and biosynthetic precursors. AcCys is ultimately converted to pyruvate through the activity of cysteine desulfhydrase, an activity which was shown to be present in the *M. smegmatis* extracts. Before the desulfhydrase reaction can take place, AcCys has to be deacetylated to form Cys, through the activity of a deacetylase enzyme. The genes encoding for the two enzymes necessary for AcCys catabolism still needs to be identified.

1.3 Mycothiol biosynthesis

Mycothiol is produced in a four step biosynthetic pathway (Scheme 1.2). MshA catalyzes the first step in which *N*-acetylglucosamine (αGlcNAc) from UDP-αGlcNAc is transferred to *myo*-inositol, producing αGlcNAc-Ins. αGlcNAc-Ins is deacetylated by MshB to form αGlcN-Ins and thereafter αGlcN-Ins is ligated to L-cysteine. This ligation reaction is ATP-dependent and is catalyzed by MshC, forming Cys-αGlcN-Ins. In the final step of this pathway MshD transfers an acetyl group from acetyl-CoA to Cys-αGlcN-Ins to produce mycothiol.

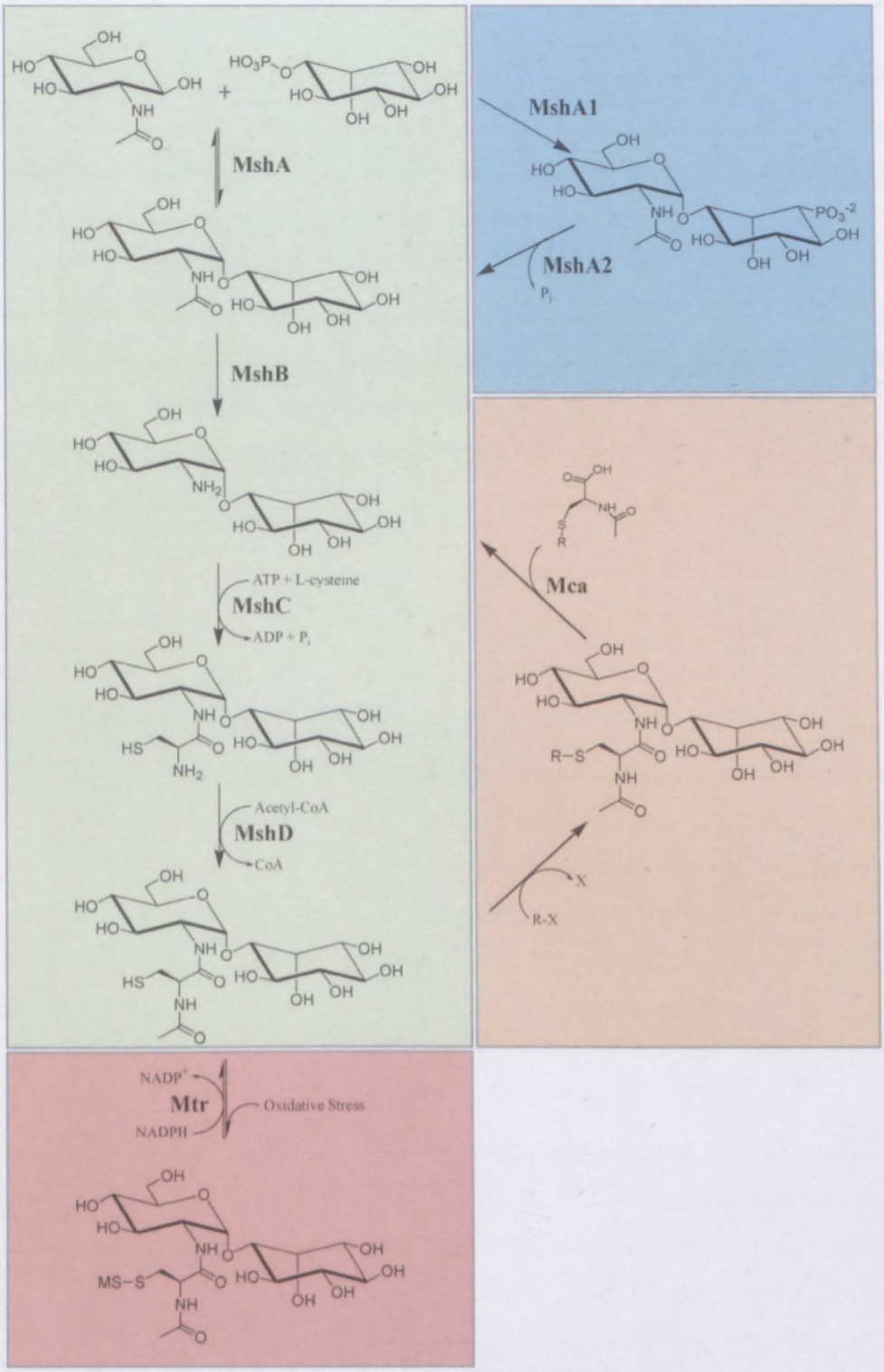

Scheme 1.2: Biosynthesis and reactions of mycothiol.

1.3.1 MshA

MshA belongs to the glycosyltransferase family 4 as shown by the CAZy database (*21*). This family of glycosyltransferases which includes sucrose synthetase, mannosyl transferase and αGlcNAc transferase, has two highly conserved motifs present in the glycosyl transferase domains (*23*). These motifs were also found to be conserved in MshA. In the *M. smegmatis* mutant of MshA, a glycine in the first conserved motif was changed to an asparagine, which resulted in a complete loss of αGlcNAc-Ins synthesis. This demonstrated that the first conserved motif is important for the activity of MshA. The second conserved motif containes the Glu-X_7-Glu signature sequence found in all family 4 glycosyltransferases. The homology of MshA with the family 4 glycosyltransferases enzymes is proof that the glycosyltransferase is necessary for the biosynthesis of αGlcNAc-Ins (*22*).

The gene encoding MshA, *Rv0486* or *mshA*, was identified by Newton *et al.* while studying mycothiol deficient *M. smegmatis* mutants (*22*). Later studies of MshA indicated that the enzyme is essential for the growth of *M. tuberculosis* (*24*). Its essentiality was determined with targeted gene disruption studies. It is also postulated that a second MshA enzyme, MshA2, might exist. These two enzymes, MshA and MshA2, together would be responsible for the synthesis of αGlcNAc-Ins (Scheme 1.2, blue square). Thus, MshA catalyze the transfer of UDP-αGlcNAc to 1L-Ins-1-P, to form GlcNAc-(α1,3)-1L-Ins-1-P which is subsequently dephosphorylated by MshA2 to produce αGlcNAc-Ins. The enzyme MshA2 is yet to be identified.

1.3.2 MshB

MshB is homologous to the mycothiol-dependent detoxification enzyme mycothiol conjugate amidase (Mca) and was identified as the first committed enzymatic step involved in the mycothiol biosynthesis (*25*). Results obtained from the study of MshB showed that it has a high specificity for GlcNAc-Ins and it does not show the large spectrum of deacetylase or amidase activity relative to its homolog, Mca. It was found that there is almost 10× more GlcNAc-Ins than GlcN-Ins present inside the cell. This suggests that MshB could be the control point in the mycothiol biosynthesis pathway and that large quantities of mycothiol could be produced on demand through the deacetylation of the reservoir of GlcNAc-Ins.

In subsequent MshB disruption studies it was confirmed that MshB is responsible for the deacetylation of GlcNAc-Ins and thus the synthesis of mycothiol (*26*). It was also discovered that although a *mshB* deficient strain of *M. smegmatis* produced lesser amounts of mycothiol than the non-mutant strain, the production of mycothiol did not stop altogether. It was suggested that the basal levels of mycothiol present in the mutant strain could be contributed to the activity of Mca, but overexpression of Mca in the mutant strain did not increase the amount of mycothiol. This also showed that MshB is not essential for *M. tuberculosis* growth.

Maynes *et al.* first solved the crystal structure of MshB and also proposed a catalytic mechanism for the deacetylation activity, which was later confirmed by another study (*27, 28*). The deacetylation follows the well known general acid-base catalysis (GABC) mechanism. The crystal structure of MshB, first solved by Maynes *et al.* in 2003 (*27*), supported this general mechanism. MshB is a metalloprotein that is dependant on a Zn^{2+} ion for its deacetylase activity. The metal ion is pentavalent coordinated with the His13, Asp16, His147 residues of MshB as well as two water molecules.

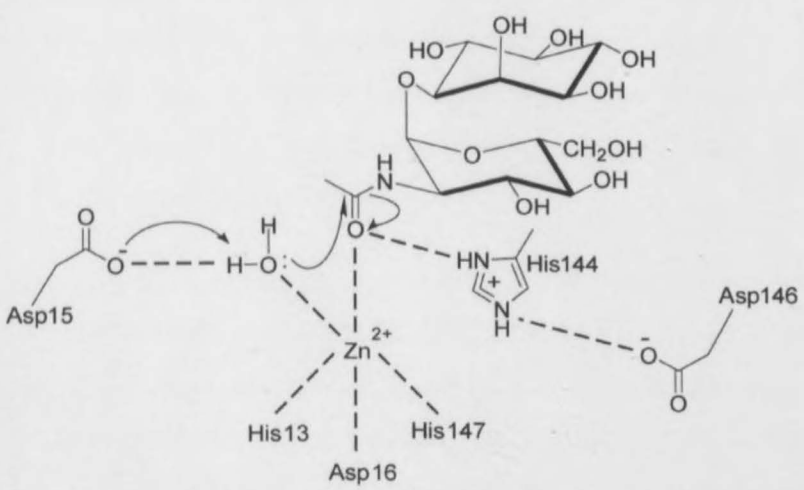

Scheme 1.3: Catalytic mechanism for MshB as proposed by Maynes *et al.*(*27*)

The proposed catalytic mechanism for MshB is shown in Scheme 1.3. As α-GlcNAc-Ins bind to MshB the one water molecule coordinated with the Zn^{2+} ion is replaced by the carbonyl oxygen of the acetyl group (*27*), leaving the second water molecule in a good position for a nucleophilic attack on the carbonyl carbon of the acetyl group. The nucleophilic attack is assisted by the base carboxylate of Asp15. A transition state

where the negatively charged oxygen is stabilized by the Zn^{2+} ion and imidazolium of His144 has been proposed. In the last step of the deacetylation, proton transfer to the nitrogen of α-GlcN-Ins is mediated through the acid function of Asp15. The reported crystal structure architecture and function were later confirmed by another study by McCarthy *et al.*, 2004 (*28*).

1.3.3 MshC

MshC is encoded for by the gene *Rv2130c* or *mshC*. This gene was previously named *cysS2* because it was thought that the gene encodes for a second copy of the cysteinyl-tRNA synthetase in the *M. tuberculosis* genome. The true identity of *cysS2* was discovered in a study where an enzyme showing MshC activity was purified from *M. smegmatis* cell lysate (*29*). In a homology search of the N-terminal sequence of this enzyme against the *M. tuberculosis* genome, *cysS2* was the only significant sequence found with a 80% homology for a 20 amino acid N-terminal sequence. These findings were confirmed when *cysS2* was cloned and expressed to produce an enzyme with MshC activity. Although MshC is not a cysteinyl-tRNA synthetase, MshC and CysS share a couple structural similarities. Both MshC and CysS have the HIGH and KMSKS motifs conserved in all class I aminoacyl-tRNA synthetases. Although the obvious relationship between these two enzymes, the *M. smegmatis* MshC enzyme was found to be active in di- and tetrameric states under different physiological conditions. CysS is normally active as a monomer.

The ligation of cysteine to αGlcN-Ins can be divided into two half reactions (Scheme 1.4) (*30*). In the first half (**a**) of the reaction ATP first binds to MshC followed by cysteine (Cys), forming an MshC-ATP-Cys complex. MshC releases a pyrophosphate molecule upon formation of the cysteine-adenylate compound which is still bound to the active site. In the second half (**b**) of the reaction αGlcN-Ins bind to MshC and the amide bond between αGlcN-Ins and Cys is formed with the cleavage of the adenylate anhydride, resulting in Cys-αGlcN-Ins and AMP. The order in which Cys-αGlcN-Ins and AMP is released from the active site is yet unknown, but if considering the catalytic mechanism of CysS it is postulated that Cys-αGlcN-Ins is released prior to AMP.

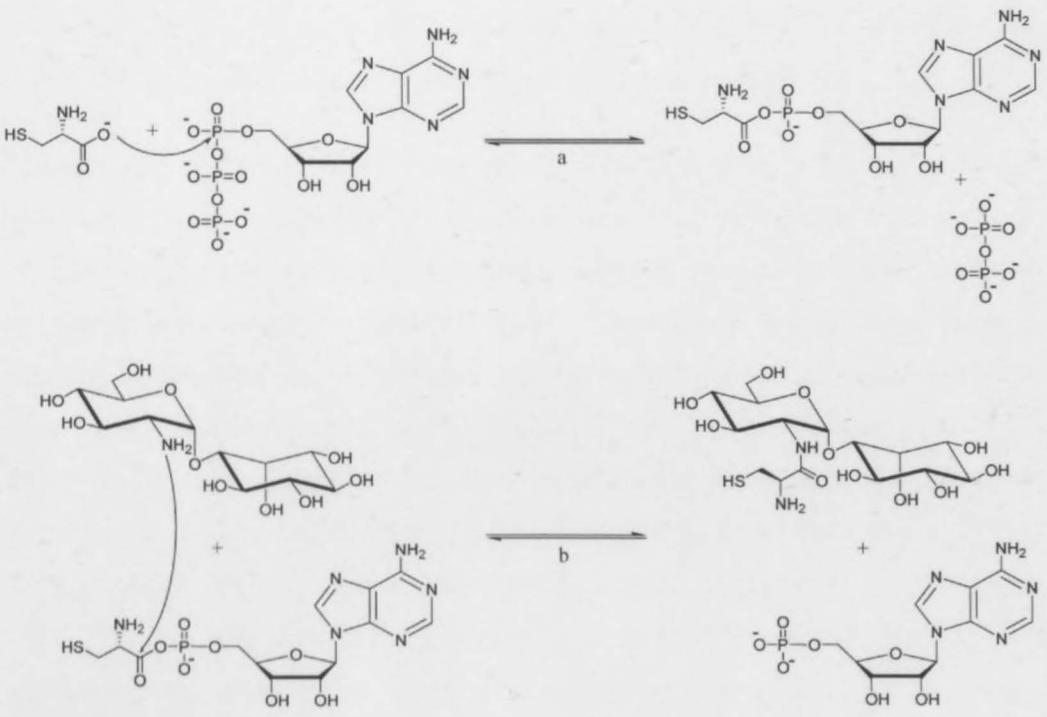

Scheme 1.4: Proposed mechanism for the cysteine transfer to GlcN-Ins by MshC.

1.3.4 MshD

MshD belongs to the GCN5-related *N*-acetyltransferases (GNAT), which catalyzes the transfer of the acetyl-CoA (AcCoA) acetyl group to a free amine. The gene encoding for MshD, *Rv0819* or *mshD*, was also identified while studying MSH deficient *M. smegmatis* mutants (*31*). MshD's sequence is twice the length of the characteristic GNAT protein, because it consists of two tandem-repeated GNAT domains on the N- and C-terminals. Of the two domains, the C-terminal domain has a higher similarity with other GNAT proteins, suggesting that this domain is involved with AcCoA binding. In a later study it was determined that both domains bind acetyl-CoA (*32*), although the binding sites are different. The C-terminal domain's active site is very similar to that of other GNAT proteins. AcCoA bind to this domain in such a way, that the acetyl group is presented in the open active site. The active site is a solvent exposed groove between the N- and C-terminal domains. AcCoA bind to the N-terminal domain so that the acetyl group is buried and not positioned for acetyl transfer. These findings are all based on the crystal structure of MshD, which was

determined in the presence of AcCoA and coenzyme A (CoA). This was also the first crystal structure solved for a mycothiol biosynthesis pathway enzyme.

The structure of the MshD-AcCoA complex showed that the active site groove is much larger than required for Cys-αGlcN-Ins substrate binding (*32*). Further crystal structure studies performed with the bound substrate showed that MshD undergo conformational changes in which the two GNAT domains are brought closer together, resulting in new interactions between the domains (*33*). Several of these interactions are mediated by the bound substrate. The size of the groove is reduced to a narrow tunnel, thereby promoting catalysis. In the smaller active site the substrate free amine is positioned close and in the correct orientation towards the acetyl group of AcCoA for nucleophilic addition of the amine on the carbonyl of the acetyl group (Scheme 1.5). Glu234 acts as a general base through interactions with a water molecule, and accepts a proton from the free amine of Cys-GlcN-Ins. The AcCoA acetyl group is kept in position through hydrogen bonding with the amide backbone of Leu238. This interaction would also stabilize the tetrahedral intermediate. After acetyl transfer the sulfhydryl of CoA is protonated by the Tyr294 residue. This proposed catalytic mechanism is common in many GNAT enzymes.

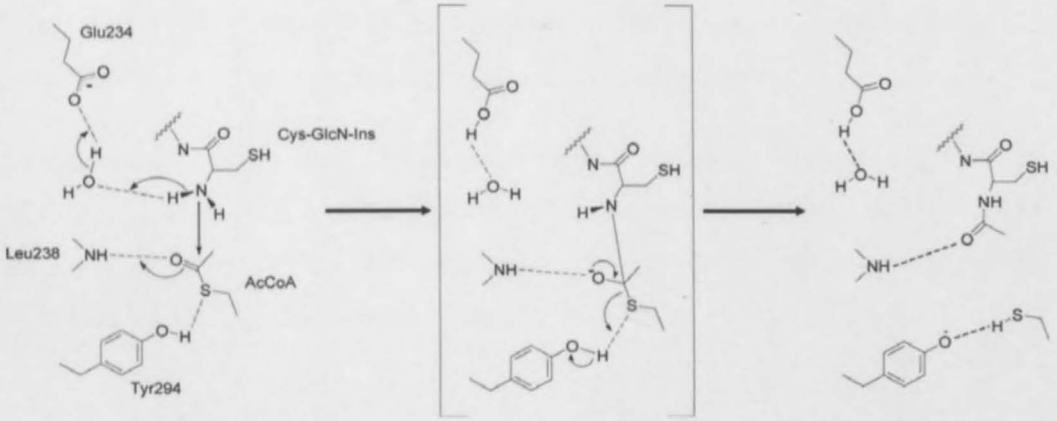

Scheme 1.5: Proposed catalytic mechanism for MshD

This crystal structure study also revealed that AcCoA is presently bound to the N-terminal domain and does not exchange with the solvent. This means that the cofactor was incorporated during protein folding and it is postulated that the AcCoA structure

helps with protein stability. This feature is unique to MshD and is not seen in other GNAT enzymes (*33*).

1.4 Drug targets and evaluation methods

Mycothiol performs critical functions within the mycobacterial cell and it is clear that the enzymes involved in the MSH metabolism are potential drug targets against *M. tuberculosis*. The biosynthetic enzymes appear to be the most attractive targets, with most of the enzymes essential for the survival of *M. tuberculosis*. MshA, MshC and MshD are required for the production of MSH and consequently, the inactivation of their genes is lethal and severely limits the survival of *M. tuberculosis*. Inactivation of *mshB* reduces the production of MSH and through the Mca production of GlcN-Ins, the cell is still able to synthesize MSH and survive. Furthermore, Mca deficient *M. smegmatis* mutants are more susceptible to antibiotics and the inactivation of Mtr reduces the growth of *M. tuberculosis*.

Thus far, most of the efforts involving inhibitor design against the abovementioned enzymes have gone towards designing inhibitors and substrate analogues against Mca. These will be fully discussed in Chapter 4. Also, the homology between Mca and MshB suggests that some mycothiol-related molecules may show activity with both enzymes. However, this has only been shown to be the case for a limited number of compounds, and others should thus be tested in a similar fashion.

Lastly, current assay methods employed for the screening of inhibitors and substrate analogues against Mca and MshB all involve derivatisation techniques followed by HLPC-UV analysis. These techniques seriously restrain the efficiency of inhibitor screening and will be discussed in Chapter 3.

1.5 Conclusion

With the emergence of MDR- and XDR-TB, tuberculosis has become an ever greater health problem worldwide, especially in developing countries. The need for faster development of new drug candidates against TB is therefore also growing. In our study we aimed to improve the efficiency by which potential new drugs can be screened for activity against existing targets in the mycothiol pathway and any other

mycothiol dependent processes. For the successful development of a drug discovery protocol and the improvement of existing assay methods a few basic tools are needed. They are: key enzymes, better analytical methods and easily accessible substrates or substrate analogues. In this study we aim to work toward a drug discovery protocol (Scheme 1.6) for the development of inhibitors or substrate analogues against abovementioned enzymes. We intend to use MshB's substrate specificity, as a primary screen for scaffolds that display binding modes similar to its natural substrate, αGlcNAc-Ins. Enzyme kinetic data along with computational molecular modeling will be used as a guide to build inhibitor libraries for all downstream enzymes in the MSH pathway, in particular Mtr. Hence, compounds that show adequate activity with MshB would be further derivatised to serve as either substrate analogues or inhibitors for Mtr, as well as the other MSH pathway enzymes. Compounds that show encouraging activity with MshB will be subjected to further modification in order to optimize binding with MshB.

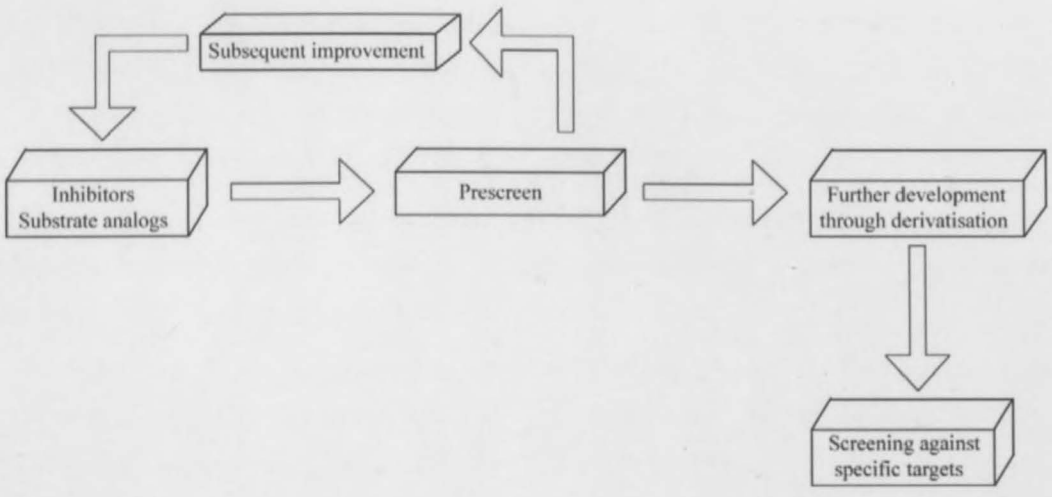

Scheme 1.6: Proposed drug discovery protocol.

In Chapter 2 we will report the expression and purification of the enzymes crucial to this study. The recombinant expression of Mtr in *E. coli* was for the first time successfully performed during this study. Furthermore, we will discuss the development of a HPLC-ESI/MS(TOF) method for the quantitation of mycothiol pathway intermediates in Chapter 3. The synthesis of substrate analogues against the expressed enzymes and their evaluation will be discussed in Chapters 4 and 5 respectively.

1.6 References

(1) Flynn, J. L., and Chan, J. (2001) Immunology of tuberculosis. *Annual Review of Immunology 19*, 93-129.

(2) World Health Organisation (WHO) -

http://www.who.int/tb/challenges/xdr/en/index.html

http://www.who.int/tb/dots/dotsplus/faq/en/index.html

(Last accessed: 29 December 2007).

(3) Global tuberculosis control: surveillance, planning, financing. WHO report 2007, World Health Organisation (WHO/HTM/TB/2007.376).

(4) Joshi, J. M., and Gothi, D. (2006) Multi-drug resistant pulmonary tuberculosis. *Current Respiratory Medicine Reviews 2*, 53-57.

(5) Raviglione, M. C., and Smith, I. M. (2007) XDR tuberculosis - implications for global public health. *New England Journal of Medicine 356*, 656-659.

(6) Newton, G. L., Arnold, K., Price, M. S., Sherrill, C., Delcardayre, S. B., Aharonowitz, Y., Cohen, G., Davies, J., Fahey, R. C., and Davis, C. (1996) Distribution of thiols in microorganisms: mycothiol is a major thiol in most actinomycetes. *Journal of Bacteriology 178*, 1990-1995.

(7) Newton, G. L., Av-Gay, Y., and Fahey, R. C. (2000) A novel mycothiol-dependent detoxification pathway in mycobacteria involving mycothiol S-conjugate amidase. *Biochemistry 39*, 10739-10746.

(8) Patel, M. P., and Blanchard, J. S. (1998) Synthesis of Des-*myo*-Inositol Mycothiol and Demonstration of a Mycobacterial Specific Reductase Activity. *Journal of the American Chemical Society 120*, 11538-11539.

(9) Misset-Smits, M., van Ophem, P. W., Sakuda, S., and Duine, J. A. (1997) Mycothiol, 1-O-(2'-[N-acetyl-L-cysteinyl]amido-2'-deoxy-alpha-D-glucopyranosyl)-D-*myo*-inositol, is the factor of NAD/factor-dependent formaldehyde dehydrogenase. *FEBS letters 409*, 221-222.

(10) Norin, A., Van Ophem, P. W., Piersma, S. R., Persson, B., Duine, J. A., and Jornvall, H. (1997) Mycothiol-dependent formaldehyde dehydrogenase, a prokaryotic medium-chain dehydrogenase/reductase, phylogenetically links different eukaroytic alcohol dehydrogenases--primary structure, conformational modelling and functional correlations. *European journal of biochemistry / FEBS 248*, 282-289.

(11) Bzymek, K. P., Newton, G. L., Ta, P., and Fahey, R. C. (2007) Mycothiol import by *Mycobacterium smegmatis* and function as a resource for metabolic precursors and energy production. *Journal of Bacteriology 189*, 6796-6805.

(12) Bornemann, C., Jardine, M. A., Spies, H. S. C., and Steenkamp, D. J. (1997) Biosynthesis of mycothiol: elucidation of the sequence of steps in *Mycobacterium smegmatis*. *Biochemical Journal 325*, 623-629.

(13) Steffek, M., Newton, G. L., Av-Gay, Y., and Fahey, R. C. (2003) Characterization of *Mycobacterium tuberculosis* Mycothiol S-Conjugate Amidase. *Biochemistry 42*, 12067-12076.

(14) Metaferia, B. B., Ray, S., Smith, J. A., and Bewley, C. A. (2007) Design and synthesis of substrate-mimic inhibitors of mycothiol-S-conjugate amidase from *Mycobacterium tuberculosis*. *Bioorganic & Medicinal Chemistry Letters 17*, 444-447.

(15) Knapp, S., Amorelli, B., Darout, E., Ventocilla, C. C., Goldman, L. M., Huhn, R. A., and Minnihan, E. C. (2005) A family of mycothiol analogs. *Journal of Carbohydrate Chemistry 24*, 103-130.

(16) Rawat, M., Uppal, M., Newton, G., Steffek, M., Fahey, R. C., and Av-Gay, Y. (2004) Targeted mutagenesis of the *Mycobacterium smegmatis mca* gene, encoding a mycothiol-dependent detoxification protein. *Journal of Bacteriology 186*, 6050-6058.

(17) Dosanjh Nirpjit, S., Rawat, M., Chung, J.-H., and Av-Gay, Y. (2005) Thiol specific oxidative stress response in Mycobacteria. *FEMS microbiology letters 249*, 87-94.

(18) Patel, M. P., and Blanchard, J. S. (1999) Expression, Purification, and Characterization of *Mycobacterium tuberculosis* Mycothione Reductase. *Biochemistry 38*, 11827-11833.

(19) Patel, M. P., and Blanchard, J. S. (2001) *Mycobacterium tuberculosis* mycothione reductase: pH dependence of the kinetic parameters and kinetic isotope effects. *Biochemistry 40*, 5119-5126.

(20) Hayward, D., Wiid, I., and van Helden, P. (2004) Differential expression of mycothiol pathway genes: are they affected by antituberculosis drugs? *IUBMB life 56*, 131-138.

(21) Campbell, J. A., Davies, G. J., Bulone, V., and Henrissat, B. (1997) A classification of nucleotide-diphospho-sugar glycosyltransferases based on amino acid sequence similarities. *The Biochemical Journal 326*, 929-939.

(22) Newton, G. L., Koledin, T., Gorovitz, B., Rawat, M., Fahey, R. C., and Av-Gay, Y. (2003) The glycosyltransferase gene encoding the enzyme catalyzing the first step of mycothiol biosynthesis (*mshA*). *Journal of Bacteriology 185*, 3476-3479.

(23) Cumino, A., Curatti, L., Giarrocco, L., and Salerno, G. L. (2002) Sucrose metabolism: Anabaena sucrose-phosphate synthase and sucrose-phosphate phosphatase define minimal functional domains shuffled during evolution. *FEBS Letters 517*, 19-23.

(24) Buchmeier, N., and Fahey, R. C. (2006) The *mshA* gene encoding the glycosyltransferase of mycothiol biosynthesis is essential in *Mycobacterium tuberculosis* Erdman. *FEMS Microbiology Letters 264*, 74-79.

(25) Newton, G. L., Av-Gay, Y., and Fahey, R. C. (2000) N-acetyl-1-D-*myo*-inosityl-2-amino-2-deoxy-α-D-glucopyranoside deacetylase (MshB) is a key enzyme in mycothiol biosynthesis. *Journal of Bacteriology 182*, 6958-6963.

(26) Rawat, M., Kovacevic, S., Billman-Jacobe, H., and Av-Gay, Y. (2003) Inactivation of *mshB*, a key gene in the mycothiol biosynthesis pathway in *Mycobacterium smegmatis*. *Microbiology 149*, 1341-1349.

(27) Maynes, J. T., Garen, C., Cherney, M. M., Newton, G., Arad, D., Av-Gay, Y., Fahey, R. C., and James, M. N. G. (2003) The Crystal Structure of 1-D-*myo*-Inosityl 2-Acetamido-2-deoxy-α-D-glucopyranoside Deacetylase (MshB) from *Mycobacterium tuberculosis* Reveals a Zinc Hydrolase with a Lactate Dehydrogenase Fold. *Journal of Biological Chemistry 278*, 47166-47170.

(28) McCarthy, A. A., Peterson, N. A., Knijff, R., and Baker, E. N. (2004) Crystal Structure of MshB from *Mycobacterium tuberculosis*, a Deacetylase Involved in Mycothiol Biosynthesis. *Journal of Molecular Biology 335*, 1131-1141.

(29) Sareen, D., Steffek, M., Newton, G. L., and Fahey, R. C. (2002) ATP-dependent L-cysteine:1D-*myo*-inosityl 2-amino-2-deoxy-α-D-glucopyranoside ligase, mycothiol biosynthesis enzyme MshC, is related to class I cysteinyl-tRNA synthetases. *Biochemistry 41*, 6885-6890.

(30) Fan, F., Luxenburger, A., Painter, G. F., and Blanchard, J. S. (2007) Steady-State and Pre-steady-State Kinetic Analysis of *Mycobacterium smegmatis* Cysteine Ligase (MshC). *Biochemistry 46*, 11421-11429.

(31) Koledin, T., Newton, G. L., and Fahey, R. C. (2002) Identification of the mycothiol synthase gene (*mshD*) encoding the acetyltransferase producing mycothiol in actinomycetes. *Archives of Microbiology 178*, 331-337.

(32) Vetting, M. W., Roderick, S. L., Yu, M., and Blanchard, J. S. (2003) Crystal structure of mycothiol synthase (*Rv0819*) from *Mycobacterium tuberculosis* shows structural homology to the GNAT family of *N*-acetyltransferases. *Protein Science 12*, 1954-1959.

(33) Vetting Matthew, W., Yu, M., Rendle Phillip, M., and Blanchard John, S. (2006) The substrate-induced conformational change of *Mycobacterium tuberculosis* mycothiol synthase. *The Journal of Biological Chemistry 281*, 2795-2802.

Chapter 2

Cloning, expression and purification of *M. tuberculosis* mycothiol related enzymes

2.1 Introduction

As discussed in Chapter 1, MshB is the second enzyme in the mycothiol biosynthetic pathway (*1*). This enzyme catalyses the deacetylation of GlcNAc-Ins to produce GlcN-Ins, the second intermediate in the pathway. Mycothiol Disulfide Reductase (Mtr), is responsible for the reduction of the mycothiol disulfide (MSSM) to produce two equivalents mycothiol (MSH) (*2*). The gene sequences of both MshB and Mtr are known, these being *Rv1170* (*mshB*) and *Rv2855* (*mtr*) respectively. This makes it possible for these genes to be amplified from *M. tuberculosis* genomic DNA and cloned into expression plasmids for overexpression and subsequent purification. In this chapter we report the expression and purification of both the MshB and Mtr enzymes.

2.2 MshB

Previously MshB was cloned into and expressed using the pET22b(+) expression plasmid (*1, 3, 4*). This expression plasmid is part of the pET System (Novagen) of expression plasmids used to clone and express recombinant proteins in *E. coli*. When using pET22b(+), proteins are expressed connected to a C-terminal 6 x Histidine tag (His_6-tag). In this study MshB was cloned and expressed using pET28a(+), which is also part of the pET System. With pET28a(+) one has the option of expressing the recombinant protein with a C- or N-terminal His-tag. MshB was previously expressed with a C-terminal His-tag.

2.2.1 *Cloning and expression*

The *Rv1170* or *mshB* gene was amplified from genomic *M. tuberculosis* H37Rv DNA. During amplification an N-terminal NcoI-site and a C-terminal XhoI-site was introduced, which made it possible for the PCR product to be cloned into pET28a(+) (Novagen pET expression system) in such a way that MshB would be expressed with a C-terminal 6 x histidine tag (His-tag). The His-tag has a high affinity and binds to Ni^{2+} ions, which makes the purification of the protein possible through immobilized metal affinity chromatography (IMAC). The formation of the pET28a(+)-*mshB* expression plasmid was verified through digestion screening.

Expression trails were conducted to find the correct combination of expression parameters for soluble expression. These parameters are: the concentration of isopropyl-β-D-thiogalactoside (IPTG) used to induce expression, the temperature at which expression cultures were incubated after induction and the time allowed for expression to continue. The expression trails were performed in *E. coli* BL21*(DE3). The expected results were achieved after the expression was left overnight at 22°C and more specifically at an IPTG concentration of 0.1mM (Figure 2.1).

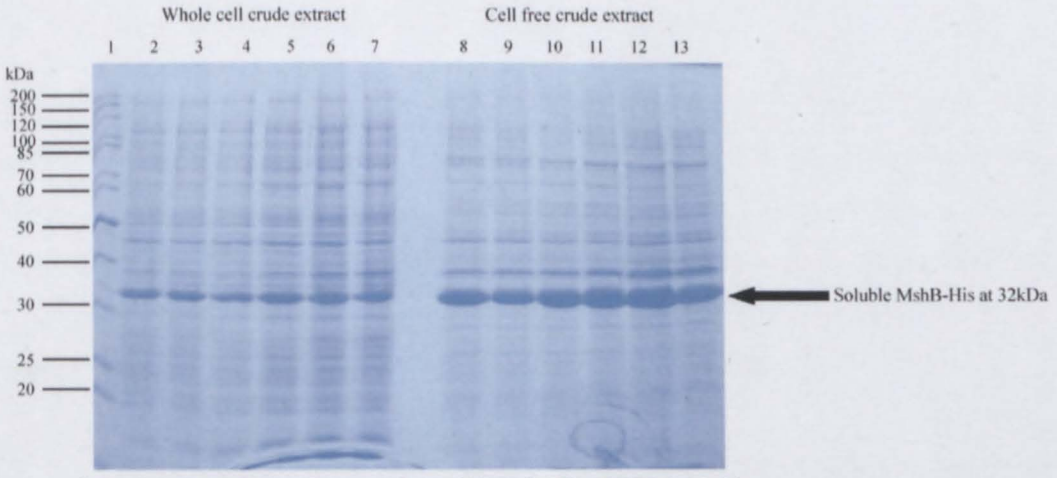

1. PageRuler Protein Ladder (Fermentas) **2.** 1.0mM IPTG **3.** 0.75mM IPTG **4.** 0.5mM IPTG **5.** 0.2mM IPTG **6.** 0.1mM IPTG **7.** 0.05mM IPTG **8.** 1.0mM IPTG **9.** 0.75mM IPTG **10.** 0.5mM IPTG **11.** 0.2mM IPTG **12.** 0.1mM IPTG **13.** 0.05mM IPTG

Figure 2.1: Expression trail of pET28a(+)-mshB at 22°C, overnight and different IPTG concentrations (as indicated).

2.2.2 Purification of MshB

The expression conditions discovered above were used in a large scale expression (see 2.5.4.2) of MshB-His. The purification from bacterial lysate was performed using the automated ÄKTA*prime*-system with a 1ml HisTrap FF column (Amersham Bioscience). The HisTrap FF column is Ni-NTA-based and thus preloaded with Ni^{2+} ions. The program used to purify the protein was an automated gradient run. Before the protein was loaded onto the column, the column was equilibrated with 10 column volumes of H_2O and 5 column volumes of binding buffer (20mM Tris-HCl, 5mM imidazole, 500mM NaCl, pH 7). After protein loading a wash step with 10 column volumes binding buffer followed before another 5 column volumes wash step in which the elution buffer (20mM Tris-HCl, 500mM NaCl, 50mM imidazole, pH 7.9) concentration was increased to 15%. This second wash step was necessary to elute any nonspecifically bound proteins. The MshB-His protein was eluted by increasing the concentration elution buffer to 100% over 10 column volumes. A flow rate of 1ml/min was maintained over the run and protein elution was monitored at 280nm. The protein concentration was determined with a Bradford assay to be 4.5mg/ml.

2.3 Mycothiol Disulfide Reductase (Mtr)

Mtr was previously cloned into and expressed from the mycobacterial expression plasmid, pMV261. *M. smegmatis* was used as expression host (*2, 5, 6*). During this study various methods of cloning and expression were used in an attempt to solubly express Mtr in *E. coli* as expression host. The pET28a(+) expression plasmid was used to expressed Mtr with a C- and N-terminal His-tag. The Gateway® expression system was used to express Mtr with different fusion protein tags.

2.3.1 Cloning and Expression of Mycothiol Disulfide Reductase with a N-terminal His-tag

The *mtr* gene was amplified from *M. tuberculosis* H37Rv genomic DNA. An N-terminal NdeI-site and a C-terminal XhoI-site were introduced, which was used to clone the PCR product into pET28a(+) (Novagen pET expression system). Using the NdeI and XhoI sites ensures that Mtr will be expressed with an N-terminal 6 x histidine tag (His-tag) for purification through IMAC. The pET28a(+)-*mtr* construct

was verified with restriction enzyme analysis and sequencing. *E. coli* BL21(DE3) was used as expression host. The first expression trails were performed in the same manner as for MshB-His, but no soluble His-Mtr was obtained (Figure 2.2).

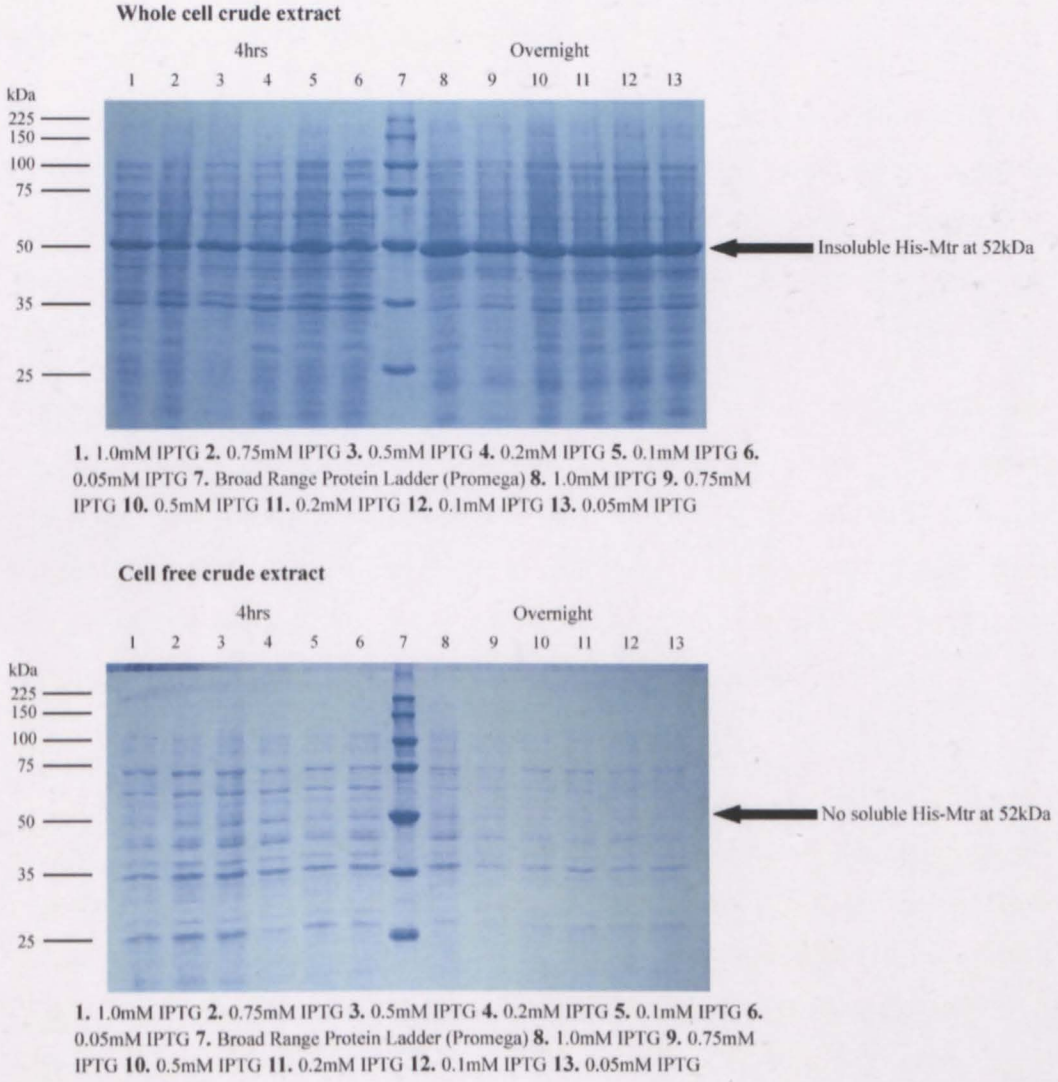

Figure 2.2: First pET28(+)-*mtr* expression trail performed at 22ºC, 4h and overnight, and at different IPTG concentrations (noted in the figure)

2.3.2 Other attempts at soluble expression and purification of His-Mtr

2.3.2.1 Addition of Ethanol and Gly-Gly

It has been demonstrated that the addition of ethanol and gly-gly could help improve the solubility of otherwise insoluble proteins (*7, 8*). *E. coli* Bl21(DE3) cells

containing the pET28a(+)-*mtr* construct was induced to express His-Mtr in the presence of 0.5%, 1.0% and 1.5% ethanol and 1.0M gly-gly, which was added to the growth media. Unfortunately, no soluble His-Mtr was obtained.

2.3.2.2 Co-expression with pRARE plasmids

The pRARE 2 plasmid encodes for tRNAs of scarce codons. Scarce codons are the codons whose tRNA's is not usually used by *E. coli* for the translation of its native RNA to protein. It has been shown that the introduction of the tRNAs of these scarce codons (AUA, AGG, AGA, CUA, CCA, GGA and CGG) improve the translation efficiency, which lead to soluble recombinant protein (*9*).

In the translation of the *mtr* gene 25 scarce codons (3AUA, 1AGG, 4CUA, 6GGA and 11CGG) are used (Graphical Codon Usage Analyser, http://gmmmcua.schoedl.de/sequential_v2.html). In order to provide the tRNAs of these scarce codons, the pET28a(+)-*mtr* plasmid was co-expressed with the pRARE2 plasmid that expresses the tRNAs of all seven scarce codons mentioned here. However, the co-expression did not solve the insolubility problem.

2.3.2.3 Co-expression with Chaperone Plasmids

In another attempt to solublilize His-Mtr the pET28a(+)-*mtr* plasmid was co-expressed with a series of five chaperone plasmids (Takara Bio Inc.). Each of these chaperone plasmids encodes for a different "team" of molecular chaperone proteins (Table 2.1), which was shown to improve the solubility of recombinant proteins (*10, 11*).

Table 2.1: Takara Chaperone Plasmid sets

Plasmid	Chaperons	Promoter	Inducer	Resistance
pG-KJE8	dnaK-dnaJ-grpE-groES-groEL	*araB* and Pzt1	L-arabinose Tetracycline	Cloramphenicol
pGro7	groES-groEL	*araB*	L-arabinose	Cloramphenicol
pKJE7	dnaK-dnaJ-grpE	*araB*	L-arabinose	Cloramphenicol
pG-Tf2	groES-groEL-tig	Pzt1	Tetracycline	Cloramphenicol
pTf16	tig	*araB*	L-arabinose	Cloramphenicol

Molecular chaperone proteins prevent the aggregation of insoluble proteins, called inclusion bodies, by assisting them to fold correctly into their tertiary structure (*12*). This plasmid set uses six different chaperones and co-chaperones in different combinations. Trigger factor or tig is a 50kDa *E. coli* protein that was shown to have Peptidyl-prolyl *cis/trans* isomerase (PPIase) activity and was found to be associated with the 50S ribosome subunit (*13, 14*). These PPIases catalyzes the *cis-trans* isomerization of proline imidic bonds in newly synthesized peptides, thus helping with protein folding (*15*). DnaK belongs to the Hsp70 family of heat shock proteins. All the members of this family have two domains, a C-terminal peptide binding and N-terminal ATPase domain (*16*). GrpE and DnaJ are two co-chaperones that are essential for DnaK activity. While GrpE promotes nucleotide exchange by DnaK, DnaJ helps with the binding of DnaK to the target polypeptides (*16, 17*). GroES is a type I chaperone which also helps with protein refolding in conjunction with a co-chaperone like GroEL. During the ATP dependent protein folding mechanism the target protein is enclosed in the GroES ring structure by GroEL, after which it is released to the cytosol (*16, 18*).

The co-expression of pET28a(+)-*mtr* with the five different chaperone plasmids was performed at 37°C and 30°C for 4h respectively. The expression of Mtr was induced with a final IPTG concentration of 0.5mM (Figure 2.3). The expression of the chaperons was induced with each respective plasmid's corresponding inducer (Table 2.1).

Initial analysis suggested that soluble expression of His-Mtr was achieved by co-expression with of the pTf16 plasmid. Attempts at verifying these results through a large scale expression and purification failed as no significant amounts of purified protein was obtained. The flow through, wash and elution fractions were analyzed on a 12% SDS-PAGE gel, which showed no significant protein bands at 52kDa. It was hereby concluded that His-Mtr was not soluble. The trigger factor has a molecular weight of 50kDa and if overexpressed to the extent that it can be visualized on a SDS-PAGE gel, it could explain the bands mistaken for soluble His-Mtr.

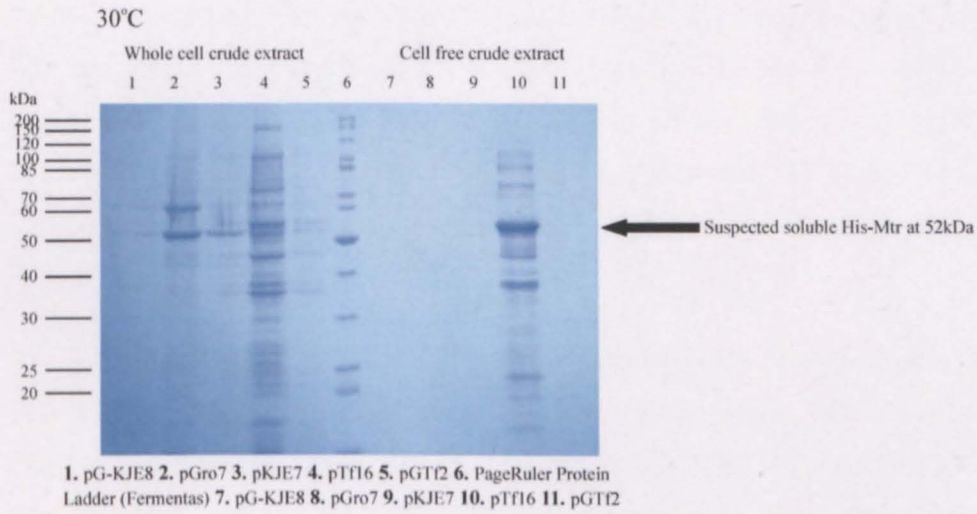

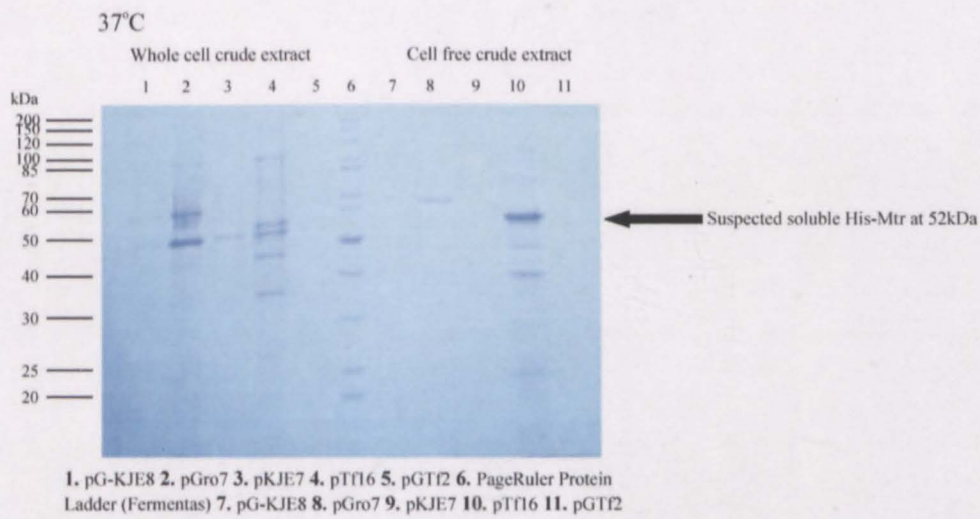

Figure 2.3: Expression trails where pET28a(+)-mtr was co-expressed with the different chaperone plasmids. The trails were conducted at 30°C and 37°C respectively; expression was induced with 0.5mM IPTG and allowed to continue for 4h.

2.3.2.4 Attempted Solublisation with Emulgen®

Emulgen® is used in the purification of cyctochrome P450 enzymes from yeast (*19*) or animal liver cell microsomes (*20*). We used Emulgen® 913 (Kao Corporation) as described by Hara *et al.* (*19*) in an attempt to solubilise His-Mtr from the whole cell fractions. However, no soluble protein was obtained (data not shown).

2.3.3 Cloning and expression of Mtr with fusion protein tags

Another method by which insoluble recombinant proteins could be solubilised is by means of expressing the target protein connected to a fusion protein tag (*21*). During this study we used the Gateway® Expression System (Invitrogen) which allows you to create a wide range of expression plasmids, all with different fusion protein tags. The target gene is cloned into an entry plasmid, which is then used in a gene transfer (LR) reaction with different destination plasmids (containing the fusion protein tags), creating a series of expression plasmids.

The *mtr* was cloned into two different entry plasmids, pENTR4N and pENTR4NT. The pENTR4N-*mtr* constructs were used in LR reactions with five different destination plasmids: pDEST15, pDEST532, pDEST544, pDEST566 and pET160DEST (Table 2.2). The resulting expression vectors were verified by restriction enzyme analysis with the Bsp14071 enzyme.

Table 2.2: Gateway destination plasmids used and their corresponding expression plasmids

Destination Plasmid	Fusion tag	Expression Plasmid	Inducer	Recombinant Protein Size
pDEST15	GST	pEXP15-*mtr*	IPTG	76kDa
pDEST532	His-GB1	pEXP532-*mtr*	IPTG	57kDa
pDEST544	His-NusA	pEXP544-*mtr*	IPTG	104kDa
pDEST566	His-MBP	pEXP566-*mtr*	IPTG	94kDa
pET160DEST	His	pET160EXP-*mtr*	IPTG	52kDa

2.3.3.1 Expression attempts

Expression trails were performed with pEXP544-*mtr*, pEXP15-*mtr* and pEXP566-*mtr*. The trail with pEXP544-*mtr* and pEXP15-*mtr* did not produce soluble expression of the fusion-tag Mtr proteins. In the trails with pEXP566-*mtr* it seemed like the His-MBP (Maltose binding protein) tagged Mtr protein was expressed soluble (Figure 2.4).

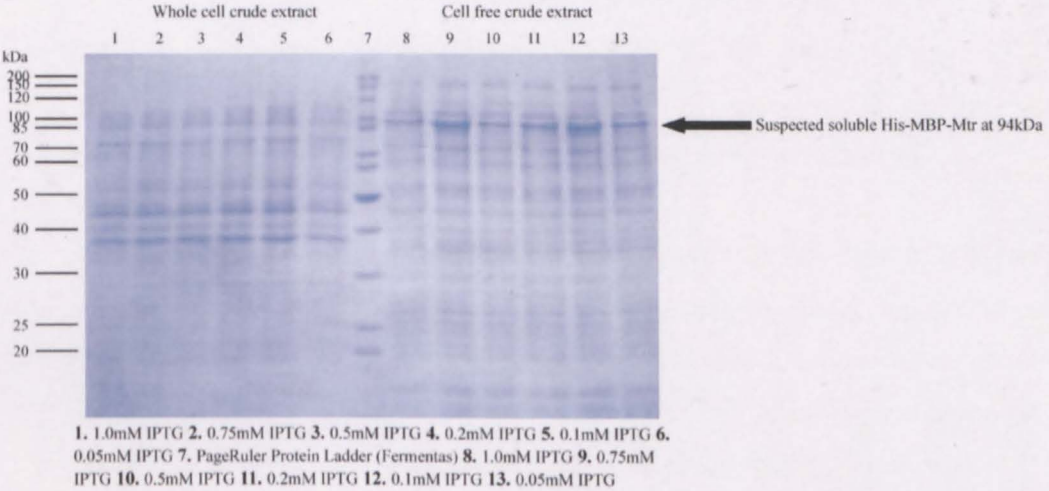

Figure 2.4: pEXP566-*mtr* expression trail performed at 37°C, 3h and different IPTG concentrations (as indicated).

A large scale expression and purification, with the ÄKTA*prime*-system, of the His-MBP-Mtr fusion protein was attempted. Expression was induced with a final IPTG concentration of 0.75mM. Subsequently, the expression was allowed to continue for 3h at 37°C. A very small elution peak was obtained during the purification. The elution fractions were analyzed on a 12% SDS-PAGE gel. The same 94kDa band (as shown in Figure 2.4) was present in addition to a large amount of other proteins which eluted in the same fractions.

Another expression trail was performed to investigate if the time allowed for expression after induction had an influence on the amount of His-MBP-Mtr present in the cell free extracts. The trail was performed at 37°C with a final IPTG concentration of 0.75mM. Expression was allowed to continue for 3, 5, 7 and 16h (overnight) respectively. The best protein expressions were obtained at 3 and 5h. Another large

scale expression and purification was attempted whereby 5h were allowed for induction. The results were similar to those described above.

It was then decided to co-express His-MBP-Mtr with the chaperone plasmids, to investigate if it would improve the amount of soluble protein expression. After numerous attempts to transform competent *E. coli* Bl21(DE3) containing pEXP566-*mtr* with the chaperone plasmids (Table 2.1), only pG-Tf2, pG-KTE8 and pGro7 could be successfully transformed. Expressions were performed as described in 2.3.2.3. Unfortunately there was no improvement in the amount of protein expressed.

2.3.4 Mtr expression with a C-terminal His-tag and subsequent purification

All pervious attempts to express soluble Mtr with N-terminal tags have failed, thus soluble expression was attempted with a C-terminal His-tag using pET28a(+) as expression plasmid. A new set of PCR primers were designed that introduce an N-terminal NcoI-site and a C-terminal XhoI-site during the PCR amplification of the *mtr* gene. Thus, when cloned into pET28(+)a, Mtr would now be expressed with a C-terminal His-tag. The pET28a(+)-*mtr*CT expression plasmid was verified through digestion screening. Expression trails were conducted at 37°C and 22°C, overnight and at different IPTG concentrations as indicated in Figure 2.5. Soluble Mtr-His expression was seen in both expression trails.

The 0.1mM and 0.05mM cell free extracts of the 22°C expression trail was purified using a His SpinTrap® (GE Healthcare) and analyzed on a 12% SDS-PAGE gel, in which soluble Mtr-His was seen as a faint band at 52kDa (data not shown). A relatively large scale expression was performed at 22°C for 16h, using a final IPTG concentration of 0.1mM, followed by purification on the ÄKTA*prime*-system, using a 1ml HiTrap® Chelating HP column (Amersham Bioscience). This column is Ni^{2+}-IDA based which requires the loading of Ni^{2+} onto the column as part of the ÄKTA*prime* automated program.

A self-programmed gradient run, with a flow rate of 1ml/min, was used to purify Mtr-His. After the column was equilibrated with 5 column volumes of H_2O, Ni^{2+} was loaded onto the column by washing it with 5 column volumes of a 100mM $NiSO_4$

solution. This was followed by a wash step with 5 column volumes H_2O and before the protein was loaded the column was again equilibrated with 10 column volumes of binding buffer (20mM Tris-HCl, 5mM imidazole, 500mM NaCl, pH 7). Another wash step of 10 column volumes binding buffer followed after the protein was loaded. The non-specifically bound proteins were eluted with 10 column volumes binding buffer in which the elution buffer (20mM Tris-HCl, 500mM NaCl, 50mM imidazole, pH 7.9) concentration was increased to 15%($^{V}/_{V}$). Mtr-His was eluted by increasing the concentration of the elution buffer to 100% over 10 column volumes. Protein elution was detected at 280nm. The protein concentration was determined to be 0.80mg/ml by means of a Bradford assay.

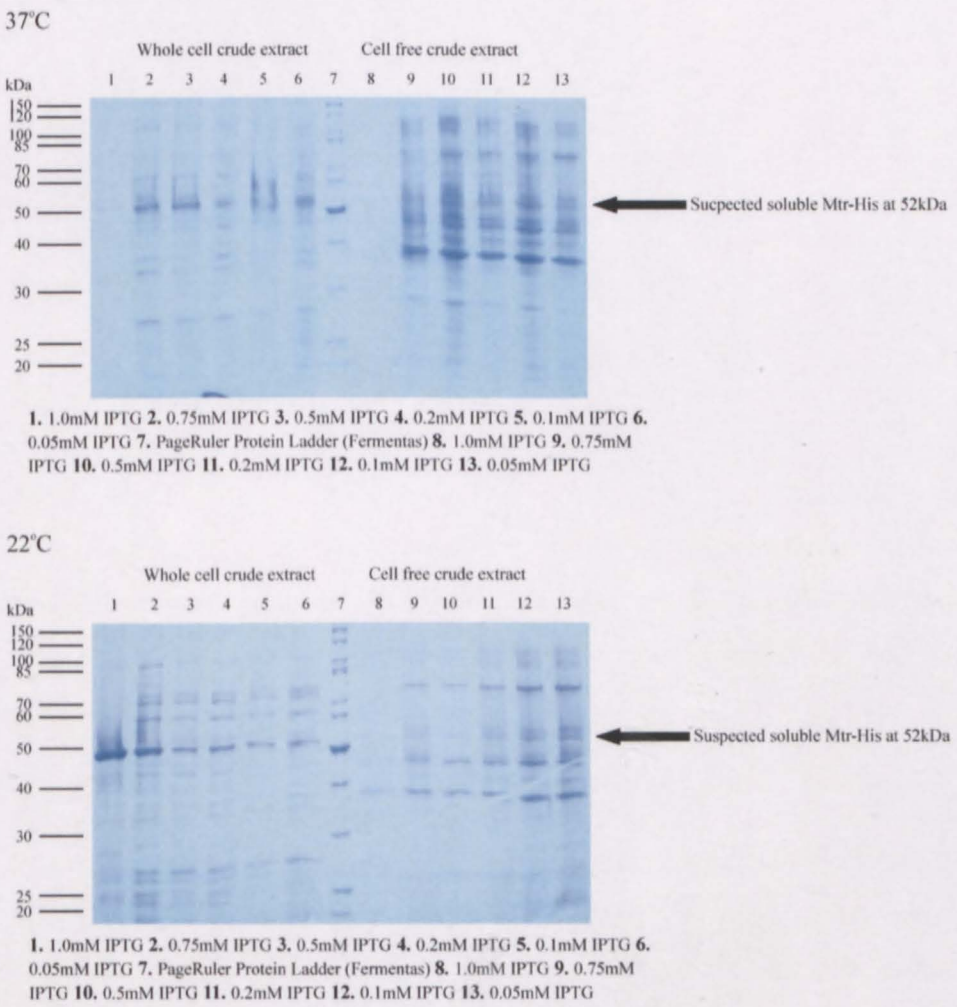

Figure 2.5: Expression trail of pET28(+)-*mtr*CT at 37°C and 22°C, overnight and different IPTG concentrations (as indicated).

The flow through, wash and elution fractions of the purification run, was analyzed on a 12% SDS-PAGE gel (Figure 2.6). Although some of the soluble Mtr-His was lost in the wash (elution of non-specifically bound proteins) step, there was still a sufficient amount of bound protein on the column for an acceptable yield.

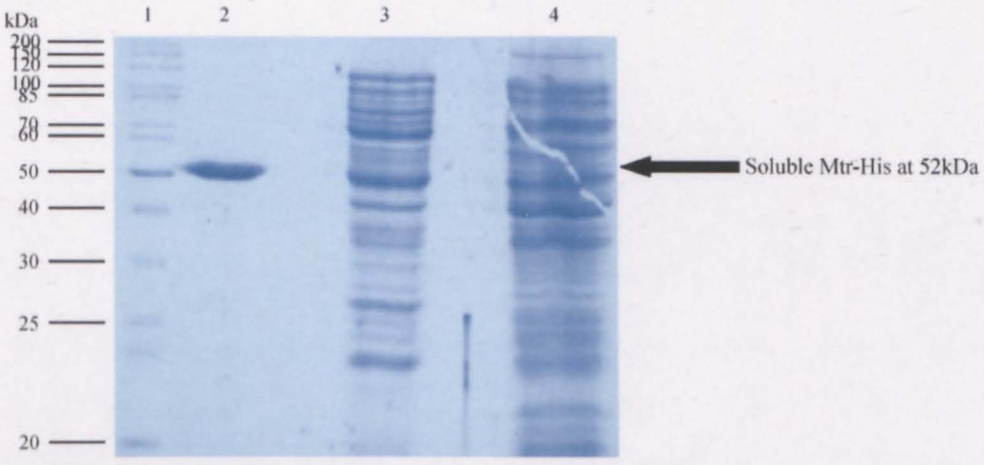

1. PageRuler Protein Ladder (Fermentas) **2.** Eluted soluble Mtr-His **3.** Wash fraction **4.** Flow through fraction

Figure 2.6: SDS-PAGE analysis of the purification of soluble Mtr-His.

2.4 Conclusion

2.4.1 MshB

In our study MshB was expressed using the pET28a(+) expression plasmid. Also, the purification techniques used here allowed for better purification of MshB-His and thus gave rise to larger yields (almost nine times) of soluble MshB-His than previously achieved (*4*).

2.4.2 Mycothiol disulfide reductase

Mycothiol disulfide reductase was successfully cloned, expressed and purified during this study. Previously this could only be achieved by using *M. smegmatis* as expression host (*2, 5, 6*). Systems for the expression of recombinant proteins in *M. smegmatis* are not nearly as effective as in *E. coli*, as was proven during this study. Patel and Blanchard (*2*) could only manage to purify 2.9mg of Mtr from 5L of *M. smegmatis* culture with a long, multi-step purification procedure. During this study a

total of 21.8mg Mtr-His was purified from 2.5L of *E. coli* culture using a simple, automated procedure. Currently we are attempting to solve the crystal structure of Mtr in a collaborative effort. If successful, it will be the first crystal structure of Mtr and would be a major breakthrough for the structure based design of drugs targeting this enzyme.

2.5 Experimental

2.5.1 DNA amplification

2.5.1.1 Mycothiol Disulfide Reductase (MSSMR)

The *Rv2588* or *mtr* gene was amplified from genomic Mtb DNA strain H37Rv using the forward primer 5'-GCCCCTA**CATATG**GAAACGTACG-3' and the reverse primer 5'-AGCCAG**CTCGAG**AGGCAGAGG-3'. With these primers an NdeI (underlined) restriction enzyme site is introduced in the forward primer and an XhoI (underlined) restriction enzyme site in the reverse primer. The amplification reaction mixture was set up as follows: *Pfu* buffer, 0.4mM dNTP mix, 1mM forward primer, 1mM reverse primer, 1ng genomic DNA, varied $MgSO_4$ concentrations, 1.25U *Pfu* and distilled, deionized water (ddH_2O) to a final volume of 25µl. The PCR program had an initial step of 2 min at 94°C; followed by 30 cycles of denaturation at 94°C for 15s, annealing at 60°C for 30s and polymerization for 1min at 70°C. After the 30 cycles were completed there was a final polymerization step of 6 min at 70°C and the program ended with a hold step at 4°C. The reaction mixtures were visualized by gel electrophoresis on a 1% agarose gel and staining the gel with SYBR®gold. The bands were viewed on a Darkreader. The best product band at 1522bp was obtained at an $MgSO_4$ concentration of 3µM. The product band was purified out of the gel using the Eppendorf Perfectprep® Gel Cleanup kit. This PCR product was used in the construction of the pET28a-*mtr*, pENTR4-*mtr* and pENTR4N-*mtr* plasmids.

For the construction of the pET28a-*mtr*CT plasmid a new set of primers had to be designed, allowing the plasmid to be constructed in such a way that will make it possible for MSSMR to be expressed with a C-terminal histidine tag (His-tag). The forward primer 5'-GATGGCCCCTAC**CCATGG**AAACGTACG-3' introduced an

NcoI (underlined) restriction enzyme site and the reverse primer 5'-GCTCGCCGTTG**CTCGAG**ACGCAGGCCAAG-3' an XhoI restriction enzyme site. The same amplification reaction mixture was used for this PCR reaction, but different annealing and polymerization temperatures were used, 65°C and 77°C respectively. The reaction mixtures were visualized and the product band purified as described above. The best results were obtained at a $MgSO_4$ concentration of 3.5µM.

2.5.1.2 MshB

The *Rv1170* or *mshB* gene was amplified from genomic Mtb DNA strain H37Rv using the forward primer 5'-GGTGCCT**CCATGG**CTGAGACGCCGC-3' which introduces an NcoI (underlined) restriction enzyme site. The reverse primer 5'-CCTGGTTGGC**CTCGAG**CGTGCCGGAC-3' introduces an XhoI (underlined) restriction enzyme site. This primer set allows the pET28a-*mshB* construct to express MshB with a C-terminal His-tag. The amplification reaction mixture was setup as previously mentioned. The PCR program used an annealing temperature of 73°C and a polymerization temperature of 80°C. The reaction mixtures were visualized and the product band purified as previously described. The best results were obtained at a $MgSO_4$ concentration of 2µM.

2.5.2 Restriction Digests

The *mtr* PCR product, pET28a(+), pENTR4N and pENTR4NT were digested with NdeI and XhoI restriction enzymes (both form Fermentas). The 20µl digestions reactions were performed in Fermentas Buffer R containing BSA, 15µl PCR product/plasmid, 10U NdeI and 20U XhoI. The reactions were incubated for 2h at 37°C, after which the mixtures were visualized on a 1% agarose gel and the bands of correct size purified using the Eppendorf Perfectprep® Gel Cleanup kit.

The *mtr*CT PCR product, *mshB* PCR product and pET28a(+) digestions were performed with NcoI (New England Bio Labs) and XhoI. In these reactions 14µl PCR product/plasmid and 20U NcoI were used. The relevant bands were visualized and purified as described above.

2.5.3 Plasmid Construction

During this study two expression systems were used, pET (Novagen) and Gateway (Invitrogen), and the construction of their expression plasmids was carried out in different ways. In the pET system the PCR product was directly ligated into the expression plasmid. With the Gateway system the PCR product was first ligated into the entry plasmids, and thereafter expression plasmids were created by means of the Gateway LR reaction.

2.5.3.1 pET expression system

Only the pET28a(+) expression plasmid was used. Equal amounts of restriction digested plasmid and PCR product were added together in a volume of 5µl. Quick Ligation Reaction Buffer and 10U Quick T4 DNA Ligase (New England BioLabs) were added to the plasmid/PCR product mixture to make a final volume of 10.5µl. The reaction was incubated for 5min at room temperature. The reaction mixture was then transformed into chemically competent *E. coli* MachI cells and plate on Luria Bertani (*12*) plates containing 30mg/l kanamycin. These plates were incubated overnight at 37°C. The colonies were screened using the Colony Fast Screen kit (Epicentre). A smear of a colony was added to 25µl of EpiLyse solution 1 and mixed. After 10µl EpiLyse solution 1 was added the mixture was visualized on a 1% agarose gel, using the parent pET28a(+) as reference. Only the DNA samples that appeared larger than the pET28a(+) reference were subjected to further screening. Overnight cultures were grown from the colonies containing the target plasmids. Plasmids were purified from these cultures using the Zyppy Plasmid Miniprep I Kit (Zymo Research) and analyzed with a restriction digestion reaction. The same restriction enzymes were used, as for the digestion of the corresponding PCR product. The reactions were visualized on a 1% agarose gel and if the desired band pattern was obtained, the plasmids were stocked for further use.

2.5.3.2 Gateway expression system

2.5.3.2.1 Entry Plasmids

The pENTR4N and pENTR4NT entry plasmids were used. The ligation of the *mtr* PCR product into the two plasmids was performed in the same manner as for the pET expression system. The transformation and first and second rounds of screening were also performed as mentioned above. The only difference with the abovementioned methods is that, after the transformation of the *mtr* PCR product/pENTR4NT ligation reaction into *E. coli* MachI cells, the cells were plated on LB plates containing 12mg/l tetracycline. Plasmids that passed the screening methods were stocked for further use.

2.5.3.2.2 Gateway LR reaction

The Gateway system utilizes an expression plasmid that is created through means of a LR reaction. In this reaction a recombinant entry plasmid (2.5.3.2.1), destination plasmid and LR clonase are added together. The entry and destination plasmids both have *att*-sites and the DNA between these sites is exchanged during the LR reaction. In the recombinant entry plasmid the target gene sequencing is situated between the *att*-sites. In this system, colonies containing the required expression plasmids are selected for with two methods, namely by means of a *ccd*B-suicide gene contained between the *att*-sites of the destination plasmid and the ampicillin resistance of the destination plasmid. Thus after a LR reaction cells containing destination plasmids would not survive because of the suicide gene. This is also true for cells containing the recombinant entry plasmid because of resistance to kanamycin or tetracycline and not ampicillin. Only cells containing the newly formed expression plasmid would survive.

A destination plasmid (pDEST) and an entry plasmid were added together in a 3:1 ratio and a final volume of 3µl. To the latter was added 1µl of LR clonase buffer and 1µl of LR clonase and incubated at 25°C for 4h. The reaction was terminated by the addition of 1µl Proteinase K and incubation at 37°C for 10min. The reaction mixture was then transformed into *E. coli MachI* cells, plated on 100mg/l ampicillin containing LB plate and incubated overnight at 37°C. Overnight cultures were grown from selected colonies; the plasmids purified using the Zyppy Plasmid Miniprep I Kit

(Zymo Research) and analysed through resistriction enzyme digestion. In these plasmid digestion reactions 20U of Bsp14071 (Fermentas) restriction enzyme, Fermentas Tango buffer and purified plasmid DNA was used to provide a final volume of 16µl. The Bsp14071 enzyme cuts at the *att*-sites. Reactions were visualized on a 1% agarose gel and thereafter SYBR®gold staining the bands were viewed with the Darkreader. Plasmids with the required two band pattern were stocked for future use.

2.5.4 Protein expression and purification

All expressions were firstly conducted in small scale expression trails to determine the correct combination of parameters for soluble expression of the target proteins. After optimization of these parameters, large scale overexpressions of the target protein and protein purification was attempted. All growth media and plates used in the expression of proteins contained the required amount of specific antibiotic.

2.5.4.1 Expression trails

The desired expression plasmids were transformed into *E. coli* BL21*(DE3) cells, then plated for an overnight culture grown from a single colony. The expression trails were performed in 2ml Eppendorf® Lid_{Bac} tubes. Each tube contained 1305µl LB or AI media, 150µl overnight culture and 45µl of IPTG to obtain a final volume of 1500µl. Expression cultures (growth media and overnight culture) were incubated at 37°C in a shaking incubator. Cultures were incubated until it reached an OD_{600} reading of 0.6, after which IPTG was added. The following parameters were varied to find the optimum conditions for soluble protein expression:

1. The final IPTG concentration: 1mM, 0.75mM, 0.5mM, 0.2mM, 0.1mM and 0.05mM.

2. Time allowed for expression to continue after induction: 4h or overnight.

3. The temperature at which expression trials were conducted: 25°C, 30°C and 37°C.

At the end of the expression trails the cells where harvested by centrifugation. The cell pellets were either processed directly after the trails ended or it was stored at -20°C for later use.

2.5.4.2 Large scale expressions

For the large scale expressions 500ml LB media was inoculated with an overnight culture of *E. coli* BL21*(DE3) cells containing the specific expression plasmid. Subsequently incubation proceeded at 37°C until an OD_{600} reading of 0.5-0.6 was reached. After the desired amount of IPTG was added the expression culture was incubated according to the predetermined conditions found in the expression trails. Cells were collected through centrifugation at 4500g for 30min at 4°C. If the pellets were not processed immediately after collection they were stored at -20°C until use.

2.5.4.3 Analyzes of expression trails

The cell pellets obtained from the expression trails were re-suspended in 300µl BugBuster® protein extraction reagent (Novagen) and incubated for 20min at room temperature on a shaking platform. Cell debris was removed by centrifugation at 13000g for 20min, after which the supernatant was transferred to a clean tube and analyzed on a SDS-PAGE gel for soluble proteins. The cell debris pellet was re-suspended in 100µl elution buffer (10mM Tris-HCl, pH 8) and analyzed for insoluble proteins on a SDS-PAGE gel.

2.5.4.4 Protein purification from large scale expressions

The large scale expression cell pellets where re-suspended in a volume 10x the weight of the cell pellet with binding buffer (20mM Tris-HCl, 5mM imidazole, 500mM NaCl, pH 7). Cells were lysed by means of sonication and the cell debris separated by centrifugation at 15000g for 30min at 4°C. The supernatant was removed, followed by filtration with a Pall Acrodisc PSF GxF/GHP 0.45µm filter before it was injected into the ÄKTA*prime*-system.

The two proteins were purified using the same His-tag purification procedure, the only difference being the columns used. MshB was loaded onto a 1ml HisTrap FF

column, whereas Mtr was loaded onto a 1ml HiTrap Chelating HP column, both from Amersham Bioscience. The difference between the two columns is that the FF column is supplied preloaded with Ni^{+2} and the Chelating HP column needs to be loaded with Ni^{+2} as part of the ÄKTA*prime* program. After the His-tagged protein was loaded onto the column and non-specific bound proteins washed off, the imidazole concentration in the buffer (20mM Tris-HCl, 500mM NaCl, 50mM imidazole, pH 7.9) was increased to elute the target protein. The eluted proteins were then desalted using a 5ml HiTrap desalting column (Amersham Bioscience) and a gel filtration buffer (25mM Tris-HCl, 5mM $MgCl_2$, 5% glycerol, pH 8) on the ÄKTA*prime*-system. All the protein elution profiles were followed by UV detection at 280nm.

2.5.4.5 12% SDS-PAGE gel analysis

Proteins, either from expression trails or large scale purifications, were visualized using 12% SDS-PAGE gels. The protein samples were prepared by adding it to an equal volume of 2x SDS-PAGE loading buffer (0.125M Tris-HCl, 4% SDS, 30% glycerol, 1.5% β-mercaptoethanol and bromophenol blue, pH 6.8) and incubating it for 5min at 95°C. After the samples were loaded the gel was run in 1x SDS-PAGE running buffer (0.1% SDS, 0.025M Tris and 0.192M glycine). After completion, gels were stained with Coomassie blue stain (45ml MeOH, 40ml ddH_2O, 10ml CH_3COOH and 250mg Coomassie Brilliant Blue) for 30min and then destained for 2 hours with destaining solution (45% MeOH, 40% ddH_2O, 10% CH_3COOH).

2.5.4.6 Protein concentration determination

Concentration determination was performed using the Bradford protein assay. Bovine serum albumin (BSA) standards from Biorad were used to plot a standard curve of absorbance versus concentration. Absorbance was measured at 595nm, which is the absorption maximum of the Coomassie Brilliant Blue dye when bound to protein. The dye is added to all protein samples, standards and unknowns, and incubated for 5min at room temperature before measurements are taken. All measurements were taken with a Thermo Varioskan™ and data processing was performed with Skanit software.

2.5.5 Other attempts at soluble protein expression and purification

During this study it was necessary to perform protein expression and purification in different ways as stated in the previous section. None of the methods mentioned here was used for the large scale expression and purification of Mtr or MshB. All expression trails were performed in the 2ml Eppendorf® Lid_{Bac} tubes.

2.5.5.1 Expression in the presence of glycylglycine and ethanol

Expression trails were performed in LB media containing 0.5M or 1.0M glycylglycine (Fluka) and in LB media containing 0.5-1.5% ethanol. The expressions were incubated overnight at 37°C.

2.5.5.2 Scarce codons

Competent cells were made from *E. coli* BL21*(DE3) cells containing the pET28a-*mtr* expression plasmid. The pRARE2 plasmid was then transformed into these competent cells and plated on LB plates containing 20mg/l chloramphenicol and 30mg/l kanamycin. The expression was performed in AI media containing the abovementioned antibiotics. Expressions were allowed to continue overnight.

2.5.5.3 Chaperone plasmids

The five different chaperone plasmids were transformed into competent *E. coli* BL21*(DE3) cells containing either the pET28a-*mtr* or pEXP566-*mtr* expression plasmids. The cells were plated on 20mg/l chloramphenicol and 30mg/l kanamycin LB plates. LB media was used for these expression trails which, in additions to the antibiotics, also contained 4mg/ml L-arabinose, 10ng/ml tetracycline or both. The L-arabinose and tetracycline induces expression of the chaperons. Expression trials were incubated for 4h at 30°C and 37°C respectively after expression plasmid induction with IPTG.

2.5.5.4 His SpinTrap columns

These columns (GE Healthcare) are prepacked with Ni Sepharose™ which has a high protein binding capacity and works on the same principle as the columns used with

the ÄKTA*prime*-system. They were used to purify protein from small expression trails, in order to check if the His-tagged protein was indeed soluble and if it could be purified before the large scale purification was attempted. Buffers are accelerated through the column by means of centrifugation for 30s at 70 x g. The column was first equilibrated with 600µl of binding buffer (20mM sodium phosphate, 500mM NaCl, 20mM imidazole, pH 7.4) after which 600µl of the His-tagged protein solution was loaded. Non-specific binding proteins were washed through with 600µl binding buffer and the protein was eluted with 200µl elution buffer (20mM sodium phosphate, 500mM NaCl, 20mM imidazole, pH 7.4). The different fractions (flow through, wash and elution) were analyzed on a 12% SDS-PAGE gel.

2.5.5.5 Emulgen

Cell debris pellets were re-suspended in 3ml 0.1M Na_2SO_4 and to this different amounts of Emulgen® was added to achieve final concentrations of 1-2.5% $^{M}/_{V}$. Thereafter 3ml of a 0.05M Na_2SO_4, 1M NaCl and 10% glycerol solution was added and the mixture was allowed to stir for 4h. The cell debris was centrifuged, separated and the soluble fraction analyzed on a 12% SDS-PAGE gel.

2.6 References

(1) Newton, G. L., Av-Gay, Y., and Fahey, R. C. (2000) N-acetyl-1-D-myo-inosityl-2-amino-2-deoxy-α-D-glucopyranoside deacetylase (MshB) is a key enzyme in mycothiol biosynthesis. *Journal of Bacteriology 182*, 6958-6963.

(2) Patel, M. P., and Blanchard, J. S. (1999) Expression, Purification, and Characterization of *Mycobacterium tuberculosis* Mycothione Reductase. *Biochemistry 38*, 11827-11833.

(3) Maynes, J. T., Garen, C., Cherney, M. M., Newton, G., Arad, D., Av-Gay, Y., Fahey, R. C., and James, M. N. G. (2003) The Crystal Structure of 1-D-myo-Inosityl 2-Acetamido-2-deoxy-α-D-glucopyranoside Deacetylase (MshB) from *Mycobacterium tuberculosis* Reveals a Zinc Hydrolase with a Lactate Dehydrogenase Fold. *Journal of Biological Chemistry 278*, 47166-47170.

(4) Newton, G. L., Ko, M., Ta, P., Av-Gay, Y., and Fahey, R. C. (2006) Purification and characterization of Mycobacterium tuberculosis 1D-myo-inosityl-2-acetamido-2-deoxy-α-D-glucopyranoside deacetylase, MshB, a mycothiol biosynthetic enzyme. *Protein Expression and Purification 47*, 542-550.

(5) Patel, M. P., and Blanchard, J. S. (1998) Synthesis of Des-myo-Inositol Mycothiol and Demonstration of a Mycobacterial Specific Reductase Activity. *Journal of the American Chemical Society 120*, 11538-11539.

(6) Patel, M. P., and Blanchard, J. S. (2001) *Mycobacterium tuberculosis* mycothione reductase: pH dependence of the kinetic parameters and kinetic isotope effects. *Biochemistry 40*, 5119-5126.

(7) Yang, J., Xu, Y., Su, M., Hao, X., and Yu, W. (2005) Ethanol facilitates soluble expression of Mr 38000 protein of *Mycobacterium tuberculosis* in *E. coli*. *Disi Junyi Daxue Xuebao 26*, 360-362.

(8) Ghosh, S., Rasheedi, S., Rahim, S. S., Banerjee, S., Choudhary, R. K., Chakhaiyar, P., Ehtesham, N. Z., Mukhopadhyay, S., and Hasnain, S. E. (2004) Method for enhancing solubility of the expressed recombinant proteins in *Escherichia coli*. *BioTechniques 37*, 418, 420, 422-423.

(9) Martinez-Martinez, I., Navarro-Fernandez, J., Lozada-Ramirez, J. D., Garcia-Carmona, F., and Sanchez-Ferrer, A. (2006) Maximization of production of His-tagged glycine oxidase and its M261 mutant proteins. *Biotechnology Progress 22*, 647-652.

(10) Nishihara, K., Kanemori, M., Kitagawa, M., Yanagi, H., and Yura, T. (1998) Chaperone coexpression plasmids: differential and synergistic roles of DnaK-DnaJ-GrpE and GroEL-GroES in assisting folding of an allergen of Japanese cedar pollen, Cryj2, in *Escherichia coli*. *Applied and Environmental Microbiology 64*, 1694-1699.

(11) Nishihara, K., Kanemori, M., Yanagi, H., and Yura, T. (2000) Overexpression of trigger factor prevents aggregation of recombinant proteins in *Escherichia coli*. *Applied and Environmental Microbiology 66*, 884-889.

(12) Middelberg, A. P. J. (2002) Preparative protein refolding. *Trends in Biotechnology 20*, 437-443.

(13) Stoller, G., Rucknagel, K. P., Nierhaus, K. H., Schmid, F. X., Fischer, G., and Rahfeld, J. U. (1995) A ribosome-associated peptidyl-prolyl *cis/trans* isomerase identified as the trigger factor. *EMBO J FIELD Full Journal Title:The EMBO journal 14*, 4939-4948.

(14) Valent, Q. A., Kendall, D. A., High, S., Kusters, R., Oudega, B., and Luirink, J. (1995) Early events in preprotein recognition in *E. coli*: interaction of SRP and trigger factor with nascent polypeptides. *EMBO Journal 14*, 5494-5505.

(15) Fischer, G., and Schmid, F. X. (1990) The mechanism of protein folding. Implications of *in vitro* refolding models for *de novo* protein folding and translocation in the cell. *Biochemistry FIELD Full Journal Title:Biochemistry 29*, 2205-2212.

(16) Fink, A. L. (1999) Chaperone-mediated protein folding. *Physiol Rev FIELD Full Journal Title:Physiological reviews 79*, 425-449.

(17) Gottesman, S., Wickner, S., and Maurizi, M. R. (1997) Protein quality control: triage by chaperones and proteases. *Genes Dev FIELD Full Journal Title:Genes & development 11*, 815-823.

(18) Sigler, P. B., Xu, Z., Rye, H. S., Burston, S. G., Fenton, W. A., and Horwich, A. L. (1998) Structure and function in GroEL-mediated protein folding. *Annu Rev Biochem FIELD Full Journal Title:Annual review of biochemistry 67*, 581-608.

(19) Hara, M., Miyake, J., Asada, Y., and Ohkawa, H. (1999) Purified fusion enzyme between rat cytochrome P4501A1 and yeast NADPH-cytochrome P450 oxidoreductase. *Bioscience, Biotechnology, and Biochemistry 63*, 21-28.

(20) Arinc, E., and Lelik, H. (2002) Biochemical characteristics of purified beef liver NADPH-cytochrome P450 reductase. *Journal of Biochemical and Molecular Toxicology 16*, 286-297.

(21) Kapust, R. B., and Waugh, D. S. (1999) *Escherichia coli* maltose-binding protein is uncommonly effective at promoting the solubility of polypeptides to which it is fused. *Protein Science 8*, 1668-1674.

Chapter 3

Detection and quantitation of the mycothiol pathway intermediates

3.1 Introduction

As discussed in Chapter 1, one of the major functions of mycothiol (MSH) is maintaining the intracellular redox homeostasis, a function which is homologous to that of glutathione. A variety of analytical methods, including mass spectrometry, have been used to determine the amount of glutathione present in cells (*1*). By monitoring the depletion of glutathione in cells, the level of oxidative stress that cells are under can be determined (*2*). Thus, glutathione acts as a biomarker for determining the oxidative stress inside eukaryotic cells. In the same way MSH can also be used as a biomarker for oxidative stress. A change in the ratio of reduced MSH and oxidized mycothiol disulfide (MSSM) in cells can be used to determine the effect, if any, existing and newly-developed drugs may have on *M. tuberculosis* cells.

Current methods for determining MSH, MSSM and other mycothiol pathway intermediates most commonly utilize high pressure liquid chromatography (HPLC) and require the derivatisation of these molecules (*3, 4*). Two derivatisation methods often used in mycothiol pathway studies are monobromobimane and AccQ-Fluor (Waters Corp.) (*3-6*). Monobromobimane is used to derivatise the free thiol of MSH and AccQ-Fluor the free amine of αGlcN-Ins (Figure 3.1). MSSM levels can also be determined through monobromobimane derivatisation, but has to be preceded by the reduction of the molecule's disulfide to its free thiol form (*7*). With both of these methods a fluorogenic product is formed which is visualized using UV-HPLC.

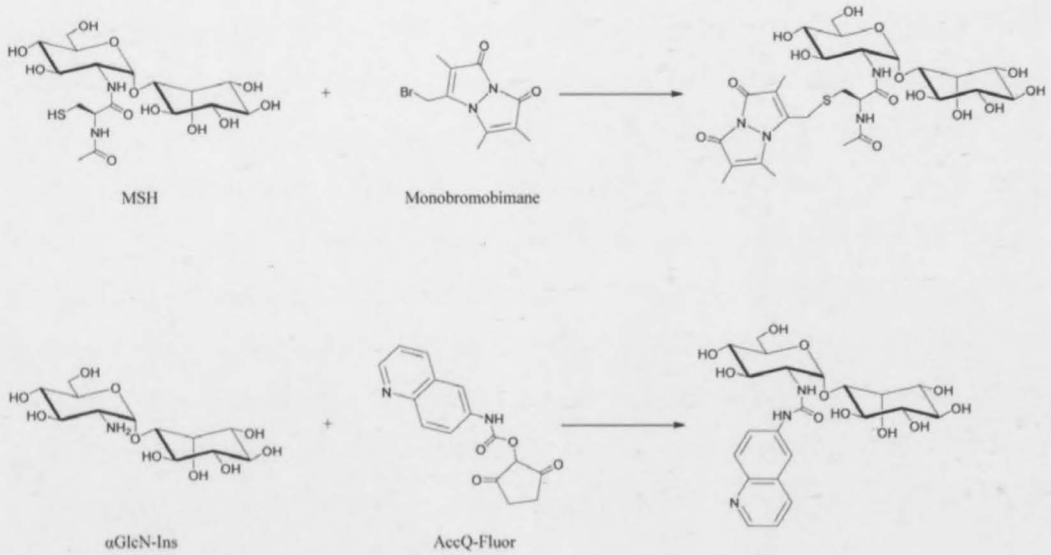

Figure 3.1: Derivatisation methods for MSH and αGlcN-Ins producing the fluorogenic products.

In this chapter we report the development of a new HPLC-ESI/MS(TOF) method for the simultaneous detection and quantitation of MSH, MSSM and other mycothiol pathway intermediates in *M. smegmatis* cell lysates without the need for any derivatisation.

3.2 Method Development

3.2.1 Analyte extraction methods

During development of our detection and quantitation method three established analyte extraction methods were compared with each other. Two of these methods use sonication as means of cell wall disruption, but differ in the extraction buffer used during sonication. In the first method the extraction buffer consists of 0.5% formic acid in 80% MeOH/H_2O (Buffer A) and was used in the extraction of nitrogen containing metabolites from *S. enterica* (*8*). The other was used in the extraction of MSH from *M. smegmatis* cells; in this case the buffer consisted of 0.25M perchloric acid and 2mM EDTA in a 40% MeCN/H_2O (Buffer B) (*9*). In the third analyte extraction method a commercially available protein extraction reagent, BugBuster® (Novagen), was used. BugBuster® reagent was originally designed to disrupt *E. coli* cell walls without the need for sonication. Using it for the disruption of the more rigid *M. smegmatis* cell walls would therefore constitute a new application for this reagent.

After evaluation of the three extraction methods, analyte extraction with BugBuster® was proven to be the best of the three methods. In comparison with the other two extraction methods, the BugBuster® method was by far the fastest and most convenient method with which large sets of samples could easily be processed. Although the sample preparation time was 2h, all the samples of a set could be processed simultaneously, which also minimizes the potential handling errors. The BugBuster® extraction method also produced better results than that of the other two methods as based on analysis of the total ion chromatograms (data not shown). Buffer B produced the worst matrix interference, of the three methods, while the main problem with buffer A was that after sonication and the removal of the cell debris by centrifugation the majority of the methanol had to be removed *in vacuo* before it could be lyophilized. This means that the samples extracted by this method was handled more than in the other two extraction methods.

3.2.2 LCMS analysis

The soluble *M. smegmatis* fractions containing the analytes were extracted using the BugBuster® method. Samples were analyzed with a gradient elution program utilizing a Synergy 4 µM Fusion RP, 250x2mm column (Phenomenex) on an ACQUITY UPLC® system (Waters Corp.). The total analysis time was 20 min. Detection was performed with a QTOF Ultima API quadrupole mass spectrometer (Micromass, Manchester, UK) and the data processed with MassLynx™ software (Micromass, Manchester, UK). The three analytes of interest were MSH, MSSM and αGlcN-Ins.

The mass spectra were acquired by ESI/MS(TOF) in the *m/z* range of 100–1000 amu during the whole chromatographic run. Three-dimensional (time, *m/z*, and intensity) chromatograms were obtained and were extracted for the exact *m/z* values corresponding to the $[M+H]^+$ species of each analyte. The extracted ion chromatogram responses were measured as area under the curve (AUC) and were correlated to analyte standards of known concentrations.

The concentration of the MSH standard was determined using a standard curve derived from a DTNB assay with a range of different glutathione (GSH) standards. This MSH standard was diluted and two different injection volumes were analyzed with the HPLC-ESI/MS(TOF) method. The responses obtained from these two

different MSH standards showed a linear response with respect to each other. This response factors were used to determine the amount of MSH present in stationary phase *M. smegmatis* cells.

3.2.2.1 αGlcN-Ins identification

To identify αGlcN-Ins in analyte samples the ion chromatograms were extracted for the 342 *m/z* ion (the mass of the αGlcN-Ins $[M+H]^+$ ion). The extracted total ion chromatogram for the αGlcN-Ins standard (synthesized via published procedure, Jardine *et al.* (*10*)) is shown below (Figure 3.2), along with its corresponding MS spectrum (Figure 3.3). The MS spectrum clearly shows the $[M+H]^+$, $[M+Na]^+$ and the $[M+H]^{2+}$ ions of the standard. Similarly, the MS spectrum of the corresponding analyte sample clearly shows the same $[M+H]^+$ value of the natural occurring αGlcN-Ins in the *M. smegmatis* extraction (Figure 3.4). αGlcN-Ins had a similar retention time of ~2.9min in both samples. An MS/MS experiment (data not shown) was also performed to show that in future, a selective ion monitoring (SIR) method could also be utilized for the identification and quantitation of αGlcN-Ins.

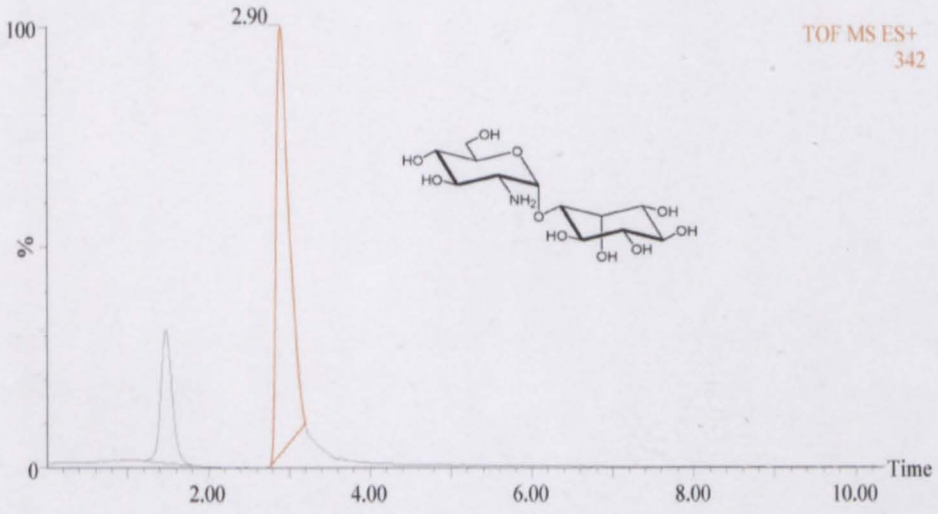

Figure 3.2: GlcN-Ins standard ion chromatogram extracted for the m/z 342 [M+H]+ ion of αGlc-Ins.

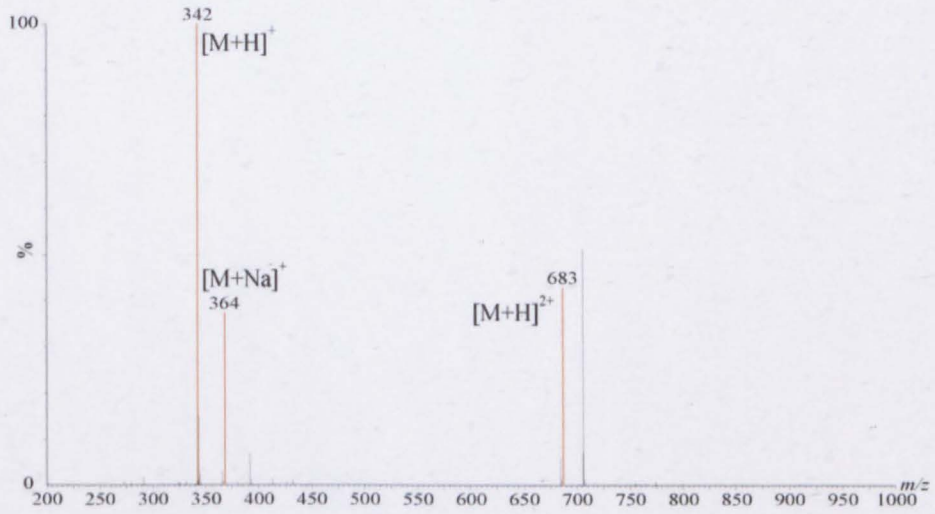

Figure 3.3: MS spectrum of the αGlcN-Ins standard.

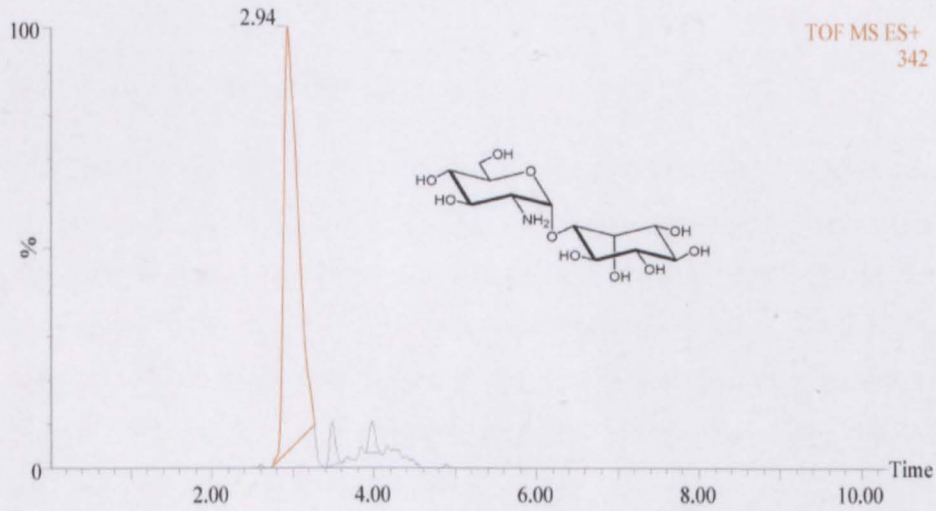

Figure 3.4: The total ion chromatogram of the *M. smegmatis* cell lysate extracted for the *m/z* 342 $[M+H]^+$ value of αGlcN-Ins.

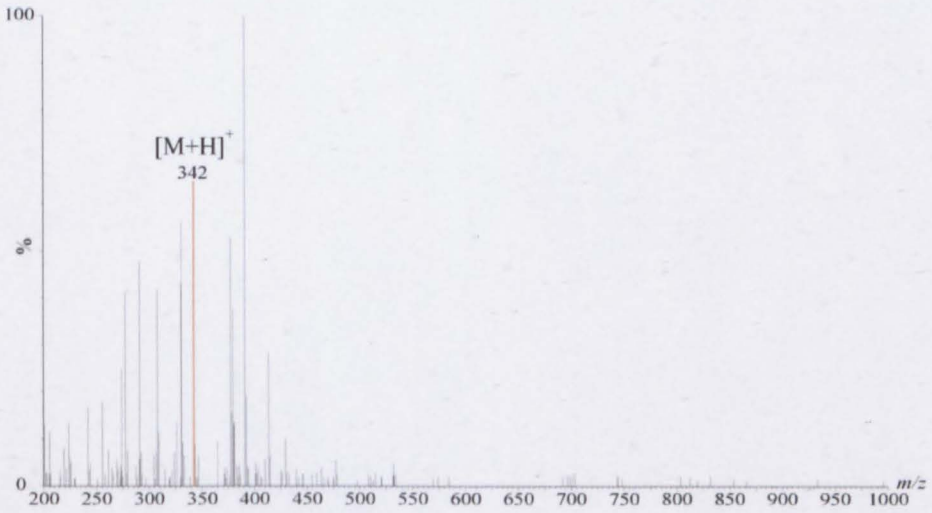

Figure 3.5: MS spectrum corresponding to the total ion chromatogram of the *M. smegmatis* cell lysate extracted for the *m/z* 342 $[M+H]^+$ ion of αGlcN-Ins.

3.2.2.2 Mycothiol (MSH) identification

To identify mycothiol the total ion chromatogram of a standard sample was extracted for the *m/z* 487 $[M+H]^+$ ion of MSH. The chromatogram and its corresponding MS spectrum is shown in Figures 3.6 and 3.7 respectively. The MS spectrum clearly shows the $[M+H]^+$ and $[M+Na]^+$ values of the MSH standard. MSH had a retention time of 4.4mins in the total ion chromatogram of the *M. smegmatis* lysate extracted for *m/z* 487 $[M+H]^+$. The corresponding MS spectra also shows the $[M+H]^+$ and $[M+Na]^+$ ions of MSH (Figure 3.9).

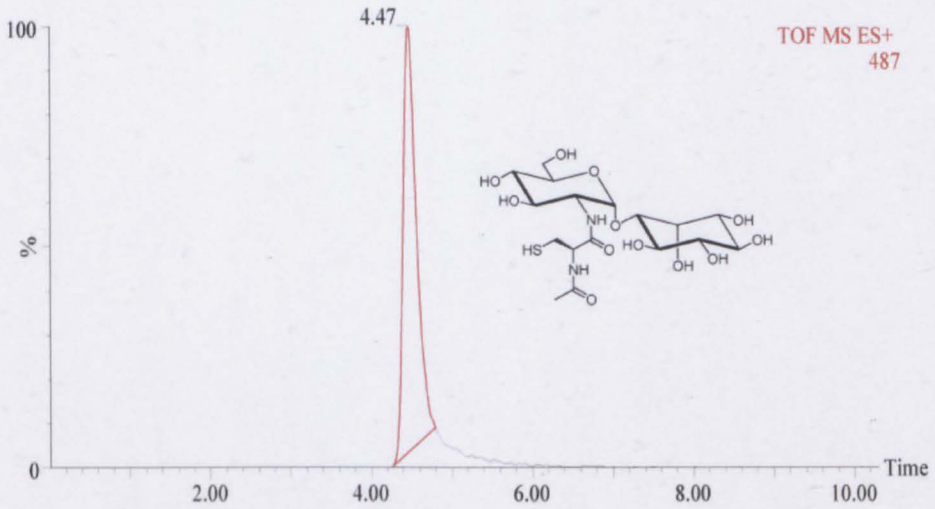

Figure 3.6: MSH standard ion chromatogram extracted for the *m/z* 487 $[M+H]^+$ ion of MSH.

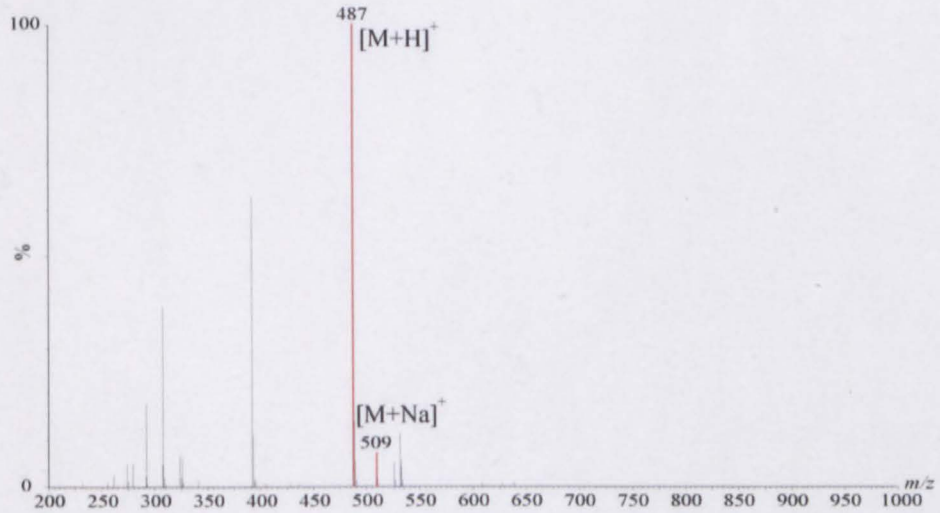

Figure 3.7: MS spectrum of the MSH standard

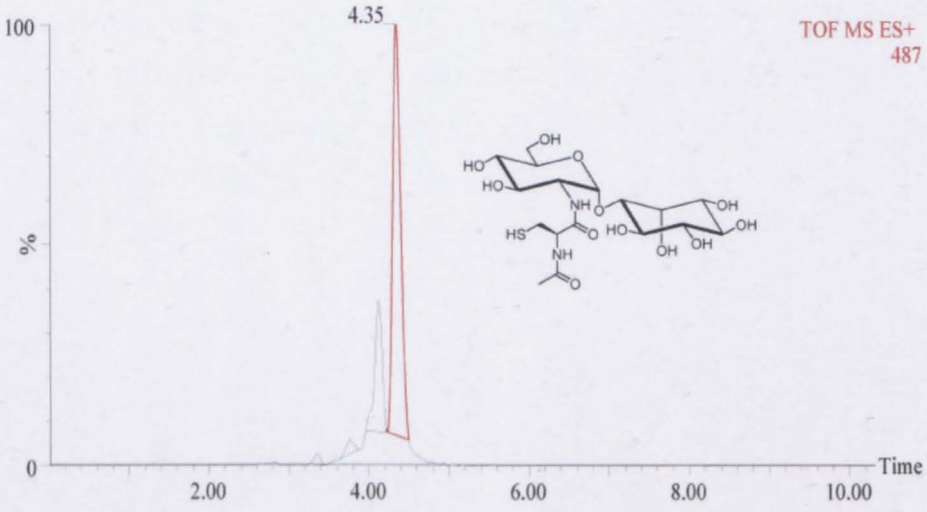

Figure 3.8: The total ion chromatogram of the *M. smegmatis* cell lysate extracted for the *m/z* 487 $[M+H]^+$ ion of MSH.

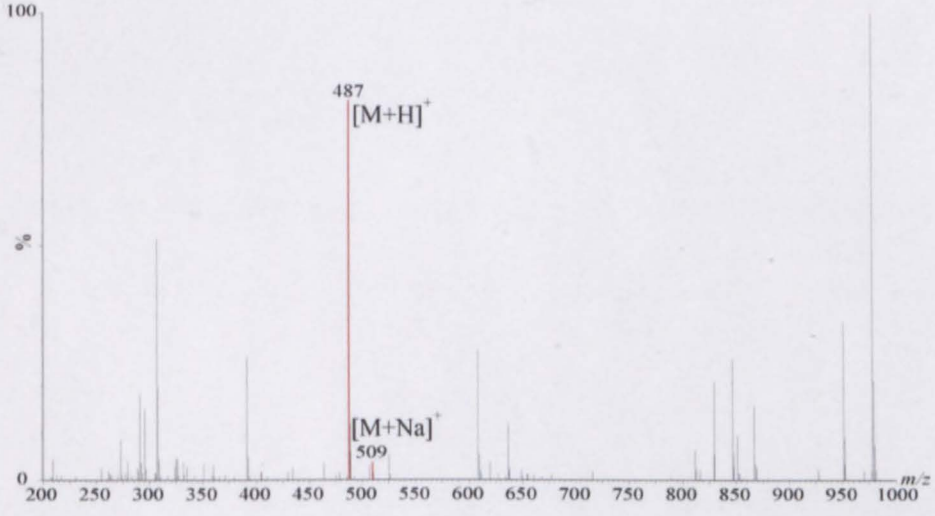

Figure 3.9: MS spectrum corresponding to the total ion chromatogram of the *M. smegmatis* cell lysate extracted for the *m/z* 487 $[M+H]^+$ ion MSH.

3.2.2.3 Mycothiol disulfide (MSSM) identification

Mycothiol disulfide could be identified by extracting the total ion chromatogram for the *m/z* 971 $[M+H]^+$ ion of MSSM. The chromatogram for the MSSM standard is shown in Figure 3.10, and its corresponding MS spectrum in Figure 3.11. The MS spectrum shows the $[M+H]^+$ ion and the weak $[M+Na]^+$ ion of the standard. Similar results were obtained when *M. smegmatis* lysate was analyzed, although the peak

obtained by extracting the total ion chromatogram for the *m/z* 971 $[M+H]^+$ ion had a slightly delayed retention time compared to that of the standard (Figure 3.12). The corresponding MS spectrum (Figure 3.13) also shows the $[M+H]^+$ ion and a weak $[M+Na]^+$ ion of MSSM.

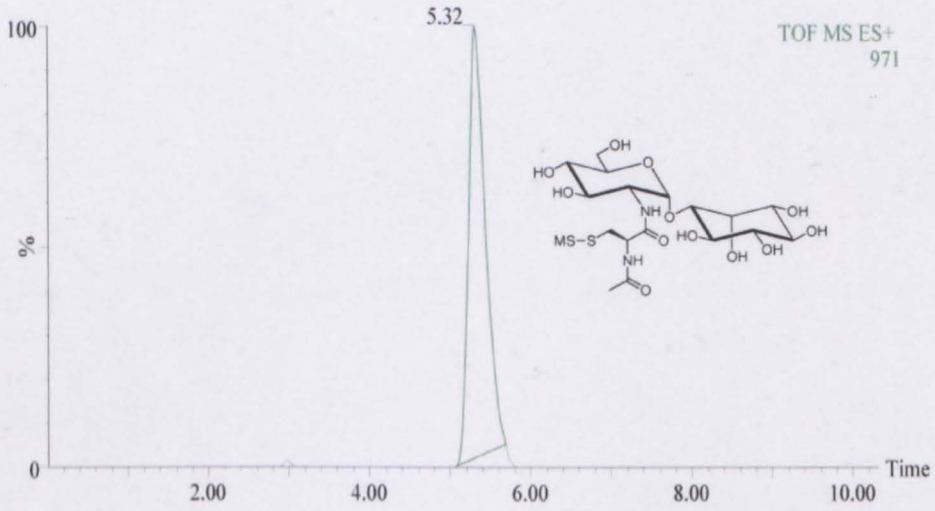

Figure 3.10: MSSM standard ion chromatogram extracted for the *m/z* 971 $[M+H]^+$ ion of MSSM.

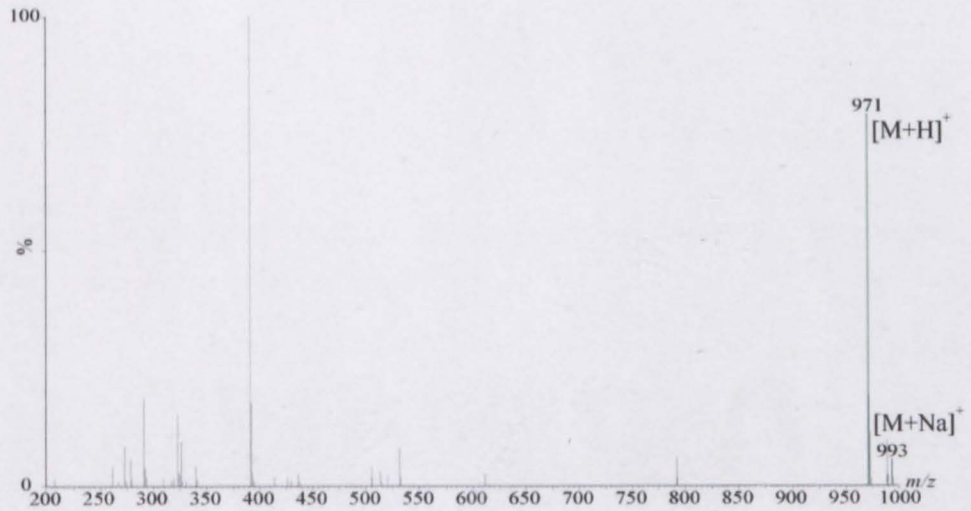

Figure 3.11: MS spectrum of the MSSM standard.

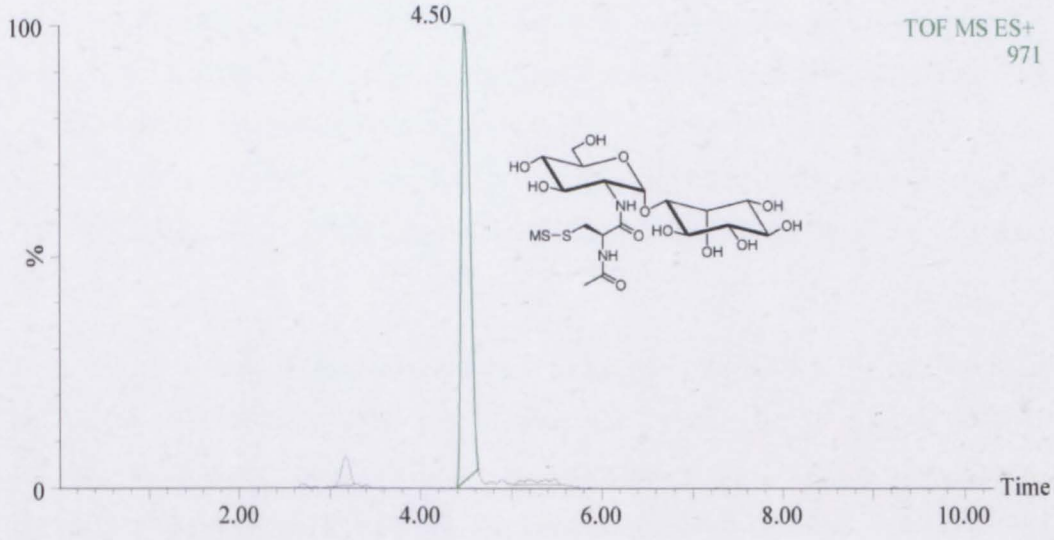

Figure 3.12: The total ion chromatogram of the *M. smegmatis* cell lysate extracted for the *m/z* 971 $[M+H]^+$ ion of MSSM.

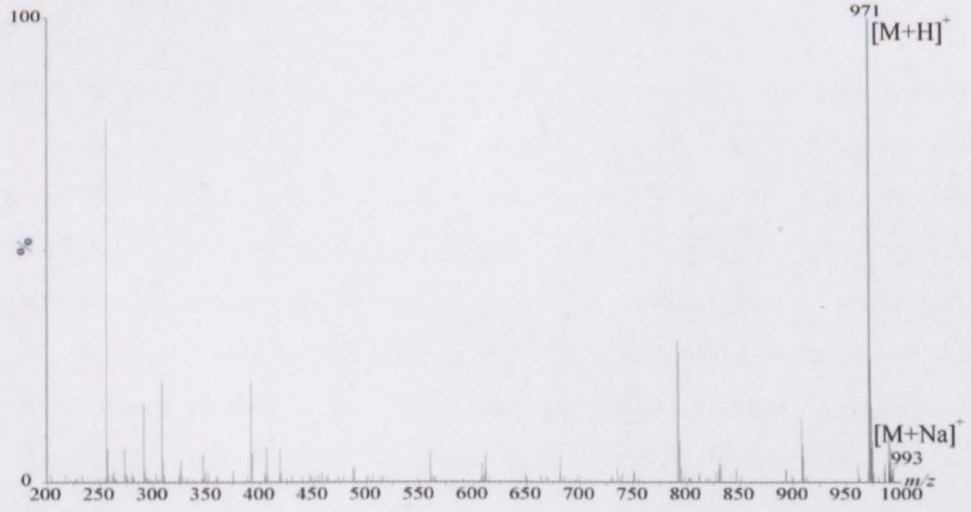

Figure 3.13: MS spectrum corresponding to the total ion chromatogram of the *M. smegmatis* cell lysate extracted for the *m/z* 971 $[M+H]^+$ ion of MSSM.

3.2.3 Induction of oxidative stress

In a study performed by Ung *et al.*, cellular stress were invoked in *M. bovis* BCG cells with the addition of diamide or hydrogen peroxide (H_2O_2) to stationery phase cultures. Both diamide and H_2O_2 induced oxidative stress inside cells. Diamide or *N,N,N',N'*-tetramethylazodicarboxamide penetrates the cell and causes specific oxidation of intracellular low molecular weight thiols to their disulfide forms. This form of

oxidative stress is called disulfide stress and leads to the buildup of foreign disulfide bonds in the cytoplasm (*11*). The authors monitored the MSH and MSSM levels after oxidative stress was induced and reported depletion of the MSH and a change in the basal MSH:MSSM levels. These authors used the monobromobimane derivatisation and HPLC detection method mentioned in section 3.1 for the quantitation of MSH and MSSM.

To test if our LCMS method could be used to detect differences in the MSH:MSSM ratios under different cell growth conditions, the experiments of Ung *et al.* were repeated by inducing oxidative stress in stationary phase *M. smegmatis* cultures. Cultures at stationary phase provides a more accurate representation of the MSH and MSSM levels inside the cell, as it eliminates the effect of oxidative stress caused by cellular respiration.

3.2.3.1 Analyte extraction done with all three methods

In an attempt to reproduce the results obtained by Ung *et al.*, all three extraction methods were used. For each of the sonication methods (with buffers A and B) a set of 4x300ml *M. smegmatis* cultures were grown until stationary phase. In two of the cultures oxidative stress was not induced (blank cultures) and diamide or H_2O_2 was added to the remaining two cultures in a final concentration of 5mM and 10mM respectively. At each time point (0, 1, 4 and 8h) after oxidative stress was induced, a 50ml sample of each of the four cultures were taken. Cells were collected through centrifugation and stored at -20°C until the extractions were performed.

For the BugBuster® method, fifteen 1.5ml *M. smegmatis* cultures, in 2ml Lid_{Bac}® tubes (Eppendorf), were grown until it reached stationary phase. Oxidative stress was induced by the addition of diamide to five tubes and H_2O_2 to another five of the tubes. Nothing was added to the remaining five tubes (blank cultures). At the previously mentioned time points three tubes were removed, one for the blank culture and one of each stress-induced culture (as induced by addition of either diamide or H_2O_2). The cells were also collected and stored until extractions could be done.

Two major shortcomings were discovered with this method. The first is that more than half the culture medium evaporated from the 1.5ml culture tubes intended for the

BugBuster® extraction. This was proof that the Lid_{Bac}® tubes and membrane lids designed for the growth of *E. coli* is not suitable for the long incubation periods required for *M. smegmatis* culturing. Thus, the data obtained from these extractions were not representative of the oxidative stress the cells were experiencing. The second shortcoming with this method is the length of time it took to extract fifteen samples using the sonication methods. Thus, the latter methods were not well suited for development into a high-throughput quantitation of MSH:MSSM under various cell growth conditions. The BugBuster® extraction method was in many aspects better suited for the task.

3.2.3.2 Analyte extraction with the BugBuster® method

As was seen above (sections 3.2.1 and 3.2.3.1) the BugBuster® extraction method is better suited for the processing of large sets of samples and the Ung *et al.* experiment was repeated, this time only using the BugBuster® method for analyte extraction. It was also decided to induce oxidative stress in only one *M. smegmatis* culture using H_2O_2. The reason for choosing H_2O_2 is twofold. First, in the Ung *et al.* experiment larger differences in MSH and MSSM levels were observed in the presence of H_2O_2. Second, H_2O_2 is a reactive oxygen species that is released during the "oxidative burst" inside macrophage phagosomes as a natural defense against a *M. tuberculosis* infection.

Two *M. smegmatis* cultures (300ml) were grown until they reached stationary phase, after which H_2O_2 (final concentration of 10mM) was added to one of the two cultures. The other culture served as the control. At 0, 1 and 6h after oxidative stress was induced, three aliquots of 15ml each were taken from each of the two cultures. The cells were collected by centrifugation, washed and stored at -20ºC until further use. After all the samples were collected extraction was performed with the BugBuster® method as described above and submitted for LCMS analysis.

At the 0h time point all the MSH and MSSM levels are similar (Figure 3.14). This is expected, since the cells are in stationary phase and the amount of oxidative stress they are subjected to should be similar and would be reflected in their MSH and MSSM levels. However, analysis of cultures removed at the 1h time point shows that

dramatic changes in the MSH and MSSM levels have taken place in the cells to which H_2O_2 was added. An even bigger change was observed at the 6h point. This is a consequence of the induced oxidative stress the cells were experiencing. This is in contrast to the MSH and MSSM levels of the blank samples analyzed at the 1h point, which were still similar to their original values, although there was a slight elevation in the amount of MSH. There was a big change in the MSH and MSSM levels of the blank sample at the 6h point. This seems to indicate that even cells in the blank samples start to experience oxidative stress without the addition of any oxidative agents.

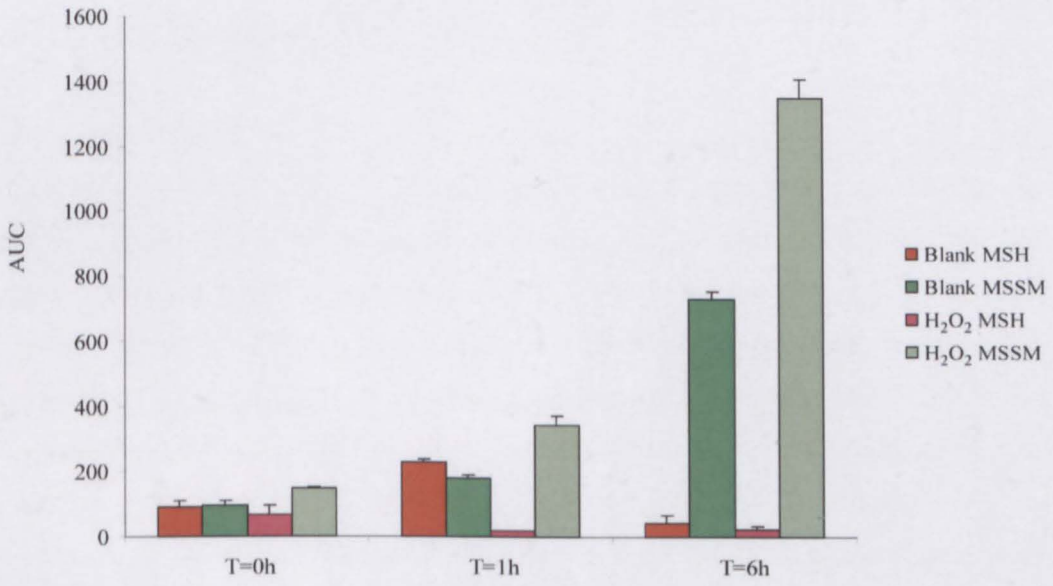

Figure 3.14: Bar graph depicting the changes in MSH and MSSM levels over time.

3.3 Conclusion

A new method for the simultaneous detection and quantitation of MSH and MSSM has been developed. With this method there is no need for the derivatisation of these two analytes. It is shown that this method can be used not only to determine the MSH and MSSM levels inside *M. smegmatis*, but also to detect αGlcN-Ins, an intermediate in the biosynthesis of MSH. The results of the HPLC-ESI/MS(TOF) method show that it is capable of resolving the three analytes in the same run with αGlcN-Ins, MSH and MSSM having retention times of 2.9, 4.4 and 5.3min respectively. Also the commercially available BugBuster® protein extraction reagent was used in a new

application and with great success. All the analytes could be detected using BugBuster® extractions, which demonstrated a great improvement on prior extraction methods.

The calculated amount of MSH present in the 0h time point stationary phase cells was a factor of ten more than that previously reported by Ung *et al.* (*7*) and Newton *et al.* (*3*). A full analytical evaluation of this quantitation method is currently in progress, but the preliminary results indicate superior sensitivity of this LCMS-based method over the established protocols.

3.4 Experimental

3.4.1 Culturing

The *M. smegmatis* ATCC 19420 cell stock was a gift from Prof. Daan Steenkamp, Medical School, University of Cape Town. All *M. smegmatis* culturing and experiments were done in Middlebrook 7H9 Broth (Difco) to which 5% glycerol and 0.05% Tween 80 (Sigma) was added. No antibiotics were used. Before every experiment an "overnight" *M. smegmatis* culture was grown for 24h at 37°C. This culture was used to inoculate the experimental culture media. The inoculated cultures were incubated for 35h at 37°C. This gave the cells enough time to reach the stationery phase, as all experiments were performed at stationary phase *M. smegmatis* cultures. After incubation the cells were collected through centrifugation for 30min at 4500rpm. The resulting cell pellets were processed accordingly.

3.4.2 Extraction methods

3.4.2.1 Sonication with buffer A

This method was used to extract nitrogen containing metabolites from *Salmonella enterica* (*8*). The cell pellet was resuspended in 80% MeOH/H_2O solution containing 0.5% formic acid followed by disruption by sonication. After sonication the cell debris was removed by centrifugation, the methanol was evaporated *in vacuo* and the remainder of the aqueous supernatant was lyophilized overnight. The resulting residue

was reconstituted in 1ml 50% MeCN/H_2O, spun through a NANOSEP 3K OMEGA size exclusion centrifugal column (Pall) and submitted for LCMS analysis.

3.4.2.2 Sonication with buffer B

Steenkamp *et al.* (*9*) used this method to purify mycothiol from *M. smegmatis*. In this method the cells were also disrupted through sonication, but the extraction buffer used consisted of 0.25M perchloric acid and 2mM EDTA in a 40% MeCN/H_2O. After the cell debris was removed the supernatant was directly lyophilized overnight. The resulting residue was processed as mentioned above before LCMS analysis.

3.4.2.3 BugBuster® extraction method

BugBuster® protein extraction reagent (Novagen) was also used to extract the analytes. Cell pellets were resuspended in five times less extraction buffer than the culture sample the cell were pelleted from. The suspensions were incubated for 40min at room temperature on a shaking platform. The cell debris was removed through centrifugation and the supernatant lyophilized overnight. The remaining residue was redissolved in 50% MeCN/H_2O and processed as mentioned above.

3.4.3 LCMS analysis

Samples were analyzed on an ACQUITY UPLC® system (Waters Corp.) with an autosampler and a Synergy 4 µM Fusion RP, 250x2mm column (Phenomenex). The sample injection volume was 20µl and the auto sampler syringe was washed with solvent A (0.1% formic acid in water) before each injection. A gradient elution program with a flow-rate of 0.20 ml/min was used for the analysis. The gradient was as follows: 100% solvent A for 8 min; 7 min linear increase up to 95% solvent B (0.1% formic acid in acetonitrile); 95% B step for 3 min; 95% solvent A from 18 to 20 min. The total analysis time was 20 min.

Detection was performed on a QTOF Ultima API quadrupole mass spectrometer (Micromass, Manchester, UK). Analytes were detected in the positive ion mode. The capillary voltage was set at 3500 V. The source temperature and the nebulization gas temperature were set at 120 °C and 400 °C, respectively. The cone voltages were set at 35V. Data was processed using MassLynx™ software (Micromass, Manchester, UK).

3.4.4 Induction of oxidative stress

3.4.4.1 Analyte extraction done with all three extraction methods

M. smegmatis stock (260µl) was used to inoculate 13ml of 7H9 media and incubated for 24h at 37°C. This culture was used to inoculate the four 300ml and fifteen 1.5ml (in 2ml Eppendorf Lid_{BAC}® tubes) cultures used in the experiment. A 50ml sample was taken out of each of the four 300ml cultures before H_2O_2 (final concentration of 10mM) was added to one culture and diamide (final concentration of 5mM) to another, in order to induce oxidative stress. Nothing was added to the other two 300ml cultures, as they were used as blanks. The samples taken before the diamide and H_2O_2 was added, was used as the 0h time point samples. Samples (50ml) were also taken at the 1, 2, 4 and 8h time points. Cells from these samples were collected by means of centrifugation and pellets were stored at -20°C until processing.

In the case of the 1.5ml cultures, samples were not taken, as the whole sample was used. Thus at the 0h time point, four of the 1.5ml cultures were removed and cells collected through centrifugation. Diamide was added to four samples and H_2O_2 to the other four of the remaining 1.5ml cultures, resulting in final concentrations of 5mM and 10mM respectively. At each of the other time points, an additional four cultures were removed, one to which diamide was added, one to which H_2O_2 was added and two to which nothing was added. Each time the cells were cetrifuged and stored at -20°C until required.

Each of the pellets obtained from the 50ml samples were divided into two pellets with equal mass, resulting in a total of 24 pellets. Sonication with buffer A was used to process 12 of the pellets and the remaining 12 was processed using sonication with buffer B. The cell pellets from the 1.5ml cultures were extracted with the BugBuster® method, but the resuspended cells were incubated for 120min instead of the 40min.

3.4.4.2 Analyte extraction with the BugBuster® method

Two 300ml stationary phase *M. smegmatis* cultures were prepared as described above. Three 0h time point samples (15ml each) were taken from each culture before the addition of H_2O_2. H_2O_2 was added to one of the cultures to a final concentration of

10mM. The other culture was used as control and nothing was added to it. Another 3x15ml samples were taken from each culture at the 1h and 6h time points. Cells were collected through centrifugation and stored at -20°C until required. Extractions were performed by resuspending the cells in 1ml of BugBuster® protein extraction reagent followed by incubation for 120 min at room temperature on a shaking platform. Cell debris was removed by centrifugation and the supernatant lyophilized overnight. The resulting residue was reconstituted in 250µl 50% MeCN/H_2O, spun through a NANOSEP 3K OMEGA centrifugal column (Pall) and submitted for LCMS analysis.

3.4.5 Statistical Data Analysis

All statistical data analysis and graphical presentation of the data was performed with Microsoft® Office Excel 2003.

3.5 Reference

(1) Bouligand, J., Deroussent, A., Paci, A., Morizet, J., and Vassal, G. (2006) Liquid chromatography-tandem mass spectrometry assay of reduced and oxidized glutathione and main precursors in mice liver. *Journal of Chromatography, B: Analytical Technologies in the Biomedical and Life Sciences 832*, 67-74.

(2) Rossi, R., Dalle-Donne, I., Milzani, A., and Giustarini, D. (2006) Oxidized forms of glutathione in peripheral blood as biomarkers of oxidative stress. *Clinical Chemistry (Washington, DC, United States) 52*, 1406-1414.

(3) Newton, G. L., Arnold, K., Price, M. S., Sherrill, C., Delcardayre, S. B., Aharonowitz, Y., Cohen, G., Davies, J., Fahey, R. C., and Davis, C. (1996) Distribution of thiols in microorganisms: mycothiol is a major thiol in most actinomycetes. *Journal of Bacteriology 178*, 1990-5.

(4) Anderberg, S. J., Newton, G. L., and Fahey, R. C. (1998) Mycothiol biosynthesis and metabolism. Cellular levels of potential intermediates in the biosynthesis and degradation of mycothiol in *Mycobacterium smegmatis*. *Journal of Biological Chemistry 273*, 30391-30397.

(5) Newton, G. L., Av-Gay, Y., and Fahey, R. C. (2000) N-acetyl-1-D-*myo*-inosityl-2-amino-2-deoxy-α-D-glucopyranoside deacetylase (MshB) is a key enzyme in mycothiol biosynthesis. *Journal of Bacteriology 182*, 6958-6963.

(6) Newton, G. L., Ko, M., Ta, P., Av-Gay, Y., and Fahey, R. C. (2006) Purification and characterization of *Mycobacterium tuberculosis* 1D-*myo*-inosityl-2-acetamido-2-deoxy-α-D-glucopyranoside deacetylase, MshB, a mycothiol biosynthetic enzyme. *Protein Expression and Purification 47*, 542-550.

(7) Ung, K. S. E., and Av-Gay, Y. (2006) Mycothiol-dependent mycobacterial response to oxidative stress. *FEBS Letters 580*, 2712-2716.

(8) Lu, W., Kimball, E., and Rabinowitz, J. D. (2006) A High-Performance Liquid Chromatography-Tandem Mass Spectrometry Method for Quantitation of

Nitrogen-Containing Intracellular Metabolites. *Journal of the American Society for Mass Spectrometry 17*, 37-50.

(9) Steenkamp, D. J., and Vogt, R. N. (2004) Preparation and utilization of a reagent for the isolation and purification of low-molecular-mass thiols. *Analytical Biochemistry 325*, 21-27.

(10) Jardine, M. A., Spies, H. S. C., Nkambule, C. M., Gammon, D. W., and Steenkamp, D. J. (2002) Synthesis of mycothiol, 1D-1-O-(2-[N-acetyl-L-cysteinyl]amino-2-deoxy-α-D-glucopyranosyl)-*myo*-inositol, principal low molecular mass thiol in the actinomycetes. *Bioorganic & Medicinal Chemistry 10*, 875-881.

(11) Dosanjh Nirpjit, S., Rawat, M., Chung, J.-H., and Av-Gay, Y. (2005) Thiol specific oxidative stress response in Mycobacteria. *FEMS microbiology letters 249*, 87-94.

Chapter 4

Alternate substrates of MshB and Mtr

4.1 Introduction

As discussed in Chapter 1, mycothiol (MSH) has a very unique structure, which in the past has inspired the synthesis of analogues of the parent structure and of its biosynthetic pathway intermediates (Figure 4.1).

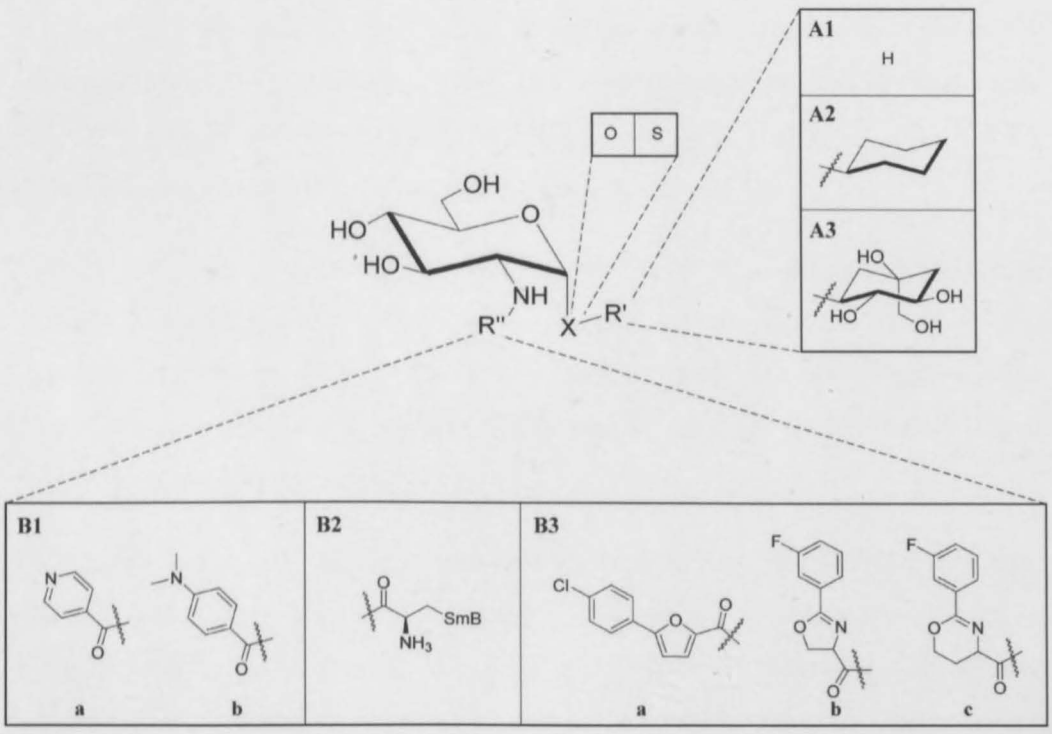

Figure 4.1: Key substrate analogues of mycothiol and its pathway intermediates.

The first reported MSH analogue was a cyclohexyl thioglycoside obtained by Knapp *et al.* through the free radical reaction of 2-acetamido-2-deoxy-3,4,6-tri-*O*-acetyl-1-α-thio-D-glucopyranose (αGlcNAc-mercaptan) with cyclohexene (Figure 4.1, **A2**)(*1*). The advantage of thioglycosides is that generally they are kinetically more stable than oxygen glycosides with respect to enzymatic hydrolysis by glycosidases (*2*). This

means that inside a cell thioglycosides are not hydrolyzed easily, increasing the chance of the thioglycoside reaching its intended target. The cyclohexyl thioglycoside was later used as a scaffold in the synthesis of a library of 36 substrate analogues for mycothiol-*S*-conjugate amidase (Mca) (*3*). The compounds in the library differed from one another by the moieties bound to the free amine through an amide bond.

Metaferia *et al.* used a natural product inspired pseudo-disaccharide scaffold to synthesize a series of inhibitors of MshB. These inhibitors again differed from one another by the moieties bound to the free amine. The inhibitors that showed the best inhibition had the moieties **B3a-c** (Figure 4.1), which were all derived from natural products (*4*). Newton *et al.* showed that the natural glucosamine-inositol disaccharide connected to a monobromobinane (mB) derivatised cysteine (Figure 4.1, **B2**) through a peptide bond with the glucosamine amine, is a better substrate for MshB than its natural substrate αGlcNAc-Ins. The reasons for this increased activity are still unknown. Also αGlcNAc, with no moieties bound to the anomeric oxygen (Figure 4.1, **A1**), is a 100 times less active with MshB than αGlcNAc-Ins (*5*).

A library of substrate mimicking inhibitors was also synthesized and tested against Mca (*6*). The authors used a quinic acid (Figure 4.1, **A3**) containing scaffold, with an *O*-glycosidic bond, as the basis for their inhibitor library. The two compounds that showed the best inhibition were derivatised with substituents **B1a** and **B1b** (Figure 4.1) on the glucosamine amine.

Thus, as was proven in the discussion above, the αGlcNAc or αGlcNAc-mercaptan moieties proved to be useful core synthons for the design of substrate analogues for MSH and its pathway intermediates. In this chapter we report on the alternate substrates for MshB and Mtr that was synthesized during this study.

4.2 Synthesis of key alternate substrate intermediates

The basic intermediates used in the synthesis of all the thioglycosides alternate substrates for MshB during this study is 2-acetamido-2-deoxy-3,4,6-tri-*O*-acetyl-1-α-thio-D-glucopyranose (αGlcNAc mercaptan) (**4.7**). Compound **4.7** was synthesized through the route depicted in Scheme 4.1, which is well characterised in previous glycosidic studies (*7-9*). 1,3,4,6-Tetra-*O*-acetyl-glucosamine hydrochloride (**4.4**), an

intermediate in the synthesis of compound **4.7**, was also used in the synthesis of des-*myo*-inositol mycothiol disulfide (DI-MSSM)

1,3,4,6-Tetra-*O*-acetyl-glucosamine hydrochloride (**4.4**) was synthesized from the commercially available D-glucosamine hydrochloride (**4.1**) as described by Myszka *et al.* (*7*). 1,3,4,6-Tetra-*O*-acetyl-2-deoxy-2-acetamido-β-D-glucopyranose (β-D-GlcNAc) (**4.5**) was prepared by the reaction of 1,3,4,6-tetra-*O*-acetyl-glucosamine hydrochloride (**4.4**) with pyridine and acetic anhydride. The β-D-GlcNAc (**4.5**) was reacted with Lawesson's reagent to produce the GlcNAc-thiazoline (**4.6**). The thiazoline ring of GlcNAc-thiazoline (**4.6**) was hydrolyzed to produce αGlcNAc mercaptan (**4.7**). Both the synthesis and the hydrolysis of the thiazoline ring was previously described by Knapp *et al.* (*8, 9*).

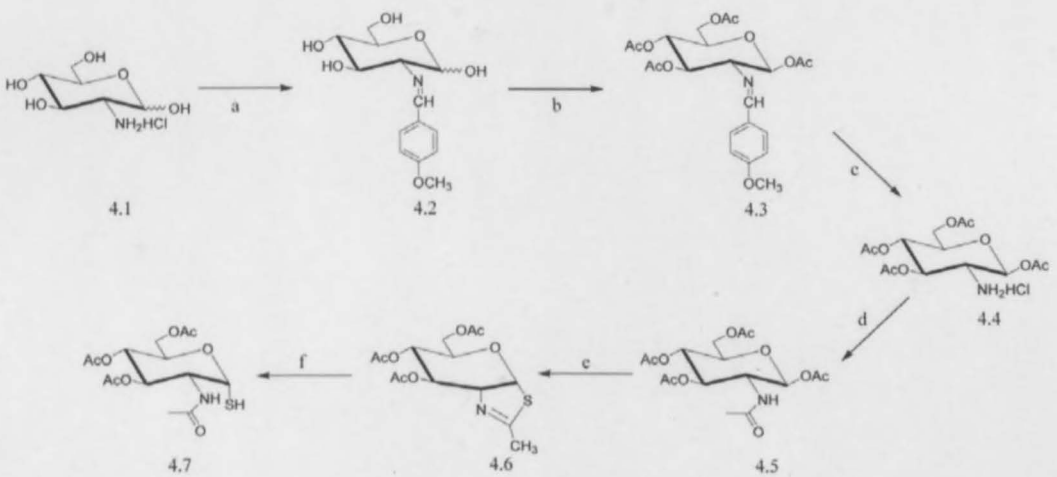

Scheme 4.1: Reagents and conditions: (a) aq 1M NaOH, p-CH_3O-C_6H_4-CHO; (b) Py, Ac_2O; (c) acetone 5M HCl; (d) Py Ac_2O; (e) Lawesson's reagent, toluene, 80°C; (f) TFA, wet MeOH

4.3 Thioglycosides

4.3.1 Thioglycoside disaccharides

As discussed previously, the largest part of the MSH molecule is the glucosamine-inositol disaccharide moiety. This disaccharide moiety is the recognition site used by enzymes in the binding of MSH and its intermediates. We were interested in the binding specificity of MshB to various disaccharide scaffolds, differing in particular at the inositol or cyclohexane moiety. Thus, during this study a series of thioglycoside

disaccharides scaffolds were synthesized. These thioglycoside disaccharide scaffolds will serve as starting points for synthesis of inhibitor or substrate analogue libraries targeted against MshB and other MSH binding enzymes.

The αGlcNAc mercaptan (**4.7**) was reacted with the *O*-acetylated sugars (Table 4.1, **4.8** and **4.9**) in the presence of boron trifluoride etherate-complex (BF_3OEt_2) (see Scheme 4.2). The anomeric acetate on the monosaccharide moieties was eliminated in the process, to form the oxonium intermediate. Addition of the thiol nucleophile occurs from either side of the plane of the electrophilic anomeric centre, giving rise to the formation of α- and β-coupled *O*-acetylated products **4.11a** and **4.12a** respectively (Table 4.1).

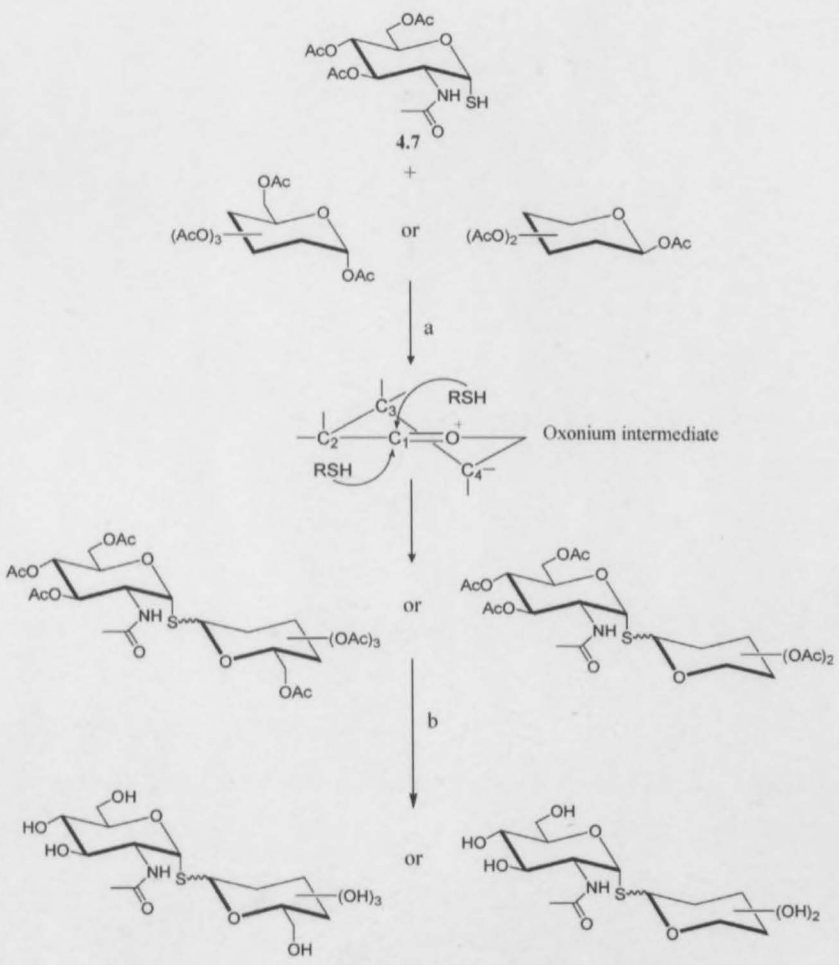

Scheme 4.2: General reaction for the synthesis of the thioglycoside disaccharide molecules.

The deacetylation of these compounds was performed with sodium methoxide in MeOH, resulting in the formation of deacetylated compounds, **4.11b** and **4.12b** (Table 4.1). The α/β anomeric proton ratios ranged from 1:1 to 1:2 as determined by the coupling constants of the anomeric protons (NMR).

Table 4.1: Synthesized thioglycoside disaccharides.

Monosaccharide	Product	δ (ppm)	Hz	α/β
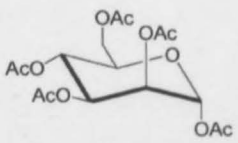 **4.8**	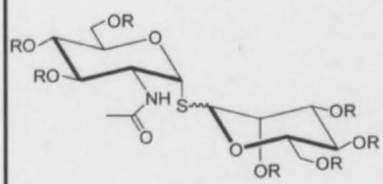 **4.11a,b**	5.0 5.1 5.4	11.7 5.57 5.46	1:2
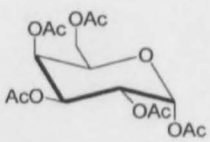 **4.9**	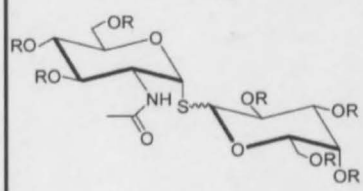 **4.12a,b**	5.0 5.2 5.5	4.75 4.82 4.90	1:1
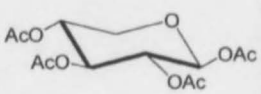 **4.10**	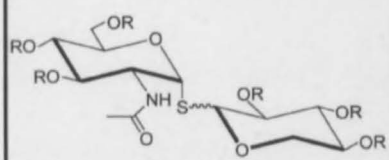 **4.13a,b** R_a = Ac R_b = H	#	#	#

[#] The synthesis of **4.13a,b** is currently in progress and no analytical data is available this time.

4.3.2 Fluorogenic substrates

As discussed in Chapter 3, current methods for the quantitation of MshB mediated *N*-deacetylated compounds all require the derivatisation of the free amine followed by HPLC-UV analysis. This limits the screening throughput of potential alternate substrates or inhibitors of MshB. However, to address this shortcoming a fluorescent binding assay was developed in a previous study for the evaluation of inhibitors against the MshB homologue Mca. In these assays MSH was derivatised with monobromobimane (MSmB) (K_m of 500±50μM) (*5*) and used as a competitive binding molecule with the possible inhibitors (*10*). The amount of cysteine-bimane

released was monitored by HPLC-UV and was a measure of the inhibitor's binding affinity to Mca.

During this study we synthesized a series of fluorogenic thioglycoside molecules as potential alternate substrates of MshB. These molecules could be used in competitive binding assays, where they serve as fluorogenic substrates by which the binding of possible inhibitors could be quantified. Since these molecules are UV active, differences in the UV or fluorescence spectra of their enzyme-mediated products could be used in the development of a high-throughput MshB assay

These substrates were synthesized through the triethylamine-mediated alkylation reactions of the free thiol of 2-acetamido-2-deoxy-3,4,6-tri-*O*-acetyl-1-α-thio-D-glucopyranose (**4.7**) and various UV active aryl- or alkyl halides (Table 4.2, **4.14-4.17**) (Scheme 4.3).

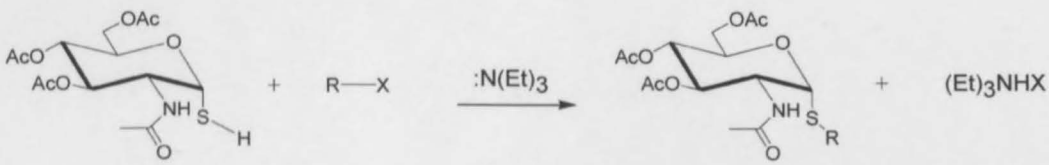

Scheme 4.3: General reaction for the synthesis of the fluorogenic substrates.

The alkylation reaction resulted in the formation of thioglycoside compounds **4.18a**, **4.19a**, **4.20a** and **4.21a** respectively (Table 4.2). The *O*-deacetylation of **4.18a-4.20a** was performed with Amberlite IRA400 (OH) resin in a 19% H_2O, 50% MeOH and 31% acetone mixture (*11*), to produce **4.18b-4.20b**. This mild deprotection was used because of the difficulties experienced with other deprotection methods. For example, in the deprotection of **4.19a** in particular it was found that the S-aryl/alkyl bond was easily cleaved if a strong base such as sodium methoxide had to be used. The coupling constants of the anomeric protons are noted in Table 4.2 and are all consistent with an α-coupled thioglycoside.

Table 4.2: Fluorogenic substrates

Alkyl/arylhalide	Product	δ (ppm)	Hz
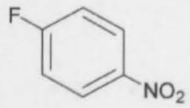 **4.14**	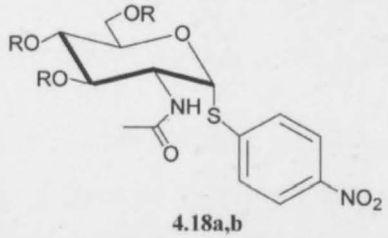 **4.18a,b**	6.1	5.36
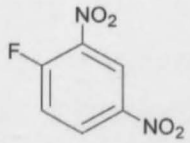 **4.15**	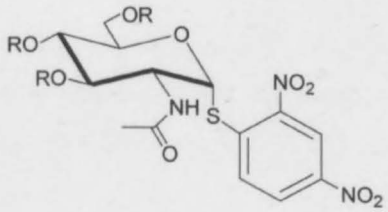 **4.19a,b**	6.1	5.44
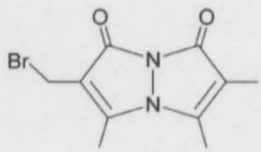 **4.16**	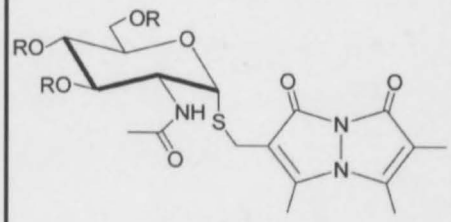 **4.20a,b**	5.5	5.51
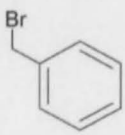 **4.17**	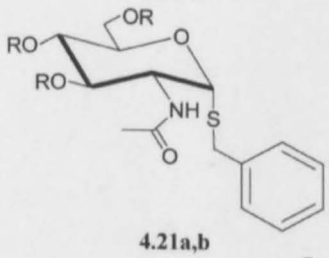 **4.21a,b** R_a = Ac R_b = H	#	#

[#] The NMR characterization of **4.18b**, **4.20b** and **4.21a** is currently in progress, after which the deacetylation of **4.21a** will be attempted.

4.4 Des-*myo*-inositol mycothiol disulfide

The synthesis of 2(*N*-acetyl-L-cysteinyl)-amino-2-deoxy-(α/β)-D-glucopyranoside (also known as des-*myo*-insitol mycothiol disulfide, DI-MSSM) was previously reported by Patel and Blanchard (*12*). This molecule is a truncated form of mycothiol as it lacks the inositol moiety. The authors used DI-MSSM as a substrate analogue (K_m of 510±40μM) for all subsequent kinetic studies of the Mtr enzyme (*13, 14*).

Since DI-MSSM is a less expensive alternative to synthetic MSH, we also set out to prepare this compound as a substrate with which the activity of the *E. coli* expressed Mtr enzyme could be tested. During this study DI-MSSM was synthesized by a different synthetic route than the one previously described.

The synthesis proceeded by the formation of amide bonds between $(Boc\text{-}Cys\text{-}OH)_2$ (**4.22**) and two equivalents of the protected glucosamine (**4.4**), to produce the disulfide compound (**4.23**). This was accomplished by an EDC coupling reaction (Scheme 4.4, route a). The acid catalyzed deprotection (Scheme 4.4, route b) of the cysteine α-amino Boc protecting group resulted in the formation of the free amine compound (**4.24**). Subsequent *N*-acetylation of compound (**4.25**) was achieved by the reaction of the free amine with an acetic anhydride-pyridine mixture (Scheme 4.4, route c). Deprotection of compound (**4.25**) with magnesium methoxide in methanol, followed by treatment with Dowex-50W, successfully gave the *O*-deacetylated compound, DI-MSSM (**4.26**). The structure of **4.26** was confirmed by ^{1}H and ^{13}C NMR spectra and correlates to that reported in the literature (*12*).

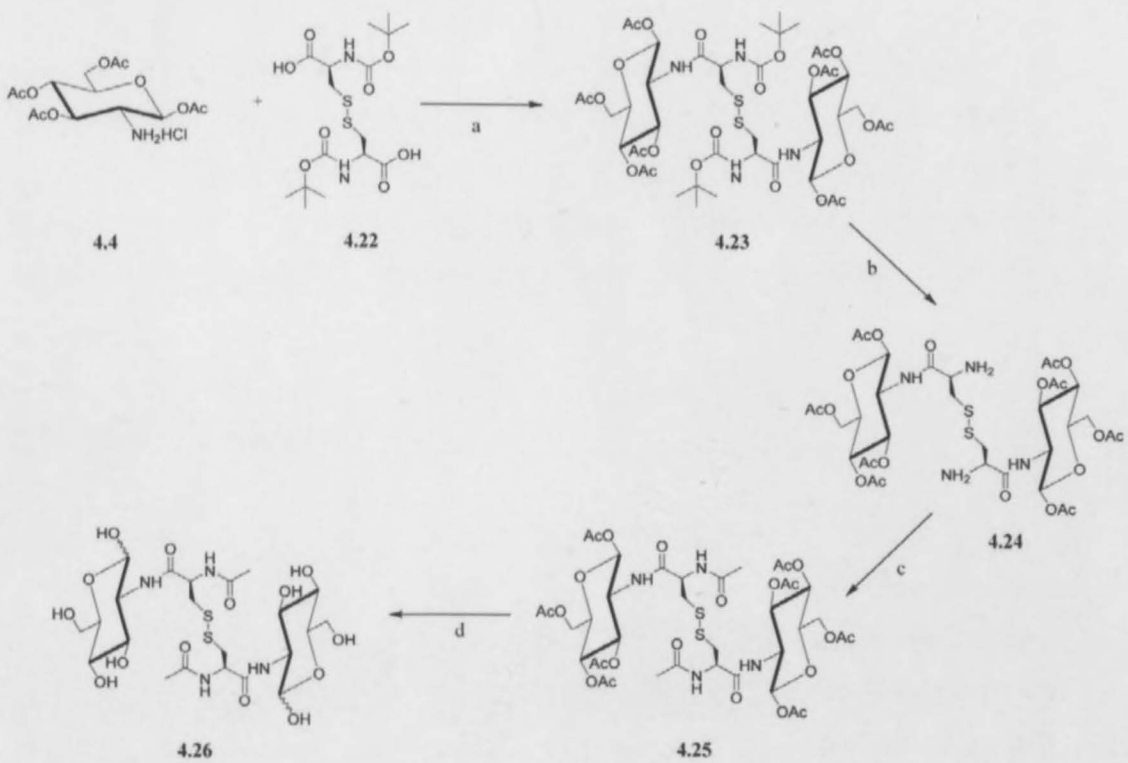

Scheme 4.4: Reagents and conditions: (a) DIPEA, HOBt, EDC; (b) 50% DCM, TFA; (c) Py Ac_2O; (d) 1. $Mg(OMe)_2$, MeOH, 2. Dowex-50W (H^+)

4.5 Conclusion

In a study performed by Newton *et al.* (*5*) it was found that there is an structural similarity in the types of molecules that effectively bind to Mca and MshB. From this finding, the cyclohexyl thioglycoside scaffold used by Knapp *et al.* (*3*) in the Mca substrate library synthesis was also later used by Metaferia *et al.* (*4*) in the synthesis of a series of inhibitors against MshB. Thus the thioglycoside disaccharides synthesized successfully during this study will serve as glycosidase resistant scaffolds for substrate libraries against other glycosyl inositol binding enzymes, like Mca and not only MshB.

We also successfully synthesized a series of fluorogenic thioglycosides. These molecules are indispensable toward the development of a high throughput screen for MshB. Another advantage of these molecules is that although the molecules are UV active, *N*-deacetylation, whether enzymatically or chemically mediated, leads to the free amine. Thus, further elaboration through the amine group could lead to molecules which may display interesting inhibition properties (*4, 15*).

The truncated analogue of mycothiol, DI-MSSM, was successfully synthesized by an improved method compared to the published synthesis (*12*). DI-MSSM's main utility lies in its ability to act as a substrate of the Mtr enzyme, and having it available allowed us to test the activity of the Mtr enzyme expressed during this study. DI-MSSM can also be used in the protein crystallization trails of Mtr, where it may serve as a ligand.

4.6 Experimental

4.6.1 General

Chemicals were purchased from Sigma Aldrich. All reactions were performed at room temperature unless specified otherwise. Flash chromatography was performed using a silica to crude reaction mixture ratio of 20:1 by weight. Thin layer chromatography (TLC) was performed on Merck Aluminium Silica gel 60 F_{254} plates. All compounds containing free amines were visualized on TLC plates by spraying the plates with ninhydrin solution (1.5% ninhydrin in n-butanol with 3% AcOH) followed by heating

the plates until the colour developed. All fluorogenic compounds were visualized on the TLC plate under UV light. ESI-MS analysis was performed on a QTOF Ultima API quadrupole mass spectrometer. ^{1}H and ^{13}C NMR was performed on the Varian Unity Inova 600MHz NMR and Varian VXR 300MHz NMR spectrometers.

4.6.2 Synthesis of thioglycoside compounds

4.6.2.1 Synthesis of 2-Acetamido-2-deoxy-3,4,6-tri-O-acetyl-1-α-thio-D-glucopyranose

1,3,4,6-tetra-*O*-acetyl-glucosamine hydrochloride (4.4). The same synthetic procedure was followed as described by Myszka *et al.* (*7*) for the preparation of 2-deoxy-2-[*p*-methoxybenzylidene(amino)]-D-glucopyranse (**4.2**). To a solution of D-glucosamine hydrochloride (25g, 0.12mol) (**4.1**) in 1M NaOH was added p-anisaldehyde (17ml, 0.14mol). The reaction was allowed to stir for 2 hr and refrigerated overnight. The white precipitate was filtered off and washed with cold water and a 1:1 EtOH, Et_2O mixture. A yield of 65% (21g) was achieved. Intermediate compound **4.2** (21g, 0.071mol) was *O*-acetylated with pyridine (135ml, 113mmol) and acetic anhydride (75ml, 0.9mol) to produce compound **4.3** (25g, 75% yield). The latter compound (25g, 54mmol) was dissolved in warm acetone (200ml) to which 5M HCl (10ml) was added. The mixture was allowed to cool, followed by the addition of 200ml Et_2O. The mixture was allowed to stir for 2 hrs, followed by refrigeration overnight. The resulting precipitate was filtered and washed with Et_2O. A yield of 80% (15g) was achieved.

1,3,4,6-tetra-*O*-acetyl-2-deoxy-2-acetamido-β-D-gluco-pyranose (4.5). Compound **4.4** (15g, 32mmol) was reacted with acetic anhydride (12ml, 3.5mmol) and pyridine (12ml, 3.5mmol) in 100ml DCM, as described by Myszka *et al.* (*7*). The reaction mixture was concentrated and stirred in a 15ml ethyl acetate/H_2O mixture for 30mins, after which 2ml 1M HCl was added. The H_2O and organic layers was allowed to separate, the ethyl acetate was dried over anhydrous

sodium carbonate, followed by the evaporation of the organic solvent *in vacuo*, producing 3.22g (26% yield) of compound **4.5**.

(3a*R*,5*R*,6*R*,7*R*,7a*R*)-5-(Acetoxymethyl-6,7-diacetoxy-2-methyl-5,6,7,7a-tetra-hydro-3a*H*-pyrano[3,2-*d*]thiazole (4.6). 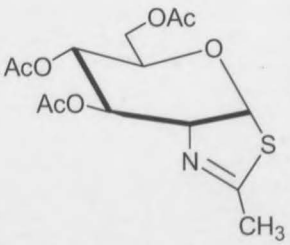 A solution of compound **4.5** (3.2g, 8.2mmol) in toluene was reacted with Lawesson's reagent (2.1g, 5.4mmol) in 30ml toluene. The reaction was heated at 80°C for 1.5 hrs, after which the pH of the reaction was adjusted by the addition of 3g sodium bicarbonate (*9*). Compound **4.6** was purified using flash chromatography (30%EtOAc/DCM) to obtain a yield of 63% (1.81g).

2-Acetamido-2-deoxy-3,4,6-tri-*O*-acetyl-1-α-thio-D-glucopyranose (4.7). 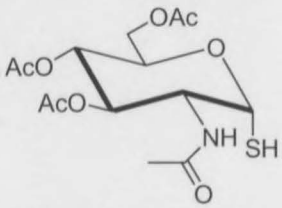 A solution of compound **4.6** (1g; 2.9mmol) in 10ml MeOH was cooled to 0°C, before TFA (300µl) and H_2O (300µl) was added (*9*). The reaction was allowed to warm to room temperature over a period of 2 hr. Subsequently, the reaction mixture was concentrated to obtain a yield of 86% (900mg) of compound **4.7**. ^1H NMR's of **4.6** and **4.7** was performed in $CDCl_3$ and identical spectra to that reported by Knapp and Myers (*9*) was obtained.

4.6.2.2 Thioglycoside disaccharides

1-*S*-(2-Acetamido-2-deoxy-3,4,6-tri-*O*-acetyl- α -D-glucopyranosyl)-1-thio-2,3,4,6-tetra-*O*-acetyl-α/□-D-mannopyranoside (4.11a). 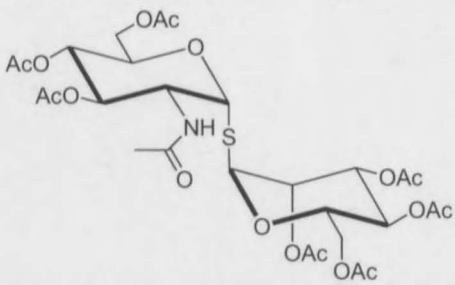 To a solution of compound 4.7 (500mg, 1.37mmol) in 10ml DCM, was added α-D-mannose pentaacetate (4.8) (530mg, 1.37mmol) and BF_3OEt_2 (500µl, 4.18mmol). The reaction mixture was allowed to stir at ambient temp under an N_2 atmosphere for 24hrs. The reaction was then concentrated and the resulting crude product was purified using flash chromatography (5%MeOH/DCM). Fractions containing the product (4.11a) were concentrated, resulting in a yield of 530mg (55%) of a colourless oil.

1-*S*-(2-Acetamido-2-deoxy-α-D-glucopyranosyl)-1-thio--α/□-D-mannopyranoside (4.11b). To a solution of compound **4.11a** (220mg, 0.317mmol) in 8ml MeOH, was added 12ml of a 180mM solution of $NaOCH_3$ in MeOH. The reaction mixture was allowed to stir for 18hrs. The reaction was purified using C18 flash chromatography (5%MeOH/H_2O), resulting in compound **4.11b** as an off white solid, with a yield of 80mg (63%).

1-*S*-(2-Acetamido-2-deoxy-3,4,6-tri-*O*-acetyl- α -D-glucopyranosyl)-1-thio-2,3,4,6-tetra-*O*-acetyl-α/β-D-galactopyranoside (4.12a). To a solution of compound **4.7** (500mg, 1.37mmol) in 10ml DCM, was added α-D-galactose pentaacetate (**4.9**) (530mg, 1.37mmol) and BF_3OEt_2 (500µl, 4.18mmol). The reaction conditions were the same as stated in the preparation of **4.11a**. The reaction mixture was concentrated and purified using flash chromatography (5%MeOH/DCM), resulting in 480mg (50% yield) of a light yellow oil (**4.12a**).

1-*S*-(2-Acetamido-2-deoxy-α-D-glucopyranosyl)-1-thio--α/β-D-galactopyranoside (4.12b). The *O*-deacetylation of compound **4.12a** to produce compound **4.12b** was performed as for compound **4.11b** above. Thus, 300mg (0.433mmol) of compound **4.12a** was deprotected to produce 85mg (49% yield) of a light yellow solid.

4.6.2.3 Fluorogenic substrates

4-Nitrophenyl 2-acetamido-2-deoxy-1-thio-3,4,6-tri-*O*-acetyl-α-D-glucopyranose (4.18a). A solution of compound **4.7** (280mg, 0.770mmol) in 5ml DCM was stirred under an N_2 atmosphere. To this solution was added 1-Fluoro-4-nitrobenzene (**4.14**)

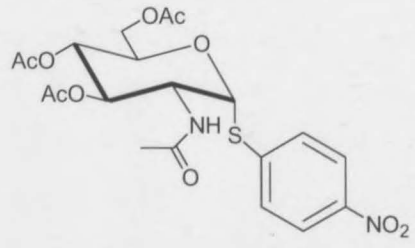

(164µl, 2.8mmol) and TEA (130µl, 1.15mmol). The reaction was allowed to stir for 24 hrs, and then concentrated. The product (4.11) was purified from the crude reaction mixture using flash chromatography (2%MeOH/DCM). Fractions containing pure compound were collected and the solvent removed *in vacuo*, resulting in 360mg (96% yield) of compound (**4.18a**) as a yellow solid. ^{1}H NMR ($CDCl_3$, 600MHz, 25°C): δ 1.974 (s, 3H), 2.026 (s, 3H), 2.061 (s, 3H), 2.081 (s, 3H), 4.070 (dd, 1H), 4.254 (dd, 1H), 4.373 (m, 1H), 4.590 (m, 1H), 5.169 (m, 2H), 5.902 (d, 1H), 6.013 (d, 1H), 7.560 (d, 2H), 8.152 (d, 2H); ESI-MS(+): *m/z* 485 $[M+H]^+$, 507 $[M+Na]^+$.

2,4-Dinitrophenyl 2-acetamido-2-deoxy-1-thio-3,4,6-tri-*O*-acetyl-α-D-glucopyranose (4.19a). To a solution of compound **4.7** (500mg, 1.37mmol) in 10ml DCM was added 1-Fluoro-2,4-dinitrobenzene (**4.15**) (173µl, 1.37mmol) and TEA (230µl, 1.65mmol). The mixture was allowed to stir under a N_2 atmosphere for 24hrs. The reaction mixture was then concentrated and the resulting crude product was purified using flash chromatography (2%MeOH/DCM). Fractions containing the product were concentrated, resulting in 570mg (78% yield) of compound (**4.19a**) as a yellow solid. ^{1}H NMR ($CDCl_3$, 300MHz, 25°C): δ 1.935 (s, 3H), 1.991 (s, 3H), 2.034 (s, 3H), 2.066 (s, 3H), 4.043 (dd, 1H), 4.265 (m, 2H), 4.626 (m, 2H), 5.235 (m, 2H), 6.100 (d, 1H), 8.045 (d, , 1H), 8.406 (dd, 1H), 9.026 (d, 1H); ESI-MS(+): *m/z* 530 $[M+H]^+$.

2,4-Dinitrophenyl 2-acetamido-2-deoxy-1-thio-α-D-glucopyranose (4.19b). To a solution of compound **4.19a** (230mg, 0.434mmol) in 18ml of H_2O (19%), MeOH (50%) and acetone (31%), was added 2.3g of Amberlite IRA400 (OH). The reaction mixture was allowed to stir for 1hr at ambient temperature. The volatile solvents were removed *in vacuo* and the residual aqueous product mixture was subjected to C-18 flash chromatography (50% MeCN/H_2O).

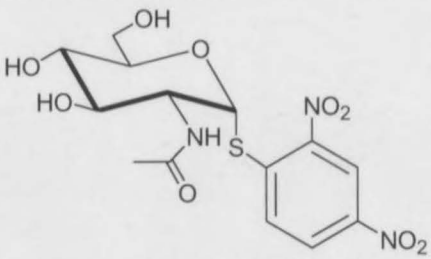

Aqueous fractions containing the compound were collected and dried by lyophilization, resulting in 50mg (28% yield) of compound **4.19b**. ^{1}H NMR (DMSO–d_6, 300MHz, 25°C): δ 1.829 (s, 3H), 3.264 (m, 1H), 3.516 (q, 1H), 3.588 (m, 2H), 3.674 (m, 1H), 3.983 (m, 1H), 4.554 (t, 1H), 5.125 (d, 1H), 5.272 (d, 1H), 6.051 (d, 1H), 8.150 (d, 1H), 8.273 (d, 1H), 8.426 (dd, 1H), 8.818 (d, 1H); ESI-MS(+): *m/z* 404 $[M+H]^+$, 426 $[M+Na]^+$.

Bimane 2-acetamido-2-deoxy-1-thio-3,4,6-tri-*O*-acetyl-α-D-glucopyranose (4.20a). To a solution of compound **4.7** (27mg, 0.074mmol) in 2ml DCM was added of monobromobimane (24mg, 0.089mmol) (**4.16**) and TEA (12µl, 0.089mmol). The reaction was allowed to stir under a N_2 atmosphere for 24 hrs, followed by the removal of the solvent *in vacuo*. The resulting crude product (**4.20a**) was purified using flash chromatography (2%MeOH/DCM). Fractions containing the compound were collected and the solvent removed *in vacuo*, resulting in 360mg (96% yield) of compound (**4.20a**) as a yellow solid. ^{1}H NMR ($CDCl_3$, 400MHz, 25°C): δ 1.844 (s, 3H), 1.884 (s, 3H), 1.940 (s, 3H), 2.058 (s, 6H), 2.092 (s, 3H), 2.379 (s, 3H), 3.729 (q, 2H), 4.095 (m, 1H), 4.251 (m, 2H), 4.468 (m, 1H), 5.038 (t, 1H), 5.139 (t, 1H), 5.667 (d, 1H), 5.813 (d, 1H); ESI-MS(+): *m/z* 554 $[M+H]^+$, 576 $[M+Na]^+$.

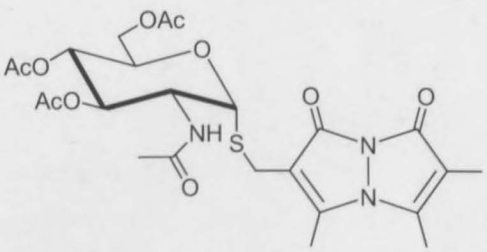

Benzyl 2-acetamido-2-deoxy-1-thio-3,4,6-tri-*O*-acetyl-α-D-glucopyranose (4.21a). To a solution of compound **4.7** (220mg, 0.61mmol) in 2ml DCM, was added benzylbromide (87µl, 0.732mmol) (**4.17**) and TEA (170µl, 1.22mmol). The reaction mixture was allowed to stir under a N_2 atmosphere for 24hrs. Subsequently the reaction was concentrated and the resulting crude product was purified using flash chromatography (2%MeOH/DCM). Fractions containing the product were concentrated, resulting in 170mg (62% yield) of pure **4.21a** as a off white oil.

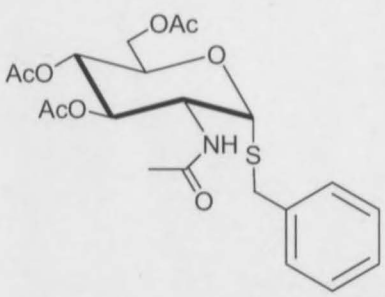

4.6.2.4 Synthesis of DI-MSSM

2(*N-tert*-Butyloxycarbonyl-L-cysteinyl)-amino-2-deoxy-1,3,4,6-tetra-*O*-acetyl-β-D-glucopyranoside disulfide (4.23). A solution $(Boc\text{-}Cys\text{-}OH)_2$ (500mg, 1.14mmol) (**4.22**), **4.4** (960mg, 2.5mmol), HOBt (380mg, 2.8mmol), 550mg 4Å molecular sieves and DIPEA (850µl, 5mmol) in 12ml dry DMF was cooled to 0°C before EDC (540mg, 2.8mmol) was added under a N_2 atmosphere. The reaction mixture was allowed to stir at 0°C for 1hr followed by room temperature over an 18hr period. The DMF was evaporated *in vacuo,* followed by the addition of 25ml of a 50% ethyl acetate/H_2O mixture and the resulting mixture was allowed to stir for 30min. The H_2O and organic layer were allowed to separate. The ethyl acetate was dried over Na_2SO_4, followed by evaporation *in vacuo*, producing 1.12g (90% yield) of **4.23** as a white solid. ^{1}H NMR (DMSO–d_6, 300MHz, 25°C): δ 1.364 (s, 18H), 1.901 (s, 6H), 1.963 (s, 6H), 2.011 (d, 12H), 2.831 (m, 4H), 3.986 (m, 6H), 4.185 (dd, 3H), 4.875 (t, 3H), 5.268 (t, 3H), 5.763 (d, 2H), 7.072 (d, 2H), 7.989 (d, 2H); ESI-MS (+): *m/z* 1099.35 $[M+H]^+$, 1122 $[M+Na]^+$.

2(L-cysteinyl)-amino-2-deoxy-1,3,4,6-tetra-*O*-acetyl-β-D-glucopyranoside disulfide (4.24). To a solution of compound **4.23** (600mg, 0.550mmol) in 5.5ml DCM at 0°C was added TFA (2.5ml, 34mmol). The reaction mixture was monitored by TLC and concentrated after being allowed to stir for 2hrs at 0°C. The reaction mixture was evaporated under reduced pressure overnight, producing 500mg (85% yield) of compound **(4.24)** as a deep red powder. ^{1}H NMR (DMSO–d_6, 300MHz, 25°C): δ 1.984 (m, 24H), 3.019 (m, 5H), 4.081 (m, 11H), 4.900 (t, 2H), 5.058 (d, 1H), 5.217 (t, 1H), 5.734 (d, 1H), 8.365 (br s, 4H); ESI-MS (+): *m/z* 901.19 $[M+H]^+$.

2(*N*-acetyl-L-cysteinyl)-amino-2-deoxy-1,3,4,6-tetra-*O*-acetyl-β-D-glucopyranoside disulfide (4.25). To a solution of compound **4.24** (500mg, 0.555mmol) in 7ml DCM, was added pyridine (215µl, 2mmol) and the reaction mixture was cooled to 0°C. Acetic anhydride (215µl, 2mmol) was added drop wise and the reaction was allowed to warm to room temperature over 18hrs. The reaction mixture was concentrated and stirred in a 15ml ethyl acetate/H_2O mixture for 30mins, after which 2ml 1M HCl was added. The H_2O and organic layers were allowed to separate. The organic layer was dried over Na_2SO_4, followed by evaporation *in vacuo* producing 380mg (69% yield) of compound **(4.25)** as a light yellow powder. ^{1}H NMR (DMSO–d_6, 300MHz, 25°C): δ 1.983 (m, 30H), 2.847 (m, 2 H), 3.990 (d, 4H), 4.182 (m, 7H), 4.879 (m, 0.6H), 5.009 (m, 2H), 5.198 (m, 2H), 5.751 (t, 1H), 5.937 (d, 1H), 8.170 (m, 3H); ESI-MS (+): *m/z* 983.29 $[M+H]^+$, 1005.29 $[M+Na]^+$.

2(*N*-acetyl-L-cysteinyl)-amino-2-deoxy-(α/β)-D-glucopyranoside disulfide (4.26). To a solution of **4.25** (200mg, 0.509mmol) in 38ml of MeOH was added $Mg(OMe)_2$ in MeOH (1.9ml of a 6% w/v) and the mixture was allowed to stir for 2hrs. The reaction was neutralized with Dowex-50W(H^+) ion-exchange resin (pH was adjusted to 6.5, monitored with pH strips), filtered and the MeOH removed *in vacuo*. The residual solvent was dried by overnight under reduced pressure, producing 50mg (42% yield) of compound **(4.26)** as a off white powder. ^{1}H and ^{13}C NMR performed in D_2O and the resulting spectra was identical to that reported in the literature (*12*). ESI-MS (+): *m/z* 647.22 $[M+H]^+$.

4.7 Reference

(1) Knapp, S., Gonzalez, S., Myers, D. S., Eckman, L. L., and Bewley, C. A. (2002) Shortcut to Mycothiol Analogues. *Organic Letters 4*, 4337-4339.

(2) Shen, H., and Byers, L. D. (2007) Thioglycoside hydrolysis catalyzed by b-glucosidase. *Biochemical and Biophysical Research Communications 362*, 717-720.

(3) Knapp, S., Amorelli, B., Darout, E., Ventocilla, C. C., Goldman, L. M., Huhn, R. A., and Minnihan, E. C. (2005) A family of mycothiol analogues. *Journal of Carbohydrate Chemistry 24*, 103-130.

(4) Metaferia, B. B., Fetterolf, B. J., Shazad-ul-Hussan, S., Moravec, M., Smith, J. A., Ray, S., Gutierrez-Lugo, M.-T., and Bewley, C. A. (2007) Synthesis of Natural Product-Inspired Inhibitors of *Mycobacterium tuberculosis* Mycothiol-Associated Enzymes: The First Inhibitors of GlcNAc-Ins Deacetylase. *Journal of Medicinal Chemistry 50*, 6326-6336.

(5) Newton, G. L., Ko, M., Ta, P., Av-Gay, Y., and Fahey, R. C. (2006) Purification and characterization of *Mycobacterium tuberculosis* 1D-*myo*-inosityl-2-acetamido-2-deoxy-α-D-glucopyranoside deacetylase, MshB, a mycothiol biosynthetic enzyme. *Protein Expression and Purification 47*, 542-550.

(6) Metaferia, B. B., Ray, S., Smith, J. A., and Bewley, C. A. (2007) Design and synthesis of substrate-mimic inhibitors of mycothiol-S-conjugate amidase from *Mycobacterium tuberculosis*. *Bioorganic & Medicinal Chemistry Letters 17*, 444-447.

(7) Myszka, H., Bednarczyk, D., Najder, M., and Kaca, W. (2003) Synthesis and induction of apoptosis in B cell chronic leukemia by diosgenyl 2-amino-2-deoxy-β-D-glucopyranoside hydrochloride and its derivatives. *Carbohydrate Research 338*, 133-141.

(8) Knapp, S., and Myers, D. S. (2002) Synthesis of αGalNAc Thio-Conjugates from an a-GalNAc Mercaptan. *Journal of Organic Chemistry 67*, 2995-2999.

(9) Knapp, S., and Myers, D. S. (2001) Alpha-GlcNAc thioconjugates. *The Journal of organic chemistry 66*, 3636-3638.

(10) Nicholas, G. M., Eckman, L. L., Newton, G. L., Fahey, R. C., Ray, S., and Bewley, C. A. (2003) Inhibition and kinetics of *Mycobacterium tuberculosis* and *Mycobacterium smegmatis* mycothiol-S-conjugate amidase by natural product inhibitors. *Bioorganic & Medicinal Chemistry 11*, 601-608.

(11) Jardine, M. A., Spies, H. S. C., Nkambule, C. M., Gammon, D. W., and Steenkamp, D. J. (2002) Synthesis of mycothiol, 1D-1-O-(2-[N-acetyl-L-cysteinyl]amino-2-deoxy-α-D-glucopyranosyl)-*myo*-inositol, principal low molecular mass thiol in the actinomycetes. *Bioorganic & Medicinal Chemistry 10*, 875-881.

(12) Patel, M. P., and Blanchard, J. S. (1998) Synthesis of Des-*myo*-Inositol Mycothiol and Demonstration of a Mycobacterial Specific Reductase Activity. *Journal of the American Chemical Society 120*, 11538-11539.

(13) Patel, M. P., and Blanchard, J. S. (1999) Expression, Purification, and Characterization of *Mycobacterium tuberculosis* Mycothione Reductase. *Biochemistry 38*, 11827-11833.

(14) Patel, M. P., and Blanchard, J. S. (2001) *Mycobacterium tuberculosis* mycothione reductase: pH dependence of the kinetic parameters and kinetic isotope effects. *Biochemistry 40*, 5119-5126.

(15) Fetterolf, B., and Bewley, C. A. (2004) Synthesis of a bromotyrosine-derived natural product inhibitor of mycothiol-S-conjugate amidase. *Bioorganic & Medicinal Chemistry Letters 14*, 3785-3788.

Chapter 5

Enzymology

5.1 Introduction

During this study we have purified the enzymes, developed the analytical methods and synthesized the substrate analogues critical to the development of the drug discovery protocol which is the aim of this study. In this chapter we report how the different aspects of this study were employed in the conduction of the enzymatic studies.

5.2 MshB

MshB is very specific for its natural substrate αGlcNAc-Ins, which is *N*-deacetylated by the enzyme to give αGlcN-Ins as product(*1*). Removal of the inositol (Ins) moiety of αGlcNAc-Ins results in a 100-fold decrease in reactivity compared to the original substrate. During this study 2,4-dinitrophenyl 2-acetamido-2-deoxy-1-thio-α-D-glucopyranose (αGlcNAc-DNP) (Table 4.2, **4.19b**) was used as alternative substrate for MshB. All enzyme reactions with MshB was performed in a reaction buffer containing 50mM HEPES and 50mM NaCl at pH 7.4 (*2*). The final concentrations of enzyme and substrate were 1.5μg/μl and 0.1mM respectively.

5.2.1 N-deacetylation of 2,4-Dinitrophenyl 2-Acetamido-2-deoxy-1-thio-α-D-glucopyranose (αGlcNAc-DNP)

5.2.1.1 LCMS analysis

The same MshB mediated *N*-deacetylation of αGlcNAc-DNP (Figure 5.1) was analyzed with the same HPLC-ESI/MS(TOF) method used in the quatitation of MSH, MSSM and αGlcNAc-Ins (Chapter 3). The enzyme reactions were incubated for 30 minutes at 37°C, after which the reaction was stopped by heat inactivation of the

enzyme. The denatured enzyme debris was removed by means of centrifugation and the reaction mixtures in the supernatant were submitted for LCMS analysis. Reaction mixtures were analyzed with a gradient elution program utilizing a Synergy 4 µM Fusion RP, 250×2mm column (Phenomenex) on an ACQUITY UPLC® system (Waters Corp.). The total analysis time was 20 min. Detection was performed with a QTOF Ultima API quadrupole mass spectrometer (Micromass, Manchester, UK) and the data processed with MassLynx™ software (Micromass, Manchester, UK).

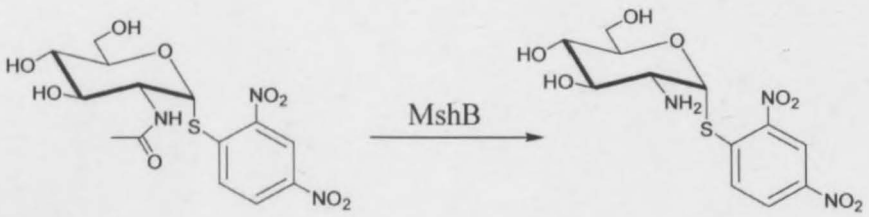

Figure 5.1: The MshB mediated *N*-deacetylation of 2,4-Dinitrophenyl 2-Acetamido-2-deoxy-1-thio-α-D-glucopyranose (**4.19b**) to 2,4-Dinitrophenyl 2-amido-2-deoxy-1-thio-α-D-glucopyranose (αGlcN-DNP)

The total ion chromatogram was extracted for the *m/z* $[M+H]^+$ ions of αGlcNAc-DNP and αGlcN-DNP, these being 404 and 362 respectively (Figure 5.2). The two compounds elute roughly one minute from each other, with the slightly more hydrophilic product (αGlcN-DNP) eluting first. The area under curve (AUC) of the two ion chromatograms of the substrate and product (Figure 5.2) are within the same range. This means that after 30 minutes. almost half of the substrate was converted to product. The total ion chromatogram of the control reaction (buffer and substrate) was extracted for the *m/z* 404 $[M+H]^+$ ion of αGlcNAc-DNP to produce a similar peak to the green peak in Figure 5.2 (data not shown). No peak was obtained when the control reaction total ion chromatogram was extracted for the *m/z* 362 $[M+H]^+$ ion of αGlcN-DNP. This confirms the N-deacetylation reaction was indeed catalyzed by MshB.

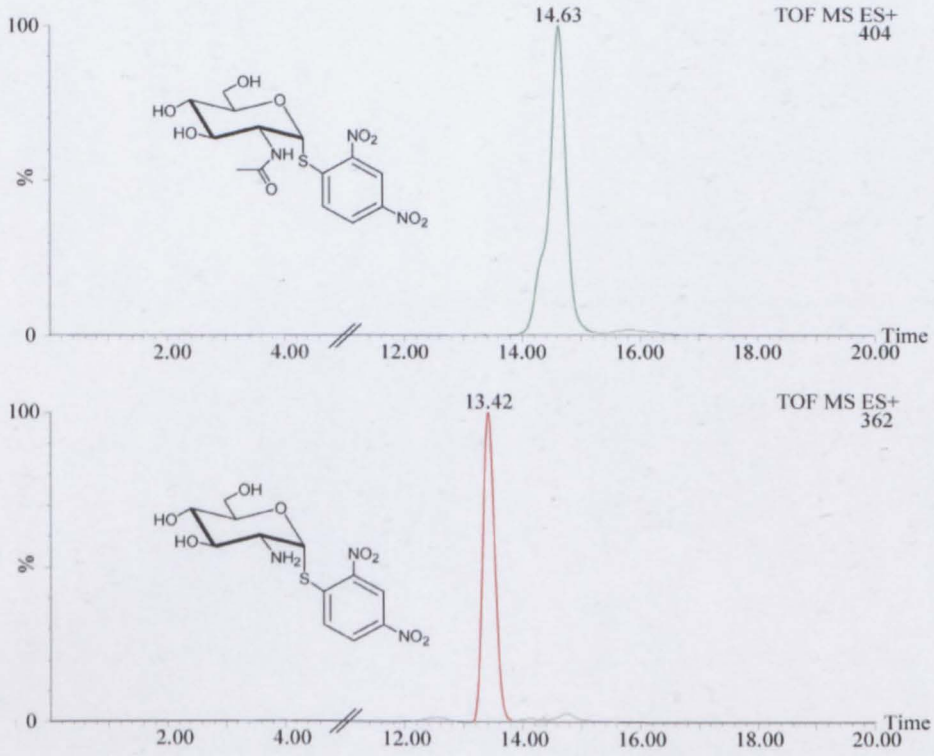

Figure 5.2: The total ion chromatogram of the MshB reaction with αGlcNAc-DNP extracted for the *m/z* 404 $[M+H]^+$ ion of αGlcNAc-DNP (green) and the *m/z* 362 $[M+H]^+$ ion of αGlcN-DNP (red).

The corresponding mass spectra of αGlcNAc-DNP and αGlcN-DNP are shown in (Figure 5.3). The two mass spectra clearly shows the *m/z* 404 $[M+H]^+$ and 426 $[M+Na]^+$ ions (green) of the αGlcNAc-DNP substrate and the *m/z* 362 $[M+H]^+$ and 384 $[M+Na]^+$ ions (red) of the *N*-deactylated product

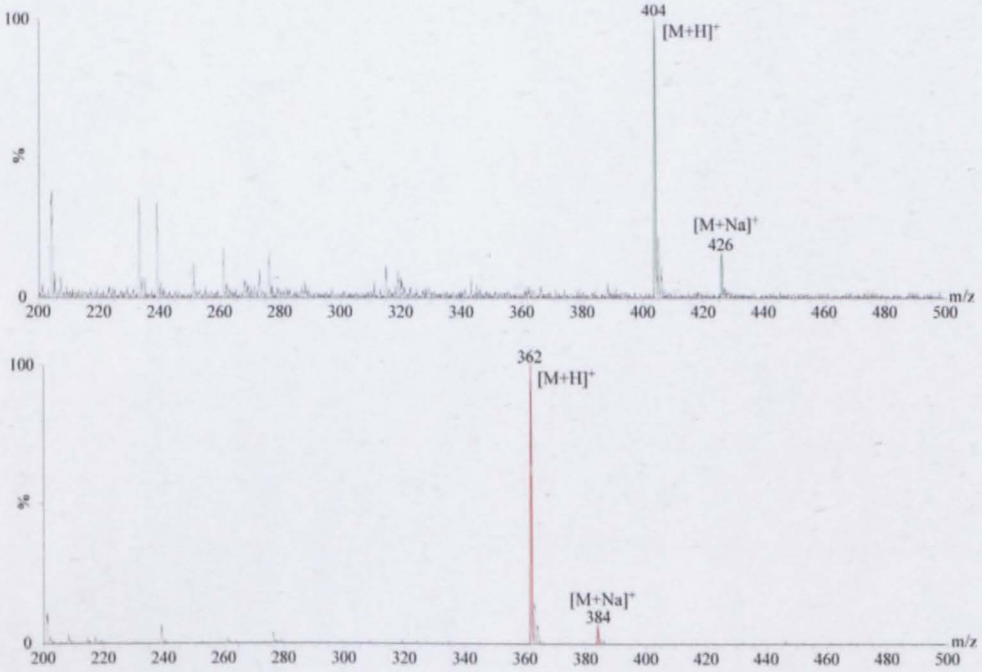

Figure 5.3: The corresponding MS spectra of αGlcNAc-DNP (green) and αGlcN-DNP (red) in the MshB reaction mixture.

5.2.1.2 HPLC analysis

During this study a HPLC method was developed to visualize the MshB reaction with αGlcNAc-DNP as substrate. The MshB enzyme reaction with α-GlcNAc-DNP was stopped at different time points and analyzed on an Agilent 1100 Series HPLC with an auto sampler and a diode array detector. The HPLC was fitted with a Synergy 4 μM Fusion RP, 250x2mm column (Phenomenex) used in all previous LCMS analyzes. The program used was a 30% MeOH/H_2O isocratic run of 10 mins. per analysis, with a flow rate of 0.350 ml/min. The substrate eluted at 5.7 mins and was monitored at 330nm. Standard substrate solutions ranging from 0mM to 0.1mM was used to produce a calibration curve. The standard curve was used to graphically visualize the depletion of αGlcNAc-DNP over time. The experiment was performed in triplicate. The enzyme reactions were stopped at 3, 5, 10, 20, 35, 60, 120 and 240 minutes, after which the enzyme was denatured and removed by centrifugation, followed by sample analysis on the HPLC. A regression curve was used to visualize the depletion of the αGlcNAc-DNP over time (Figure 5.4).

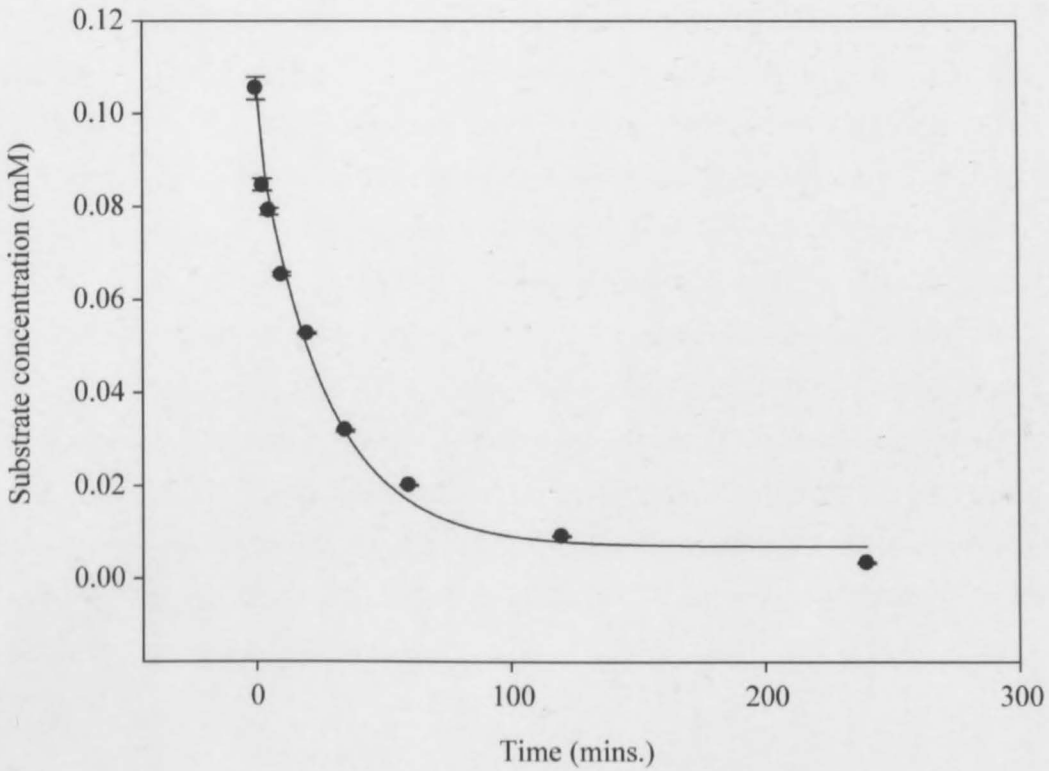

Figure 5.4: MshB mediated depletion of the αGlcNAc-DNP concentration over time.

The rate at which the 0.1mM αGlcNAc-DNP was depleted was fairly quick (Figure 5.4), with almost half of the substrate consumed within the 30mins. This quick depletion of substrate was also seen in the LCMS analyses of the enzyme reaction stopped after 30mins. (section 5.2.1.1). If these results are compared with the results obtained by Newton *et al.* (*2*) for the *N*-deacetylation of αGlcNAc-Ins by MshB, then MshB is more active with αGlcNAc-DNP than with its natural substrate. Almost double the amount of αGlcNAc-DNP is *N*-deacetylated in 30 minutes compared to αGlcNAc-Ins over the same time period.

The isocratic HPLC method poorly resolved the individual αGlcNAc-DNP substrate and αGlcN-DNP product peaks because of the similar polarity of the two compounds. The substrate peak obtained at 330nm also did not remain constant, which means that if the substrate and product co-eluted, the product does not have an absorption maximum at 330nm. Further attempts to resolve the product peak were unsuccessful.

In a study preformed by Kondo *et al.*, the authors examined the intramolecular S→N Smiles rearrangement of *S*-(2,4-dinitrophenyl)cysteine to *N*-(2,4-dinitrophenyl)cysteine (*3*). This rearrangement was performed by incubating *S*-(2,4-dinitrophenyl)cysteine with different organic bases, including imidazole. This same type of rearrangement could happen, as proposed below, in the MshB active site after the *N*-deactylation of αGlcNAc-DNP. Since the formation of the free amine was confirmed with LCMS analysis (Figure 5.2), it is possible that it could attack the C1 carbon of the dinitrophenyl moiety in a nucleophilic substitution to the ring (Figure 5.5, route a) in the presence of the imidazole side chain of His144 in the MshB active site. The spiro-Meisenheimer intermediate (**MH**) would subsequently be formed, which is then deprotonated (Figure 5.5, route b) to form ($\mathbf{M^{-1}}$). The rearrangement is completed by the concomitant breaking of the S-C bond and the protonation of the thiolate group (Figure 5.5, route c).

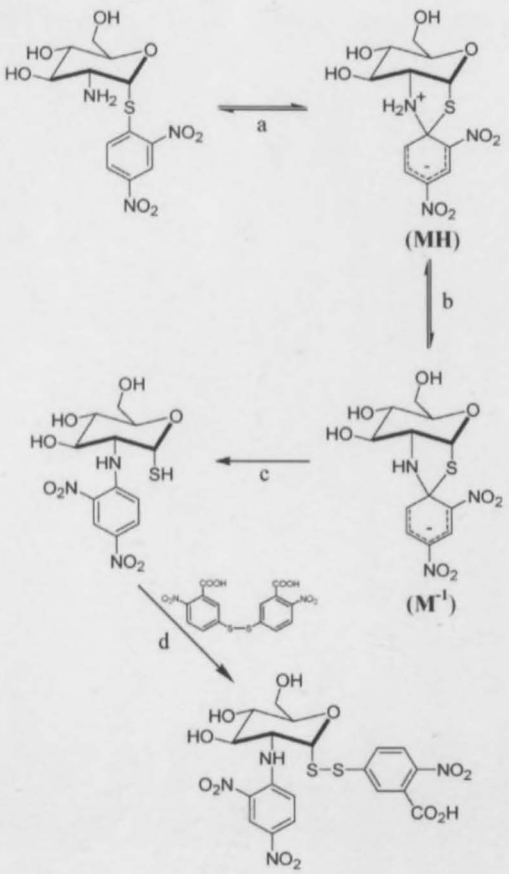

Figure 5.5: Proposed S→N Smiles rearrangement of αGlcNAc-DNP and derivatisation the free thiol product with DNTB

This rearrangement would result in the formation of a free thiol product, which could be derivatised with Ellman's Reagent (DNTB) (Figure 5.5, route d). If the MshB reaction mixture therefore give a positive (absorption at 412nm) result for a DTNB assay, it would confirm the formation of the rearrangement product.

5.2.1.3 Ellman's Reagent assay

To test this hypothesis MshB was incubated with αGlcNAc-DNP at 37°C and the reaction stopped at 3, 5, 10, 20, 35, 60 and 120mins. The enzyme debris was subsequently removed, and the reaction mixtures were transferred to new tubes for treatment with Ellman's Reagent (DTNB). DTNB is used to derivatise free thiol compounds for visualisation using spectrophotometric methods. After incubation of the DTNB reactions the reaction mixtures were transferred to a 96-well plate (Costar). The amount of DTNB derivatised compound was visualised with a Thermo Varioskan™ microplate reader at 412nm. The reaction progression curve is shown in Figure 5.6.

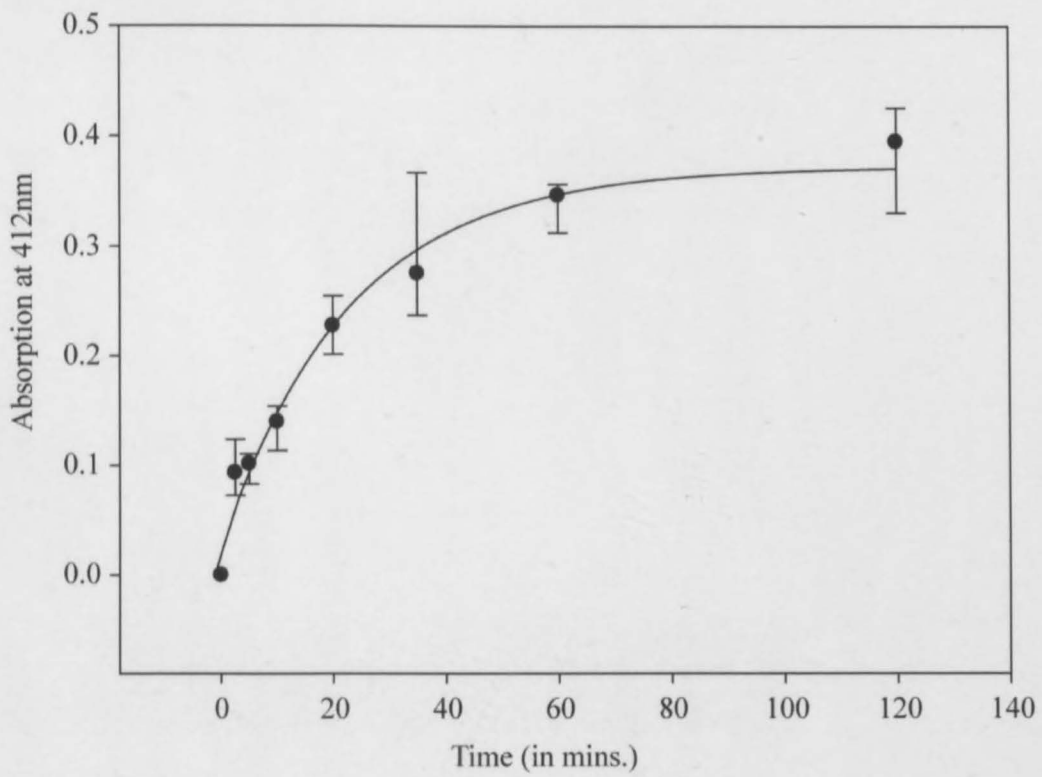

Figure 5.6: Progression curve generated by a DTNB assay

An increase of DTNB absorption over the time (Figure 5.6) in the MshB reaction with αGlcNAc-DNP means that a free thiol is formed following the *N*-deacetylation. The negative control reaction, in which no enzyme is present, did not show any absorption at 412nm. Further studies are currently underway to confirm the formation of the rearrangement product.

5.2.1.4 Inhibition study

Free thiols had been used as part of inhibitors for porcine pancreatic carboxypeptidase B (pp-CpB). The free thiol group of these inhibitors chelates the active site Zn^{2+} ion, thereby inactivating the enzyme (*4*). To determine if MshB might by inhibited by the free thiol of the rearrangement product, an experiment was performed to test if there was a difference in enzyme activity between fresh MshB and MshB that was incubated with αGlcNAc-DNP for a period of time. A set of MshB reactions was set up and incubated as described in section 5.2. They were stopped at 3, 5, 10, 20, 35, 60, 120 and 180 minutes and analyzed with the HPLC method developed during this study (Figure 5.7, curve A). A second set of MshB reactions of was first incubated with 0.1mM αGlcNAc-DNP before αGlcNAc-DNP was again added to the reactions at a final concentration of 0.1mM. The reactions of the second set were stopped at 183, 185, 190, 200, 215, 240, 300 and 360 minutes and analyzed (Figure 5.7, curve B). The regression curves of the two reaction sets are shown in Figure 5.7.

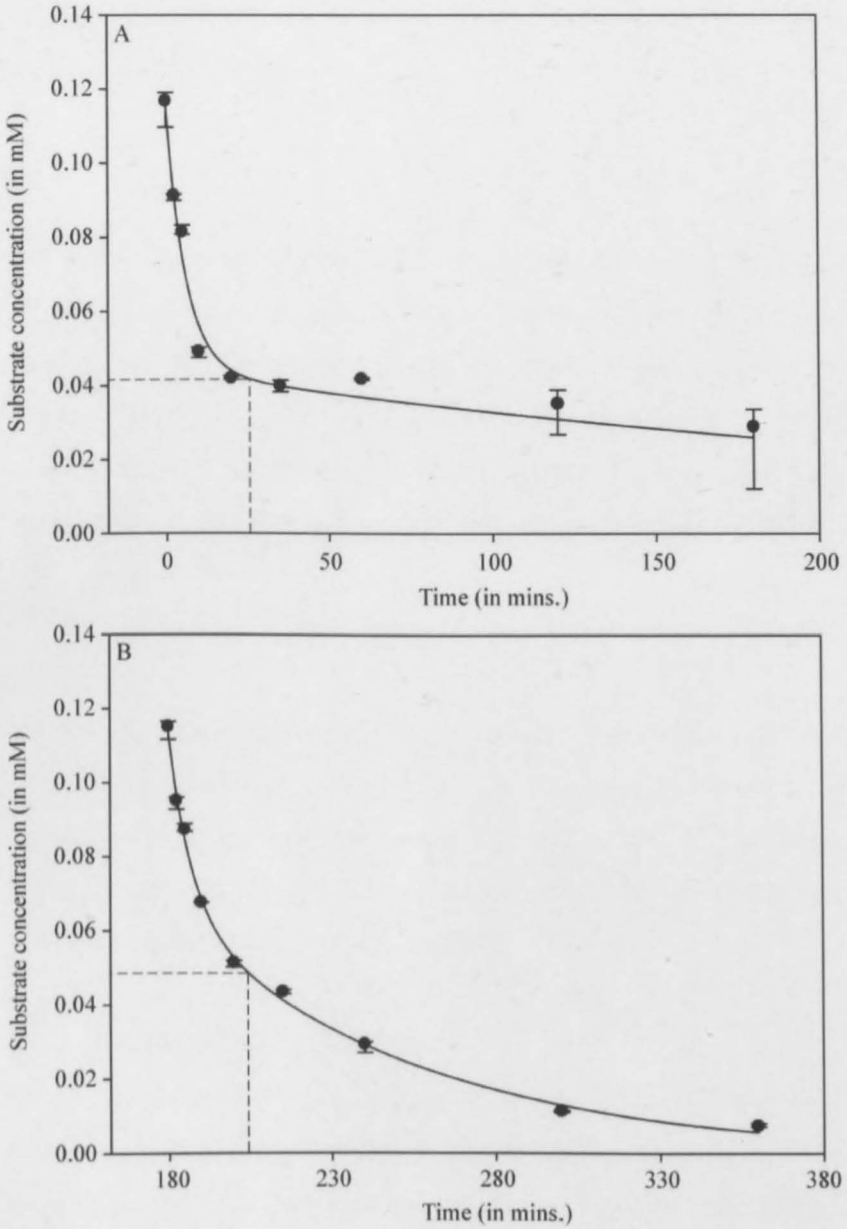

Figure 5.7: The two regression curves depicting the almost identical depletion of αGlcNAc-DNP over time. Curve A was obtained through enzymes reactions with fresh MshB and curve B with MshB incubated with αGlcNAc-DNP for 180 mins..

Results shown by the two regression curves are inconclusive. The two curves are nearly identical and in both cases most of the substrate has been depleted in the 180 minute incubation period. This means that free thiol of the rearrangement product does not inhibit MshB. However, at the 25 minute point in each of the two reactions there is almost a 10nM difference in substrate concentration in the two reaction mixtures, with the lower concentration in the fresh MshB reaction. This could mean

that the incubation of MshB with αGlcNAc-DNP for 180 minutes did have a small inhibitory effect on the enzyme.

5.3 Mtr

During this study Mtr was recombinantly expressed in *E. coli* for the first time (Chapter 2). This means that the enzyme was not produced in its native mycobacterial environment, it was not known if the enzyme would show the same activity as previously published (*5*). The activity of Mtr was tested in a steady-state kinetic assay with the synthetically prepared 2(*N*-acetyl-L-cysteinyl)-amino-2-deoxy-(α/β)-D-glucopyranoside or des-*myo*-inositol mycothiol disulfide (DI-MSSM) (**4.26**) (Chapter 4).

5.3.1 FAD scan

After Mtr was successfully expressed and purified on small scale, a fluorescent flavin adenine dinucleotide (FAD) scan was preformed. This was performed to verify that Mtr was expressed with bound FAD, which would give a good indication that the enzyme will show activity. An absorption maximum at 530nm was obtained which is consistent with the absorption maxima for FAD.

5.3.2 Activity with DI-MSSM

The kinetic parameters for Mtr were determined in a NADPH assay and were found to have a K_m = 504±109μM, V_{max} = 0.0674±0.0043nmoles/s and k_{cat} = 10.98±0.70s^{-1}. The K_m compares well with the previously published K_m values for DI-MSSM with Mtr, 410μM and 510±40μM respectively (*5, 6*). The Michealis-Menten curve fit gave an R=0.9496 (P<0.001) and is given in Figure 5.8.

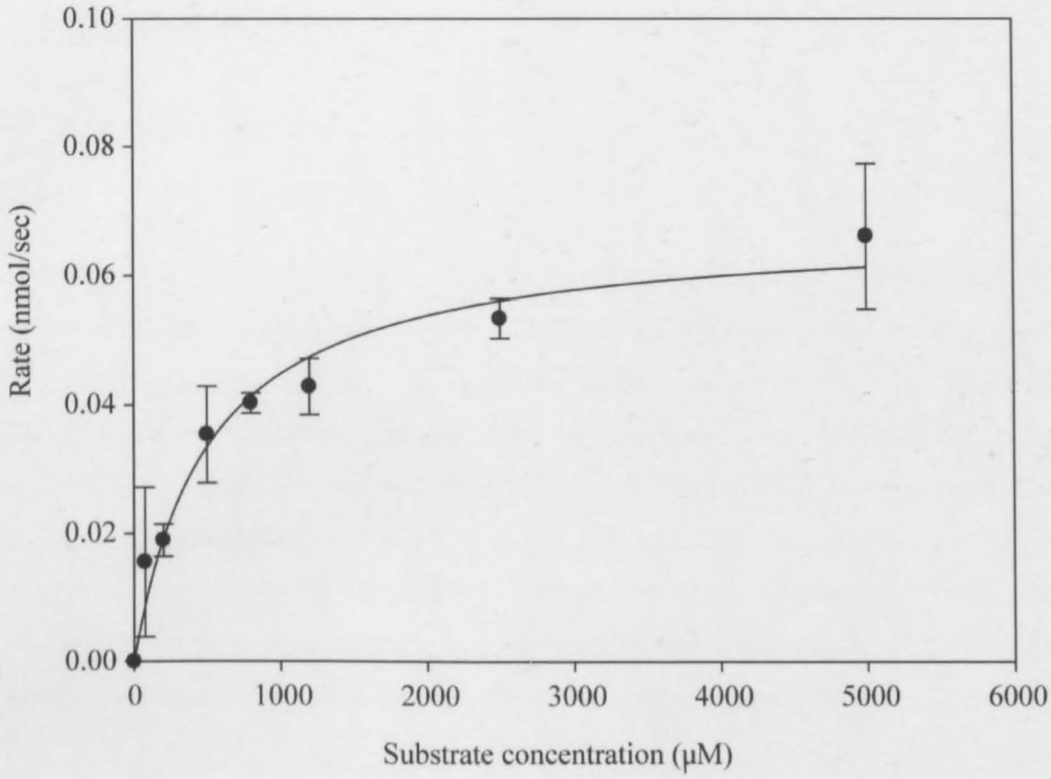

Figure 5.8: The steady state kinetics of Mtr with DI-MSSM. Each point represents the average and the bars the standard error. The solid line represents the best-fit of the data to the Michaelis-Menten equation.

5.4 Conclusion

In the reactions with MshB and αGlcNAc-DNP it was found that the *N*-deacetylation of the substrate happens twice as fast as the *N*-deacetylation of the natural substrate. It was also found that after the *N*-deacetylation of αGlcNAc-DNP, the dinitrophenyl moiety migrates from the sulfur to the free amine in an intramolecular S→N Smiles rearrangement. This is the first evidence of this type of reaction mediated by an enzyme. The formation of the rearrangement product was proven by a DTNB derivatization of the free thiol. NMR and mass spectroscopic studies are currently underway to conclusively prove the formation of the free thiol product.

The result obtained from the activity of Mtr with DI-MSSM shows that the Mtr expressed in *E. coli* is indeed active, with a K_m similar to the one previously published for DI-MSSM.

5.5 Experimental

5.5.1 Enzyme reactions

5.5.1.1 MshB reactions

The MshB reactions were performed as published by Newton et al., 2006 (*2*). All the reactions performed in preparation for LCMS and HLPC analysis was accomplished in a final volume of 250µl. The reaction mixture consisted of 1.3µl 19.2mM αGlcNAc-DNP substrate stock solution (final concentration of 0.1mM), 4.7µl 4.3mg/ml MshB stock (final concentration of 1.5µg/µl) and 244µl reaction buffer (50mM HEPES, 50mM NaCl, pH 7.4). At the specific time points the enzyme reactions were stopped by denaturing the enzyme at 95°C for 5min, after which the denatured enzyme was pelleted through centrifugation for 5min. The reaction mixtures were transferred to LCMS or HPLC vials and analyzed.

5.5.2 LCMS analysis

The same LCMS method used in the quantitation of the mycothiol pathway intermediates (Chapter 3, section 3.4.4) was used in the analysis of the MshB deacetylation of α-GlcNAc-DNP.

Samples were analyzed on an ACQUITY UPLC® system (Waters Corp.) with an autosampler and a Synergy 4 µM Fusion RP, 250×2mm column (Phenomenex). The sample injection volume was 20µl and the autosampler syringe was washed with solvent A (0.1% formic acid in water) before each injection. A gradient elution program with a flow-rate of 0.20 ml/min was used for the analysis. The gradient was as follows: 100% solvent A for 8 min; 7 min linear increase up to 95% solvent B (0.1% formic acid in acetonitrile); 95% B step for 3 min; 95% solvent A from 18 to 20 min. The total analysis time was 20 min.

Detection was performed on a QTOF Ultima API quadrupole mass spectrometer (Micromass, Manchester, UK). Analytes were detected in the positive ion mode. The capillary voltage was set at 3500 V. The source temperature and the nebulization gas temperature were set at 120 °C and 400 °C, respectively. The cone voltages were set at 35V. Data was processed using MassLynx™ software (Micromass, Manchester, UK).

5.5.3 HPLC analysis

The enzyme reactions were analyzed on a Synergy 4 µM Fusion RP, 250×2mm column (Phenomenex) on an Agilent 1100 Series HPLC with an autosampler and diode array detector. An isocratic program of 30% MeOH/H_2O was used at a flow rate of 0.350ml/min. The total analysis time was 10min. Elution of the substrate was monitored at 330nm. Data was processed with ChemStation for LC 3D software.

5.5.4 Spectrophotometric analysis

5.5.4.1 DNTB assay

MshB reactions with αGlcNAc-DNP were set up, incubated and stopped as described in section 5.5.1.1. The reaction mixtures were transferred to clean tubes and DNTB added to a final concentration of 0.1mM. The reactions were incubated at room temperature for 5 minutes after which it was transferred to a UV Corning 96 well plate. Absorption was measured at 412nm with the Thermo Varioskan™.

5.5.4.2 FAD scans

The fluorescent scan for FAD in the purified Mtr enzyme was performed with the Thermo Varioskan™. Black Corning 96-well microtitre plates were used for the fluorescent scans. The excitation wavelength was 370nm, which was scanned over an emissions wavelength range of 420-680nm with a 5nm step size. The excitation was measured at a wavelength of 512nm.

5.5.4.3 Mtr activity assay

The Mtr enzyme activity assay was performed in an UV Corning 96 well plate. The reaction was monitored through the oxidation of β-NADPH to β-$NADP^+$ at 340nm. The DI-MSSM concentration range was setup in the 96-well plate. The concentrations of DI-MSSM used were 0µM, 75µM, 200µM, 800µM, 1200µM, 2500µM and 5000µM. The enzyme reactions were initiated with the addition of the reaction mixture to the DI-MSSM concentration. The reaction mixture contained 50mM HEPES, 0.1mM EDTA, 100µM β-NADPH and 20nM Mtr, at pH 7.6.

5.5.5 Statistical Data Analysis

Sigma Plot version 9.01 (SyStat Software, Inc.) was used for all data analysis and the visualization of the data.

5.6 References

(1) Newton, G. L., Av-Gay, Y., and Fahey, R. C. (2000) N-acetyl-1-D-*myo*-inosityl-2-amino-2-deoxy-α-D-glucopyranoside deacetylase (MshB) is a key enzyme in mycothiol biosynthesis. *Journal of Bacteriology 182*, 6958-6963.

(2) Newton, G. L., Ko, M., Ta, P., Av-Gay, Y., and Fahey, R. C. (2006) Purification and characterization of *Mycobacterium tuberculosis* 1D-*myo*-inosityl-2-acetamido-2-deoxy-α-D-glucopyranoside deacetylase, MshB, a mycothiol biosynthetic enzyme. *Protein Expression and Purification 47*, 542-550.

(3) Kondo, H., Moriuchi, F., and Sunamoto, J. (1980) S→N and N→S Reverse Rearrangement of *S*- and *N*-(2,4-Dinitrophenyl)cysteines. *Journal of Organic Chemistry 46*, 1333-1336.

(4) Adler, M., Bryant, J., Buckman, B., Islam, I., Larsen, B., Finster, S., Kent, L., May, K., Mohan, R., Yuan, S., and Whitlow, M. (2005) Crystal Structures of Potent Thiol-Based Inhibitors Bound to Carboxypeptidase B. *Biochemistry 44*, 9339-9347.

(5) Patel, M. P., and Blanchard, J. S. (1999) Expression, Purification, and Characterization of *Mycobacterium tuberculosis* Mycothione Reductase. *Biochemistry 38*, 11827-11833.

(6) Patel, M. P., and Blanchard, J. S. (1998) Synthesis of Des-*myo*-Inositol Mycothiol and Demonstration of a Mycobacterial Specific Reductase Activity. *Journal of the American Chemical Society 120*, 11538-11539.

Chapter 6

Conclusion

6.1 Enzyme expression

MshB and Mtr was successfully expressed and purified during this study. The expression and purification of MshB was performed more efficiently, thus producing a higher expression yield than previously described (*1*). Also, Mtr was recombinantly expressed and purified from *E. coli* for the first time during this study. Through collaborative work, determination of the crystal structure of Mtr is under progress. If successful, this accomplishment would contribute a major step forward in the structure-based development of inhibitors and substrate analogues for Mtr.

The methods development for the soluble expression of Mtr may now be used in conjunction with site-directed mutagenesis studies for the expression of different mutant forms of the Mtr enzymes. This would be a useful tool in further studies with Mtr, especially studies involving the binding modes of different moieties.

6.2 Quantitation of mycothiol and pathway intermediates

We successfully developed a new HPLC-ESI/MS(TOF) method for the detection and quantitation of MSH and its pathway intermediates. This method was used for the simultaneous detection of MSH, MSSM, and αGlcN-Ins in *M. smegmatis* cell lysates. Unlike previous HPLC-UV detection methods, there is no need for the derivatisation of the analytes and all three analytes could be detected in a single injection of the *M. smegmatis* cell lysate. Furthermore, the method was also used to track the fluctuating MSH:MSSM levels in *M. smegmatis* cells growing under oxidative stress conditions.

Future work will focus on the determination of optimised calibration curves and on the reproducibility of the measurements of the different analytes. This would be important in the accurate determination of the amount of MSH present in *M.*

smegmatis cells and other actinomycetes, because preliminary results reported during this study would suggest that there was a large underestimation of cellular MSH levels in previous studies (*2, 3*).

The biggest advantage of this method is that the MSH biosynthetic enzymes, as well as related enzymes that utilize mycothiol, can now be studied in various physiological conditions. The effect of prospective drugs or inhibitors on these enzymes in either free or whole cell assays can now be monitored with greater ease. Thus, the development of a multiwell-based form of this method would be crucial to allow the high-throughput analysis of new or existing compounds. With our current methodology, the extrapolation of this method to a high-throughput 96-well plate format would be trivial.

6.3 Synthesis of substrate analogues

The Mtr substrate analogue, des-*myo*-inositol mycothiol disulfide (DI-MSSM), was synthesized by an improved method compared to the previous published synthesis (*4*). This substrate analogue, rather than MSSM, was used to test the activity of the recombinantly expressed Mtr. The advantage of using DI-MSSM is that it is less expensive and time-consuming to synthesize than MSSM. It can also be used as an alternative ligand in the determination of the crystal structure coordinates of Mtr.

During this study we also synthesized a range of substrate analogues for MshB. The synthesized thioglycoside disaccharides would serve as new scaffolds for the development of a new range of potential inhibitors against MshB and Mtr (with further development). We also successfully synthesized a series of fluorogenic thioglycosides. These analogues will serve a vital function in the development of new assay methods for inhibitor screening not only for MshB, but also for Mca and Mtr. The molecules designed against MshB can easily be transformed into substrate analogues for the other MSH-utilising enzymes (like Mtr) through simple synthetic methods. Future design of substrate analogues for Mtr will also exploit fluorescence resonance energy transfer (FRET) based strategies. These types of molecules will serve as competitive substrates in competitive-binding assays, where the loss of emission from the acceptor moiety would be an indication of how well the target

molecule binds to the Mtr active site (Figure 6.1). The biggest challenge in synthesizing these FRET based molecules would be to bring the donor and acceptor fluorophore moieties within an appropriate Förster distance form each other, ensuring that energy transfer would take place upon irradiation of the donor moiety.

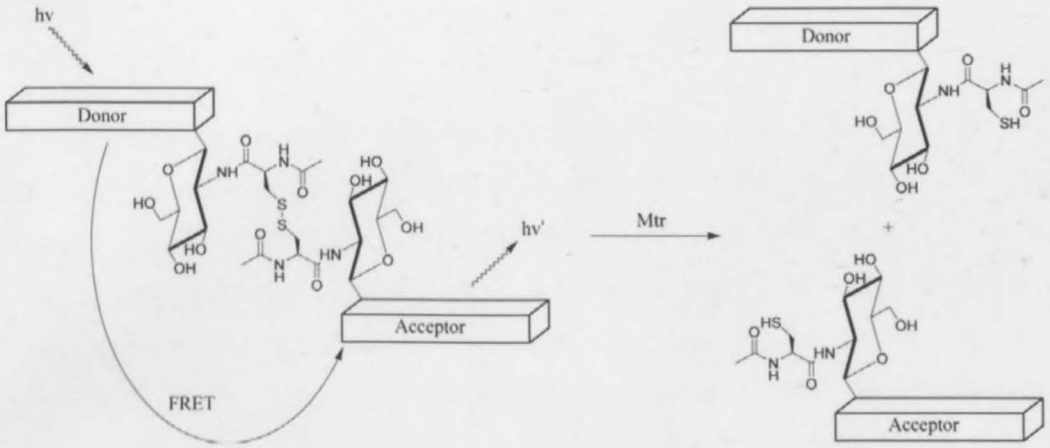

Figure 6.1: Hypothetical FRET based molecule to be used in Mtr assays.

6.4 Enzymology

The DI-MSSM substrate analogue was tested in a NADPH-dependent assay with Mtr. Nearly identical kinetic parameters to that previously reported were obtained (*5*). This concluded the first successful expression and purification of Mtr using *E. coli* as expression host.

Furthermore, αGlcNAc-DNP was used as substrate analogue in assays with MshB. LCMS analysis proved that αGlcNAc-DNP is converted to αGlcN-DNP through the action of MshB. Through a time dependent progression curve analysis of the MshB deacetylation reaction with αGlcNAc-DNP it was observed that MshB is almost twice as reactive with αGlcNAc-DNP compared to its natural substrate. Determination of the full kinetic parameters is currently underway to confirm these preliminary results. Either way, these results proved a very exciting prospect for the further development of the first photometric assay for MshB.

During the MshB-mediated *N*-deacetylation of αGlcNAc-DNP it was also discovered that the αGlcN-DNP product undergoes a S→N intramolecular rearrangement,

producing the free thiol product. This is the first evidence of an enzyme-mediated rearrangement of this type and could be exploited in the further development of inhibitors. Studies are currently underway to conclusively confirm the formation and detailed kinetics and the structure of the rearrangement product.

6.5 Final Remarks

The mycothiol pathway and related enzymes had been the focus of numerous studies. From these studies it was proven that the pathway and related mechanisms provide ample targets for the design of new drugs against *M. tuberculosis*. Active research is currently being conducted to provide lead compounds against these targets. One of the major reasons why this process is not proceeding faster is the current screening methods employed to evaluate compound libraries. During this study we have laid the foundation for the development of new analytical and screening methods, which would streamline the drug discovery process that target these enzymes and the mycothiol pathway.

6.6 References

(1) Newton, G. L., Ko, M., Ta, P., Av-Gay, Y., and Fahey, R. C. (2006) Purification and characterization of *Mycobacterium tuberculosis* 1D-*myo*-inosityl-2-acetamido-2-deoxy-α-D-glucopyranoside deacetylase, MshB, a mycothiol biosynthetic enzyme. *Protein Expression and Purification 47*, 542-550.

(2) Newton, G. L., Arnold, K., Price, M. S., Sherrill, C., Delcardayre, S. B., Aharonowitz, Y., Cohen, G., Davies, J., Fahey, R. C., and Davis, C. (1996) Distribution of thiols in microorganisms: mycothiol is a major thiol in most actinomycetes. *Journal of Bacteriology 178*, 1990-1995.

(3) Ung, K. S. E., and Av-Gay, Y. (2006) Mycothiol-dependent mycobacterial response to oxidative stress. *FEBS Letters 580*, 2712-2716.

(4) Patel, M. P., and Blanchard, J. S. (1998) Synthesis of Des-*myo*-Inositol Mycothiol and Demonstration of a Mycobacterial Specific Reductase Activity. *Journal of the American Chemical Society 120*, 11538-11539.

(5) Patel, M. P., and Blanchard, J. S. (1999) Expression, Purification, and Characterization of *Mycobacterium tuberculosis* Mycothione Reductase. *Biochemistry 38*, 11827-11833.